NTNU – Trondheim
Norwegian University of
Science and Technology

Local Structural Analysis of a Semi-Submersible Exposed to Ice Loads

Erlend Hopsdal Skjetne

Master Thesis, Spring 2015

for

Master Student Erlend Hopsdal Skjetne

Local Structural Analysis of a Semi-Submersible Exposed to Ice Loads

Lokal Strukturanalyse av en Semi-Submersible Utsatt for Islaster

With the entry of floating drilling and completion/workover units for ice infested environments on a short term basis, development of associated structural design criteria for these units are required. The capability of structures to withstand local ice loads must be investigated in terms of hull shape and structural configuration for safe operations.

The candidate shall address the following topics:

1. A summary of ice properties, ice mechanics and ice load formulations for floating hull structures is to be made.

2. Relevant loading conditions for floating units are to be discussed with focus on local strength requirements. In particular, formulations which are implemented in relevant standards are to be considered.

3. Methods for computation of linear and non-linear load-effects and the associated structural resistance are to be highlighted. Some background to the numerical algorithms which are implemented in relevant computer software which is to be applied for the different types of calculation should be given.

4. Local response calculations are performed for a particular structural component of a semi-submersible drilling unit. Parametric studies are carried out to the extent that time allows.

The work scope may prove to be larger than initially anticipated. Subject to approval from the supervisor, topics may be deleted from the list above or reduced in extent. In the thesis the candidate shall present his personal contribution to the resolution of problems within the scope of the thesis work. Theories and conclusions should be based on mathematical derivations and/or logic reasoning identifying the various steps in the deduction.

The candidate should utilise the existing possibilities for obtaining relevant literature.

The thesis should be organised in a rational manner to give a clear exposition of results, assessments, and conclusions. The text should be brief and to the point, with a clear language. Telegraphic language should be avoided.

The thesis shall contain the following elements: A text defining the scope, preface, list of contents, summary, main body of thesis, conclusions with recommendations for further work, list of symbols and acronyms, references and (optional) appendices. All figures, tables and equations shall be numbered.

The supervisor may require that the candidate, in an early stage of the work, presents a written plan for the completion of the work.

The original contribution of the candidate and material taken from other sources shall be clearly defined. Work from other sources shall be properly referenced using an acknowledged referencing system.

The thesis shall be submitted in electronic form:

- Signed by the candidate
- The text defining the scope included
- In bound volume(s)
- Drawings and/or computer prints which cannot be bound should be organised in a separate folder.

Supervisor: Professor Bernt J. Leira

Deadline: June 10th 2015

Trondheim, January 16th, 2015

Bernt J. Leira

Abstract

The subject of deep sea drilling in the Arctic is now more relevant than ever. The environment in Arctic offshore areas can be extremely harsh and the structures operating there will have to be designed accordingly.

In this thesis the main objective is to investigate the structural response of the ice belt of a four-legged semi-submersible drilling unit due to local ice loads. The design of the ice belt is based on drawings of the existing semi-submersible *Deepsea Stavanger*. This platform is not ice classed, so some modifications have been made to the original design.

The first part of the thesis is a literature review that gives an introduction to the subject of ice, from an engineering point of view, in form of a summary on different types of floating ice, ice properties and ice mechanics. Also, a study on ice loads has been conducted, with emphasis on local loads. This includes aspects of ice loads that should be considered and relevant load formulations for the semi-submersible platform. The last part of the literature review is about local strength requirements, and the Finite Element Method and how it is implemented in Abaqus.

The second part consists of the study of the ice belt, exposed to local ice loads. The study has been conducted by use of the finite element computer software Abaqus. The requirements for ice class PC4 from IACS's *requirements concerning POLAR CLASS* have been applied to the outer shell and stiffeners of the ice belt, in order to ensure that it is strengthened for ice action. A convergence check has been performed in order to determine what element type and size that was feasible to conduct the analyses with. It was found that the S4R elements with mesh size 100 mm may give non-conservative stresses, however, it was used anyway in order to limit the required computational time.

Two types of nonlinear static analyses of the ice belt have been performed; one where structure has been exposed to ISO 19906's *local pressure for thick, massive ice features* which does not account for ice classes. And one capacity check with steadily increasing loads. The aim of these types of analyses, respectively, was to check if the structure could withstand the ISO load without yielding. And to find out where on the structure and at what load magnitudes the maximum stresses reach yield and ultimate material stress. For each type of analysis several cases with different loading was investigated.

The main findings from the analyses that consider the ISO load are that yielding occurs in the structure for most of the different cases. The yielding occurs to a large extent, especially when the part of structure that has the weakest stringer structure is loaded. The results from the analyses that consider the capacity show that the largest stresses occurs in the stringer for all the different cases, even though the applied loads act over the design load patches for plates, stiffeners or bulkheads. This shows that the stringer is the weak spot of the model in the analyses performed.

The stringer, which consists of plates, stiffeners and brackets, is neither configured nor dimensioned for ice loads. This is reflected by the results in terms of its high response. The results also show that the plates, stiffeners and bulkheads have lower response, and do not yield, when exposed to the ISO load in the areas where the stringer structure is stiff. By that it can be seen that the outer hull structure does not have to be strengthened further, in order to withstand the local ISO load, as long as the stringer is sufficiently stiff.

Sammendrag

Emnet om dypvannsboring i Arktis er nå mer relevant enn noengang. Miljøet i arktiske offshoreområder kan være ekstremt rått, og konstruksjonene som opererer der må være designet deretter.

I denne masteroppgaven er hovedmålet å studere den strukturelle responsen til isbeltet av en firebeint halvt nedsenkbar drilling plattform på grunn av lokale islaster. Designet til isbeltet er basert på tegninger av den eksisterende halvt nedsenkbare plattformen *Deepsea Stavanger*. Plattformen er ikke isklasset, så derfor måtte det originale designet forandres litt på.

Den første delen av masteroppgaven er et litteraturstudie som gir en introduksjon til temaet is, fra en ingeniørs synspunkt, i form av ein oppsummering av forskjellige typer flytende is, dens egenskaper og ismekanikk. I tillegg har det blitt gjort et studie av islaster, der lokale laster spesielt har blitt vektlagt. Dette studiet inkluderer innspillende faktorer og relevante lastformuleringer for den halvt-nedsenkbare plattformen. Den siste delen av litteraturstudiet omhandler lokale styrkekrav, og elementmetoden og hvordan den er implementert i Abaqus.

Den andre delen av masteroppgaven består av studiet av isbeltet, lastet av lokale islaster. Studiet har blitt gjennomført ved hjelp av elementmetodeprogrammet Abaqus. Strukturkravene til isklassen PC4 fra IACS sitt dokument *requirements concerning POLAR CLASS* har blitt brukt for å dimensjonere isbeltets ytre skall og stivere mot islaster. En konvergenssjekk har blitt utført for å bestemme passende elementtype og maskestørrelse til bruk i analysene. Resultatene fra sjekken viste at ved bruk av S4R elementet, med maskestørrelse 100 mm, kunne man få ukonservative spenninger. På tross av dette ble denne kombinasjonen brukt for å begrense analysetiden.

To typer statisk ulineære analyser av isbeltet har blitt gjennomført. En type der konstruksjonen har blitt utsatt for ISO 19906 sitt *local pressure for thick, massive ice features* som ikke tar hensyn til isklasser, og et kapasitetstudie med økende last. Målet med disse analysene var henholdsvis å sjekke om isbeltet tåler ISO-lasten under ULS-kondisjoner (ikke gå i flyt), og finne ut hvor på konstruksjonen og ved hvilke laster de maksimal spenning når flyt- og materialkapasitetsspenning. Det ble kjørt flere analyser med forskjellige laster for de to analysetypene.

Hovedresultatene fra analysene som omhandler ISO-lasten viser at flyt oppstår i konstruksjonen i de fleste ulike analysene. Dette gjelder spesielt når den delen av konstruksjonen med svakest

stringerstruktur blir lastet. Fra analysene som omhandler kapasitet, i form av flytspenning og materialkapasitetsspenning, viser at de største spenningene oppstår i stringeren i alle analysene. Dette gjelder selv om de påførte lastene virker over designområdene for plater, stivere eller skott. Dette viser at stringeren er konstruksjonens svake punkt i de analysene som har blitt utført.

Stringeren, som består av plater, stivere og braketter, er hverken utformet eller dimensjonert for islaster. Dette gjenspeiles i av resultatene i form av dens høye respons. Resultatene viser også at platene, stiverene og skottene har lavere respons, og ikke går i flyt, når de blir utsatt for ISO-lasten i områder som har sterk stringerstruktur. På den måten kan man se at den ytre skrogstrukturen ikke trenger å bli forsterket ytterligere, for å motstå den lokale ISO-lasten, så lenge stringeren er tilstrekkelig stiv.

Preface

This document is a Master's thesis and the conclusive work of the author's Master's Degree in Marine Technology at the Norwegian University of Science and Engineering (NTNU), Trondheim. The work has been carried out in the spring of 2015 at Marinteknisk senter at Tyholt, Trondheim.

I would like thank my supervisor Professor Bernt J. Leira for all his help and guidance throughout the semester. Appreciation also goes out to Elin Crombie at Odfjell Drilling for providing drawings and information so that I was able to create a realistic model for my analyses.

Last but not least, I would to thank my fellow student Patrick Bratlie for countless discussions about modelling and Abaqus in general, in addition to my girlfriend and fellow student Britta Hanstveit for help and support in writing this thesis.

Trondheim, 10th of June 2015

Erlend Hopsdal Skjetne

Table of contents

Table of Figures

List of Tables

Abbreviation

CSA	Canadian Standards Association
DNV	Det Norske Veritas
ELIE	Extreme-level ice events
FE	Finite Element
FEM	Finite Element Method
GPa	Giga Pascal
IACS	International Association of Classification Societies
ISO	International Standardization Organization
MN	Mega Newton
MPa	Mega Pascal
PC4	Polar Class number 4
S4R	4-noded shell element with reduced integration and hourglass control
S8R	8-noded doubly-curved shell element with reduced integration and hourglass control
S8R5	8-noded doubly-curved shell element with reduced integration, hourglass control and 5 active degrees of freedom
ULS	Ultimate limit state
WMO	World Meteorological Organization

Nomenclature

ISO

a Height of the local loaded area

A Area of load patch

A_N Nominal contact area

A_0 Background area

A_L Local contact area

c Apparent keel cohesion

C_R Ice strength coefficient

e Keel porosity

F_1 Ice loads on one leg

F_c Action component due to the consolidated part of the ridge

F_k Keel action component

F_S Global force on a multi-legged structure

g Acceleration of gravity

h Ice thickness

h_1 Reference thickness of 1 m

k_j Ice jamming factor

k_n Non-simultaneous failure factor

k_s Mutual influence and sheltering effects factor

p_0^p is the background pressure

p_F Full thickness pressure load

p_G Global ice pressure averaged over the nominal contact area

p_L Local ice pressure load

w Width of the loaded area

w_L Width of the local loaded area

γ_e Effective buoyancy

γ_L Coefficient reflecting the vertical pressure distribution of the loaded area

μ_ϕ Passive pressure coefficient

ϕ Angle of internal friction

ρ_i Ice density

ρ_w Water density

IACS

a Span length

AF Hull area factor

A_{fn} Net cross-sectional area of flange

A_{pn} Net cross-sectional area of local frame

AR Load patch ratio

A_w Effective shear area

A_t Shear area from load effects

b Height of load patch

b_f Flange breadth

CF_C Crushing failure class factor

CF_D Load patch dimension class factor

D	Displacement [kt] of the structure
E	Modulus of elasticity
fa	Shape factor for the region considered
F	Force
h_{fn}	Net height of web plus flange
h_w	Web height
LL	Length of the loaded portion of the span
P	Pressure
P_{avg}	Average pressure
PFF_P	Peak pressure factor
Q	Line load
s	Stiffener spacing
t_c	Corrosion deduction
t_f	Flange thickness
t_{net}	Plate thickness required to resist the design ice load
t_{pn}	Net plate thickness
t_s	Additional thickness accounting for corrosion and abrasion
t_w	Web thickness
σ_{vM}	von Mises stress
σ_Y	Yield stress
w	Width of load patch
Z_p	Plastic section modulus

Z_{pt} Plastic section from load effects

φ_w Angle between web and the plate

FE theory

$\boldsymbol{a_j}$ Topology matrix for element j

$\boldsymbol{D}$ The plate stiffness containing the Young's modulus and the Poisson ratio

$\boldsymbol{k}$ Element stiffness matrix

K System stiffness

$\mathbf{K}$ System stiffness matrix

$\mathbf{K_I(r)}$ Incremental system stiffness matrix

r Displacement

$\boldsymbol{r}$ Global displacement vector

R   External load

$\mathbf{R}$ System load vector

$\mathbf{R}_{\text{int}}$ Internal reaction to the load

$\mathbf{R}_{\text{ref}}$ Fixed external load vector

$\boldsymbol{R^0}$ External load vector for the system

$\mathbf{S}$ Generalized nodal point force vector

$\boldsymbol{S^0}$ Nodal point forces for external load

$\boldsymbol{v}$ Nodal point displacements

$\boldsymbol{\sigma}$ Stress vector containing the normal stresses and the shear stress

σ_{P} Proportional limit

$\boldsymbol{\varepsilon}$ The strain vector containing the strains in the plane

ν Poisson ratio

λ is the loading parameter.

1   Introduction

As the time goes, the amount of easily accessible oil and gas decreases. As a consequence more and more eyes glance at the potential gold mines of the Arctic areas, where it is expected that vast amounts of oil and gas are located. Drilling in Artic ice-infested areas has been conducted for a couple of decades, at least in shallow waters near the shore. In the deep Arctic seas however, where floating offshore drilling units are required, there have not been that much activity. This is about to change, which results in a new set of engineering challenges.

Floating offshore drilling units will have to be designed according to the harsh arctic environment, where temperatures can be very low and ice-structure interaction might occur. In general, it is not economically feasible to design structures to withstand loads from the largest ice features, due to the enormous forces they represent. Therefore the structures operating in ice-infested areas often have some sort of ice management system, like e.g. an icebreaker in order to reduce the incoming ice loads. Still, the hulls of the structures must be designed to withstand the ice actions they may encounter.

For ships there are numerous standards giving rules for ice strengthening, but for column-based structures like semi-submersibles, which are well suited for deep sea drilling, there are currently none. As a consequence ship rules will have to be applied on these offshore structures. Also, in predicting accurate ice load there are challenges. The subject of ice loads is in general a very complex problem. The magnitudes of such loads depend on the type of ice, ice thickness, hull shape, whether the structures are fixed or floating, degree of ice management and more. There has been done considerable research on ice loads, due to its importance for structural design. Especially certain cases, such as e.g. level ice pushing against fixed vertical structures, have been considered in countless experiments. However, the results obtained are not suitable for all design scenarios.

In order to verify that the structures are designed and dimensioned to withstand the loads that comes with operation in ice-infested areas, structural analyses are required. Floating structures have mooring systems with a capacity that is critical not to exceed. In addition, the local resistance of the hull must be large enough to withstand the local loads from the ice.

Objective and Main Scope of Work

In this thesis the main objective is to perform a structural analysis of a semi-submersible exposed to local ice loads. The structure that will be analyzed is an ice belt as part of a larger column. Odfjell Drilling has provided drawings and information on the semi-submersible drilling platform *Deepsea Stavanger*, which is not design for arctic conditions, to the extent that a realistic model can be created.

The main scope of work presented in the thesis consists of the following efforts:

a) Giving an introduction to the subject of ice, from an engineering point of view, in form of a summary on different types of floating ice, ice properties and ice mechanics.

b) Performing a study on ice loads, with emphasis on local loads. This includes aspects of ice loads that should be considered and relevant load formulations for the semi-submersible platform.

c) Applying structural requirements, in terms of ice strengthening, to the hull structure of the semi-submersible.

d) Modelling an ice belt as part of a larger platform column in Abaqus.

e) Summarizing the Finite Element Method, in terms of linear and nonlinear theory, and how this is implemented in Abaqus.

f) Performing nonlinear static analyses of the ice belt model by use of Abaqus.

2   Floating Ice

Floating ice is the type of ice that poses a risk to floating offshore structures in polar waters. The reason for that is that it in many cases represents high loads on the structures, which unless dimensioned for may lead to catastrophes. In order to understand the loads that comes from the ice it is crucial to understand what kind of physical properties and mechanic behaviors it has. The aim of this chapter is to give this understanding, both of the ice itself and what it represents.

However, in order to follow the countless pages of information, discussions and elaborations in the material presented in this thesis, it is important to know the names of different types of floating ice. Therefore this chapter starts with a sub-chapter on nomenclature.

2.1 Nomenclature

Floating ice is divided into two main types which have different origins; sea ice and icebergs (ISO:19906, 2010). In World Meteorological Organization (1970-2014) the internationally accepted definitions of these ice types are given. Sea ice is defined as ice found at sea that consists of frozen sea water. It is common to separate sea ice into fast ice, drift ice and pack ice. Fast ice is ice that is formed along land and stays fast to the land. Drift ice is all sea ice that is not fast ice, while pack ice is high-concentrated drift ice. Icebergs are floating glacier ice which originates from land or ice shelves.

To get an overview of the different types of ice and ice features Table 2.1 was created. All definitions, except from *broken ice* which is an industry term, are found in World Meteorological Organization (1970-2014).

Table 2.1 – Types of ice and ice features

Name	Description	Thickness/Dimension
Nilas	Thin elastic crust, easily bending on waves and swell and under pressure	< 10 cm
Young ice	Ice in the transitions stage between nilas and first-year ice	10 cm to 30 cm

First-year ice	Ice that has not lived to see the first melting season	30 cm to 2 m
Second-year ice	Ice that have survived only one melting season	Normally up to 2.5 m
Multi-year ice	Ice that have survived more than one melting season	> 2.5 m
Ice sheet	Simply a sheet of ice	
Ice floe	An ice floe is a piece of ice broken off from an ice sheet	
Broken ice	Pack ice or ice floes	
Level ice	Ice that have undeformed top and bottom surfaces	
Raft ice	Ice sheets or floes that have slid on top of each other	
Ice ridge	When ice sheets or floes have driven against each other, the edges has broken due to compression and ridges up between the colliding sheets or floes	
Hummocks	An ice ridge that has stretched out in the orthogonal horizontal as well	
Rubble field	An area of extremely deformed sea ice of unusual thickness. Formed by the motion of drift ice against, or around an obstruction.	
Bergy bit	A large piece of floating ice of land origin	Showing less than 5 m above sea-level. No more than 20 m long

2.2 Properties

Just as all other materials the ice has properties. In order to understand why the properties of ice are the way they are, it can be important to know how ice are structured. In this subchapter the structure of sea ice will be described to a useful level. It will also be elaborated on some special properties that ice has. Material in this sub-chapter is mainly collected from Sanderson (1988) and Palmer and Croasdale (2013). Material found from other sources are referenced to in the text.

2.2.1 Structure

There are at least nine known structures of ice. However, only one of these are stable under natural conditions and thus of interest in this thesis. The stable ice structure is called *ice Ih* and has the molecules have a hexagonal structure. In order to understand why *ice Ih* has this structure one must look at what it is created from, namely liquid water. Water molecules forms approximate tetrahedral systems, and the hexagonal structure is more or less a repeated tetrahedral, ordered structure. Figure 2.1 illustrates this difference in molecular structures between liquid water and *ice Ih*. It can be seen that there is more space between the *ice Ih* molecules than the liquid water molecules, this is the reason why ice is less dense that water.
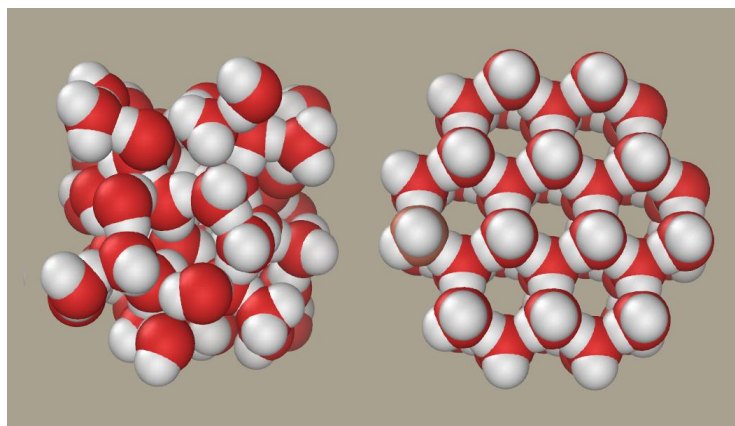
Figure 2.1 – The structure of liquid water and ice Ih (Wikipedia, 2015).

Another feature of the *ice Ih* structure is that it is formed in layers called basal planes. Each oxygen atom has three bonds within one basal plane. Across to another basal plane however, this oxygen atom has only one bond. This has consequences when the ice is to grow; it is easier to add atoms to an existing basal plane than to start growing a new one. Another consequence of this layer structure is that the ice is easier to deform parallel to the basal planes since the

deformations disrupts much fewer bonds that way, compared to deformation across the basal planes.

2.2.2 Growth

Freshwater and sea ice do not freeze in the exact same way. This is due to the density and salinity of the water. Freshwater has a maximum density at +4°C, saltwater however, becomes denser as temperature approaches the freezing limit of the water.

Say a lake of freshwater has a temperature of +8°C and the air temperature is -2°C. As the surface temperature of the lake approaches the temperature of maximum density, the surface water will sink and the warmer water, originally below the surface, will rise to the surface. This process of water mixing will carry on until the whole water column is +4°C. As the temperature of the surface water decrease further, the density will also decrease, keeping the surface water at the surface, where it eventually will freeze.

For saltwater it is required even colder conditions for ice to be formed. Since saltwater becomes denser as the temperature approaches the freezing limit, the entire water column must reach freezing temperature for ice to grow. Standard saltwater, i.e. water with a salinity of 35 ppt, has a freezing temperature of -1.91°C. So, there are both lower temperatures required, as well as more water to be cooled, in order for a given volume of saltwater to freeze than for the same volume of freshwater to freeze.

2.2.3 Density and Salinity

Water, unlike most other materials, expands when it freezes. The reason is, as explained in section 2.2.1, that there more space between the molecules in ice than in water. This is important because it is the reason why ice floats. Theoretical density of pure ice (Michel, 1978) is given in (2.1).

$$\rho_{Pure\ Ice} = 0.9166\ ton/m^3 \tag{2.1}$$

The density of the sea ice will differ slightly from the density of pure ice due to the salinity of the water. The effect of salt water in the ice will be discussed in the next paragraph, but sea ice density is given as a value between 0.915-0.920 ton/m³. From an engineering point of view, the difference in density between pure ice and sea ice is more or less negligible.

When working with sea ice it is important to realize that it is not much salt in the solid ice itself. If sea ice is melted down the resulting water will have a salinity of 5-10 ppt. The rest of the salt can be found small fluid pockets which are called brine pockets. These brine pockets are located between the columnar crystals. There is written more about columnar crystals in section 2.2.4. The pockets will weaken the sea ice compared to the freshwater ice which does not contain any salt. However, as the ice ages the brines slowly find their way out of the ice. This means in general; the older the ice is, the lower salinity it has. This is why older ice in general represents much larger loads than the new ice.

2.2.4 Anisotropy of Ice

Ice is an anisotropic material, i.e. it does not have the same properties in all directions. This can be explained by looking at the structure of the ice. If we look at Figure 2.2, which shows the structure of an ice sheet, we can see that it can be divided into three zones. The top zone is a fine-grained zone where the ice crystals are randomly orientated. The middle zone is a transition zone. These zones are obviously isotropic. The bottom zone is the columnar zone, and consists of columnar crystals. These crystals, which have small horizontal dimensions compared to the vertical, stretch over most of the ice thickness. Therefore, it is this zone that is decisive in determining the properties of the ice sheet. In the columnar zone, often called *columnar ice*, the crystals often have their horizontal axis randomly distributed in the horizontal plane. That is due to the different currents the ice has been exposed to during its growth. The result of that is an ice sheet isotropic in the horizontal directions. Though, anisotropy between the vertical direction and the horizontal directions are clear (Reddy & Swamidas, 2014).
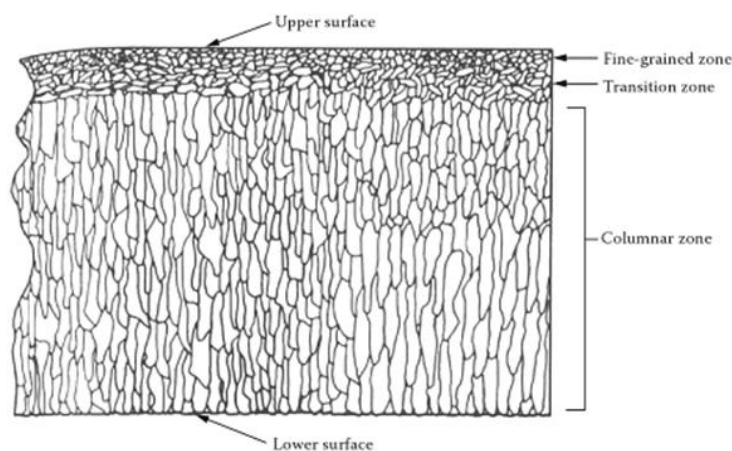
Figure 2.2 - Structure of an ice sheet (McClelland & Reifel, 1986).

2.3 Ice Mechanics

This subchapter aims to describe the mechanical behavior of ice and includes deformation types with corresponding failure modes, and mechanical properties.

2.3.1 General

When we look at ice from an engineering point of view it is sensible to describe it using the same expressions as for other solids, even though the ice itself has its own special characteristics. Ice mechanics is therefore a type of solid mechanics. That means that we do calculations for ice in the same way as we would for any other solid material, e.g. steel.

The mechanical behavior of ice is divided into two types of behaviors which are important to distinguish between. The first one is the *continuum behavior*, which the ice has in low stresses. When having this behavior it deforms elastic and/or plastic, but remains in one piece. The second behavior is the *fracture behavior* (called *brittle behavior* in Michel (1978)) which the ice has in high stress. When having this behavior the ice cracks and ultimately fractures.

What kind of behavior the ice has depends on its stress state, while the corresponding mode of failure is generally determined by the ice thickness and the geometry of the structure it interacts with.

2.3.2 Continuum Behavior and Corresponding Failure Modes

As stated above, ice can deform both elastically and plastically. However, it is not as easy to describe the deformations in ice as e.g. steel, since its deformation often is a combination of the two responses. At low stresses the ice immediately starts to deform both elastically and in creep, which is a type of plastic deformation. The deformation in creep exceeds the elastic deformation after a short time and is therefore more important to consider. The failure mode corresponding to elastic deformation is elastic buckling, but this mode is, according to Sanderson (1988), unlikely for ice with thicknesses larger than 0.5 m. The failure modes corresponding to creep behavior is creep and creep buckling. The creep buckling process is much like the creep process itself. It is a time-dependent process where the creep-rate increases as the load increases. The failure modes corresponding to continuum behavior are illustrated by Figure 2.3 and Figure 2.4, respectively. Creep behavior is generally unusual for ice interaction with vertical structures where other ice behaviors are more prominent (Palmer & Croasdale, 2013).
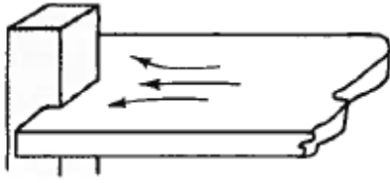
Figure 2.3 – Creep (Sanderson, 1988)   **Figure 2.4 – Buckling (Sanderson, 1988)**

2.3.3 Fracture Behavior and Corresponding Failure Modes

At high stresses ice is a very brittle material. This means that if the loads applied to the ice are high enough or act over a large enough time the ice may fail in a brittle manner, i.e. it may fracture. When ice is driven into an offshore structure fracture is the dominant mode of failure (Palmer & Croasdale, 2013). However, within fracture there are several different failure modes. We separate between bending (tensile fracture), crushing (compressive fracture), radial cracking and circumferential cracking (Sanderson, 1988). These failure modes are illustrated by Figure 3.3, Figure 2.5, Figure 2.6 and Figure 2.7, respectively.
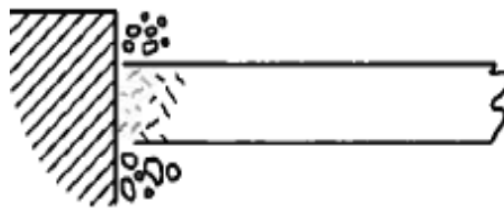
Figure 2.5 – Crushing (Sanderson, 1988)
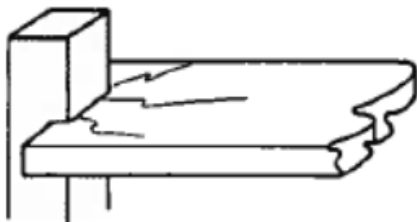
Figure 2.6 – Radial cracking (Sanderson, 1988)   **Figure 2.7 – Circumferential cracking (Sanderson, 1988)**
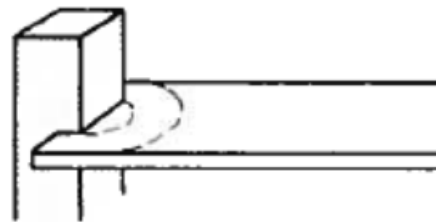
2.3.4 Mechanical Properties for Calculation of Ice Actions

The mechanical properties of sea ice depend on several different factors as e.g. temperature, salinity, density, structural orientation and thickness. But even if we have information on these factors the ice properties may vary from one part of an ice sheet to another. All numbers given in this section are found in Timco and Weeks (2010).

The most important mechanical properties of ice is the different kinds of strengths, because if one of the strengths are exceeded the ice fails. As stated earlier in this thesis, ice is an anisotropic material which means that it has different strengths in different directions, primarily in the horizontal and vertical direction. Tensile, compressive, flexural and shear strength are typical parameters in ice load calculations (ISO:19906, 2010) and therefore it is important to know what they represent.

Tensile strength is the capacity of a material to withstand stretching or pulling. This is a very important property of the ice. If the tensile strength is exceeded the ice will fail by fracturing. For a first-year sea ice sheet the horizontal tensile strength ranges from 0.2 MPa to 0.8 MPa, however, the vertical tensile strength may be up to three times higher. For multi-year sea ice the values for tensile strength ranges from 0.5 MPa to 1.5 MPa, with a tendency that strength in the vertical direction is higher than in the horizontal direction.

Compressive strength of ice is the capacity of the material to withstand loads that attempts to reduce its volume. If a compressive load on a piece of ice exceeds the compressive strength of the ice the ice will fail by fracturing. This strength, along with tensile strength, is the most important mechanical property of ice. Cracking and crushing of ice are the most common compressive failure modes in ice interaction with vertical offshore structures. In first-year ice the compressive strength normally is between 0.5 MPa and 5 MPa. Multi-year ice has approximately the same strength as first-year ice in very cold conditions (e.g. -20 °C). If the ice is warmer, however, it can be a lot stronger. The difference in compressive strength between "warm" first- and multi-year ice is due to the difference in brine volume in the ice.

Flexural strength, or bending strength, represents the highest stress in a deformed material before it fails. Ice sheets that is broken by icebreakers or sloped offshore structures, and in pressure ridge formation the ice, fails by bending. This is the reason why the flexural strength is an important parameter. In first-year ice the flexural strength ranges from up to 1 MPa, and

decreases as the brine volume increases. The strength of multi-year ice in winter ranges from 0.8 MPa to 1.1 MPa.

Shear strength of ice is the capacity of the ice in shear. In the cases of ice interaction with offshore structures ice failures in shear are not very common, as far as known today. However, stress conditions in these cases are often a combination between tensile and compressive stress and therefore it is important to consider the shear strength. The magnitude of shear strength is generally somewhere between 0.4 MPa and 1.1 MPa for different kinds of ice.

Even though there exists plenty of small scale measurements, and some full scale measurements, of the different kinds of strength, the true strengths of sea ice are hard to predict. This is due to all the factors that influence the ice and the measurements. For example floating ice is full of natural flaws and have different sizes and shapes, something that always will make a difference between realistic conditions and the conditions of a laboratory. Another factor is the complexity of the ice failure. The ice may fail in a combination of several different modes, something that is hard to register.

3 Aspects of Ice Loads

Loads from ice can in general be very high, in fact it can be the governing design criteria for structural design of offshore structures which are to operate in ice infested areas. This chapter aims to describe different important aspects and factors that influence ice loads and thus should be considered in load estimation.

3.1 Limiting Factors

As shown in Palmer and Croasdale (2013), rough calculations give reason for major concerns regarding the magnitude of ice loads in design. If we imagine a 2 meter thick level ice sheet with compressive strength of 5 MPa is driven against a vertical surface of an offshore structure with a water line length of 20 meter. By multiplying 5 MPa with the contact area of 40 m^2, we would get an ice force of 200 MN, or approximately 20 000 tons. However, as will be the topic of this sub-chapter, there are several factors that limits the magnitude of ice forces, making this calculation somewhat simpler than the reality. Information in this section is drawn from Løset and Gudmestad (2006) and Palmer and Croasdale (2013).

The limit stress scenario is when the stress in the ice reaches its capacity, or limit, and then collapse. It is then the capacity of the ice that limits the loads. The limit is either the tensile-, compressive-, flexural- or shear strength of the ice, which are described in section 2.3.4.

The limit force scenario is when the load applied to the structure is determined by the driving force of the ice. The driving force normally comes from wind and current. Such cases are when features like pressure ridges are being pushed against the structure by level ice. Then the loads are not determined by the strength of the ridge, but instead it is determined by the driving force applied to the ridge.

Limit momentum is a scenario where ice in motion interacts with the structure then loses its momentum. This is a common case when the kinetic energy of the ice does not suffice for the structure to penetrate it.

3.2 Size and Thickness Effects

A common perception about ice loads is that there is a dependence between force per area (pressure) and the contact area which have to be included in the load formulations. This effect is called the *size effect* or *area effect*. It is not certain if the effect is due to the size of the contact area, the aspect ratio of the contact area or a combination between the two of them. Seemingly, however, the ice generally fails for lower stresses for large areas than for small areas. This is elaborated on in Sanderson (1988).

In the later years this effect has been questioned, amongst other in Timco and Sudom (2013). There it is concluded that most of the data sources shows the pressure area effect, but not all. In addition, that other factors such as loading rate, failure modes, and physical and mechanical properties are in many cases far more important than *size effect* in determining load pressure.
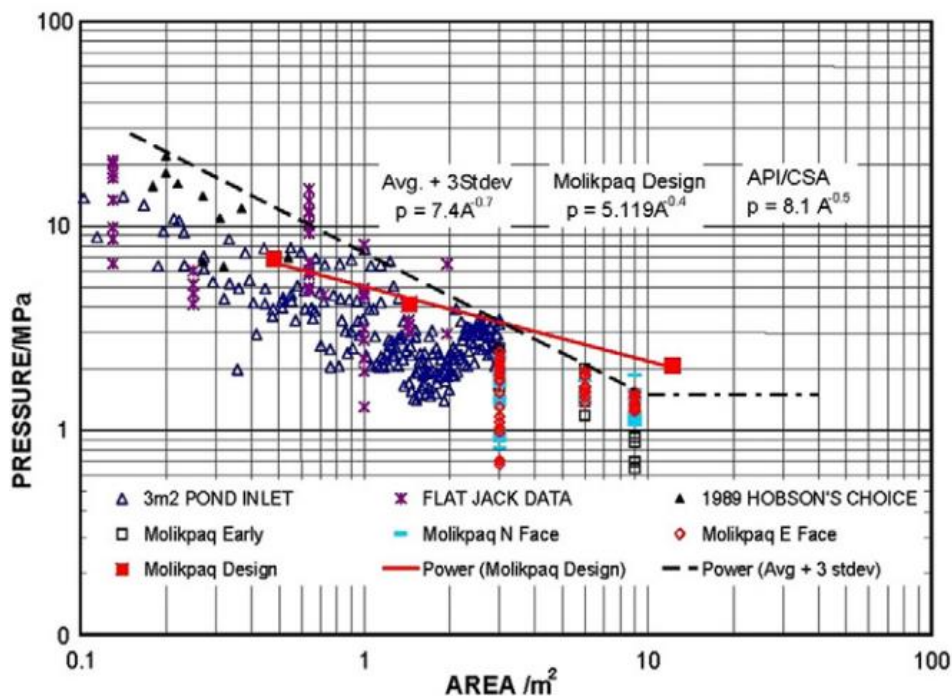
Figure 3.1 – Local pressure-area curve for fixed structures (ISO:19906, 2010).

The ice thickness is one of the most important parameters when calculating loads. An increase in ice thickness means an increase in load. Therefore it is important to know the ice thicknesses in areas where the offshores structure will be operating. Typical thickness of level ice in the western region of the Barents Sea is according to ISO:19906 (2010) approximately 1.5 m.

3.3 Vertical Structures versus Sloped Structures

As stated in section 2.3.1 the failure mode of the ice is determined by the ice thickness and the geometry of the structure it interacts with. If we look at structural geometry in the vertical plane, in the area of the structure where ice interaction might occur, there are especially two types which have been examined thoroughly in experiments; vertical structures and sloped structures. Ice interaction with the two types of structures represents different fracture mechanics and loads. References in this section are drawn from Palmer and Croasdale (2013), Løset and Gudmestad (2006) and Sanderson (1988).

For ice interaction with a vertical structure ice can show both continuum behavior and fracture behavior. If the ice is thin (approximately 0.4 m or less), slowly-moving and pushing against a vertical structure it will most likely fail by elastic buckling. If the ice is thicker it tends to crush. Crushing is generally the case that governs design and should therefore be given most attention. An important consequence of crushing is that high-pressure zones (hpzs) occur in the contact area between the ice and the structure, as well as there are other zones with little or no pressure at all. This is due to the irregular pattern of fracturing in crushing. The hpzs are important for the local ice load formulations given in ISO:19906 (2010).

Ice interaction with sloped structures normally ends with the ice failing in bending, i.e. fracture by circumferential or radial cracking. The two cracking patterns are important to separate since they can represent different loads. However, it is not straight forward to separate these because they usually appear one after the other. Which of the two cracking types that occurs first depends on the width of the structure and the thickness of the ice. Another factor that determine the loads on a sloped structure is rubble accumulation. The rubble introduces additional loads due to the weight of the rubble and friction forces between rubble and the surface of the structure.
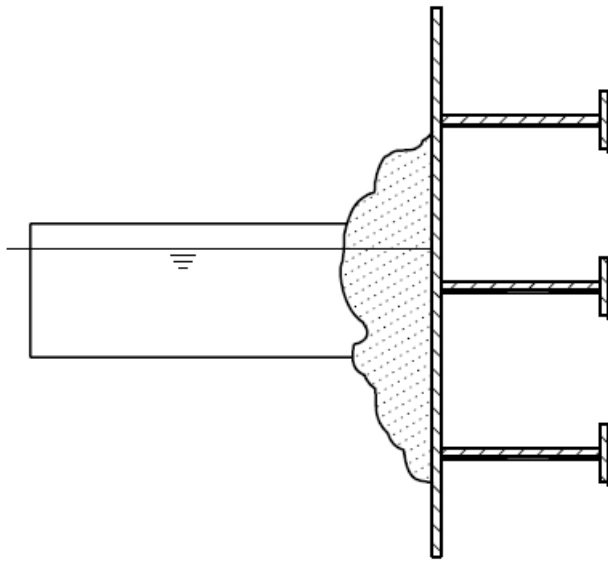
Figure 3.2 – Level ice interaction with vertical structure. Failure by crushing (ISO:19906, 2010).
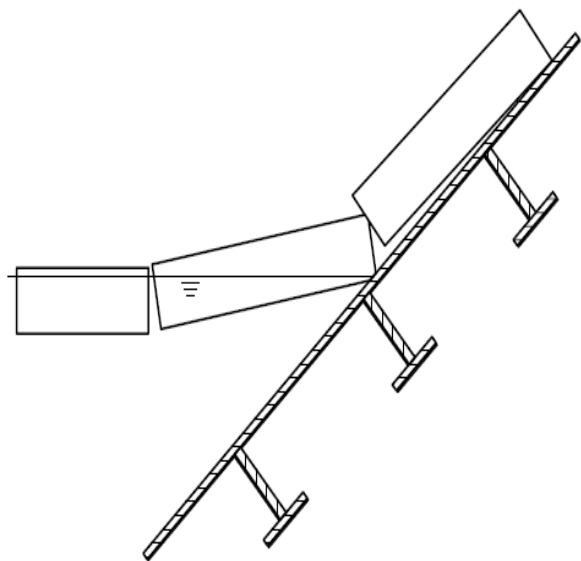
Figure 3.3 – Level ice interaction with a sloped structure. Failure by bending (ISO:19906, 2010).

In general, ice loads are significantly higher on vertical structures than on sloped structures. This is due to the respective failure modes of the ice when interacting with these types of structures. The effects of rubble accumulation on sloped structures reduces the difference in load between the two structures to some extent. Still, a sloped structure in the water line area is the most common option in design of arctic offshore structures.

3.4 Floating Hulls versus Fixed Structures

A floating hull structure will have a much larger response motion in the horizontal plane than a fixed one and therefore represents a more complex problem. As a consequence, dynamics have to be accounted for when considering ice loads. The ice loads on a floating structure may become amplified or decreased due to dynamics. The relative velocity between the structure and the ice is therefore important when determining loads.

According to Palmer and Croasdale (2013), a floater will not be designed for the worst case ice features in its operating area since the capacity of the stationkeeping system often are a limited factor. Thus some sort of ice management is expected to be required.

3.5 Ice Management

Ice management is defined as all actions that have the aim of reducing or avoid ice loads. It includes among other things ice surveillance, towing of icebergs, ice breaking and disconnection of the offshore unit. Surveillance involves detection, monitoring and forecasting. As mentioned in sub-chapter 3.4, a floating unit designed to operate in ice-infested areas is expected to have some sort of ice management. This section is based on information drawn from Palmer and Croasdale (2013).

Managed ice generally represents lower loads than unmanaged ice, since the managed ice is often broken into smaller pieces by accompanying icebreakers. Interactions with icebergs are, in theory, also avoided. However, to have an idea about the order of magnitude loads from unmanaged ice might be smart to study since it represents an upper limit of how high the loads can become. In addition the ice management can fail, resulting in loads from unmanaged ice on the floating structure.

When determining ice loads from managed ice the following factors should be considered; ice concentration, ice thickness, pressured ice and floe size. Concentration of the drift ice affects the loads on moorings significantly. The strength of the ice is important for the ice management systems, but not for the floating structure itself if the managed ice already are broken into pieces. The thickness that is important is the thickness of the ice floes and rubble fields. Pressured ice can increase loads significantly, however, it can also be handled by the ice management system.

Figure 3.4 - Lunskoye-A with an icebreaker (Sakhalin Energy, 2014)

3.6 Multi-legged structures

Ice loads on multi-legged structures can be quite complex. According to Løset and Gudmestad (2006) the following effects characterize the ice loads on such structures:

- Mutual influence of legs
- Sheltering and jamming effects
- Non-simultaneous maximum loads on legs

Mutual influence of legs occurs due to short distance between the legs. The stress conditions in the ice changes when the ice interacts with one leg before another. This influence depends largely on the diameter of the leg and the distance between them. If $Q/D > 5$ the mutual influence is negligible. Here Q is the distance between the legs and D is the diameter of the legs.

Sheltering is when a leg "shelters" another leg from the ice by creating a track of broken ice. For a rectangular, four-legged structure, this happens when the ice is driven towards the structure in the longitudinal or transverse direction. Jamming is when ice is jammed between the legs. This effect may cause an increased effective width of the structure by blocking for ice to pass through in between the legs. Examples of this are when ridges get stuck or when rubble accumulates in the area between the legs.
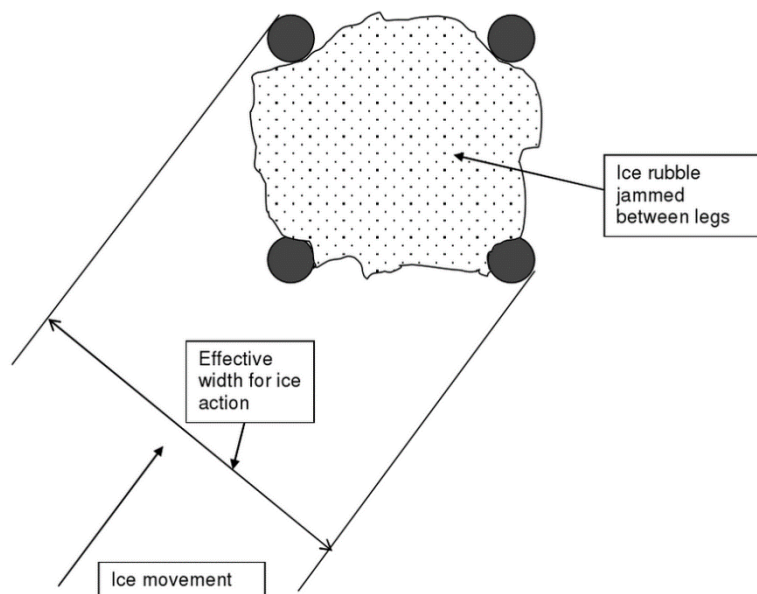
Figure 3.5 – Jamming effect causing increased effective width (Palmer & Croasdale, 2013).

Some experiments on multi-legs show that maximum load rarely is reached on several legs simultaneously. This means that the maximum global load and maximum leg load have different probability of occurrence. However, studies on the subject are limited and it should be further investigated.

4   The Semi-Submersible Drilling Unit

Column-based semi-submersible drilling units designed for ice-structure interaction are increasing in numbers. Their flexibility and mobility, combined with better solutions for dealing with the environmental challenges the Arctic represents makes them more relevant than ever.

In this thesis the structural response of an ice-belt of a semi-submersible's column exposed to local loads is investigated. The ice-belt is a modified and adapted version of a part of the aft port side column of Odfjell Drilling's semi-submersible drilling rig *Deepsea Stavanger*. *Deepsea Stavanger* is a four-columned platform which is not strengthened for ice, so some modifications, in terms of ice strengthening the original design, are required. Odfjell Drilling has provided column-stringer drawings and main particulars of the drilling rig. This is sufficient information in order to create a realistic model.

Figure 4.1 – Deepsea Stavanger (Offshore Energy Today, 2013).

Main dimensions of the ice belt are given in Table 4.1, Figure 4.2 gives an overview of where the ice belt is located, while Figure 4.3 is the drawing of the stringer plate of the ice belt. In the stringer drawing there is some structure which is a part of the mooring system. This structure is not considered when modelling the ice belt, since it is not ideal for it to interact with ice.

Table 4.1 – Main dimensions of ice belt

Length	18.4 m

Width	14.4 m
Corner Radius	3.2 m
Height	5 m
Frame Span	2.5 m

The ice belt part consists of outer shell plating with stiffeners, bulkheads and a stringer plate with stiffeners and brackets. The operational draught of the semi-submersible is 23 m and the stringer in the middle of the ice belt is located 22.5 m above the bottom of the pontoons. Since the stringer is in the middle of the ice belt height this means that the water line under normal operations will be 3 m above the bottom, and 2 m below the top of the ice belt.

----- Stiffener   - - - - Bulkhead
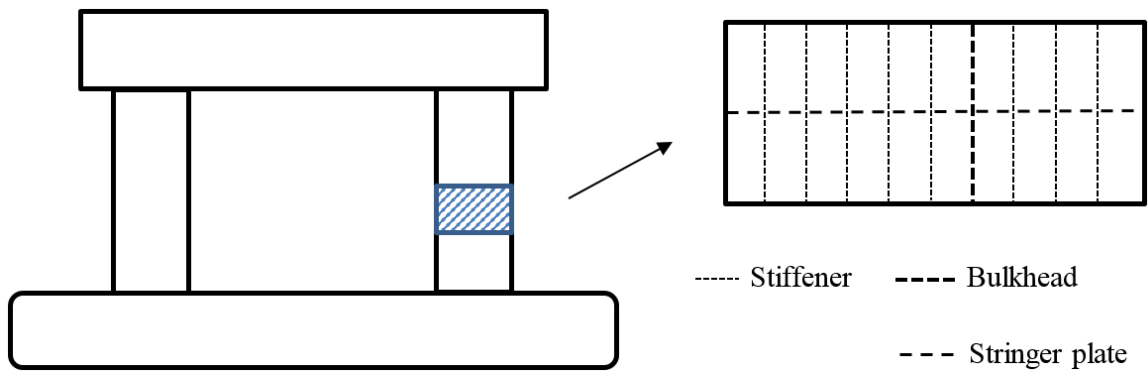
- - - Stringer plate

Figure 4.2 – The ice belt part of the column.
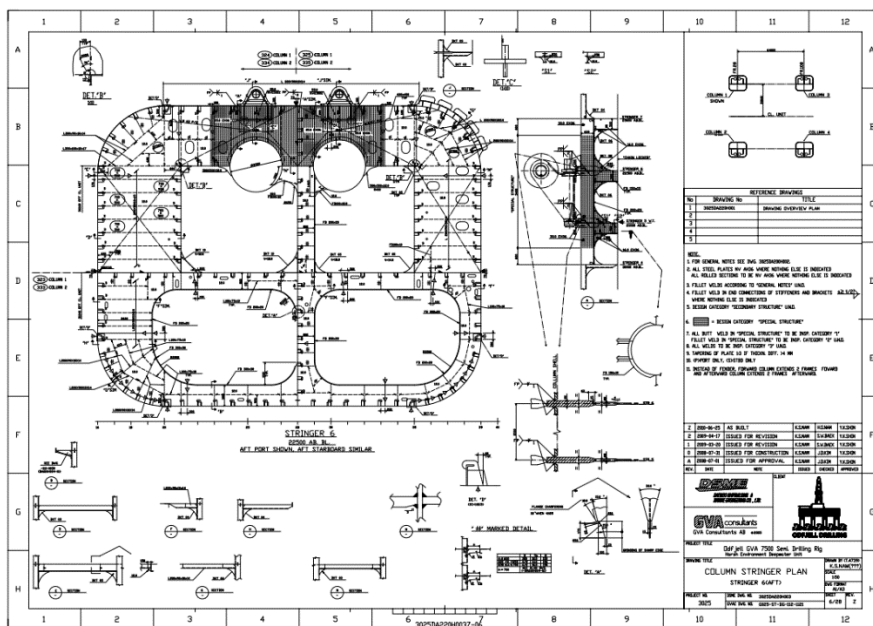
Figure 4.3 – Drawing of the stringer plate in the middle of the ice belt provided by Odfjell Drilling (Adapted from Appendix A).

5 Methods for Calculating Ice Loads on Floating Structures

In order to design hull structure for marine structures that is to interact with ice, knowledge about ice loads are required. In this chapter some different methods for calculating ice loads are presented. It should be noted that the methods for load calculation presented in this chapter are only some of the methods existing out there. The formulas given are for deterministic design only and are based on measurements and experiments. The reason for not covering probabilistic methods in this thesis is that they require a lot of data in order to be accurate.

5.1 General

Ice loads are generally described as forces or pressures acting over an area. Before going into details of calculation methods there are four terms that must be understood and separated. These are:

- Static loads
- Dynamic loads
- Global loads
- Local loads

Static loading is when there is stationary contact between the ice and the structure e.g. if an ice sheet is slowly pushing against the structure or a large ice feature is stuck to the structure while environmental forces drives the feature against the structure.

Dynamic ice loads are generally impact loads, e.g. the loads from large ice features with a certain velocity that hits the structure.

It is also a good idea to separate between global and local loads depending if we want to examine the structure in total or only parts of it, like in this thesis.

Global loads are especially important when considering overall motions and stability of offshore structures. For example when designing mooring system it is crucial to make sure that the capacity of the system is larger than the global loads the structure may be exposed to.

Local ice loads are important when only parts of a structure is to be studied. In design of hull scantlings for operations in the Arctic one should use local pressure as design load. Local ice loads from ice-structure interaction are highly irregular and very hard to model exact. Therefore local ice loads are often idealized as uniform pressure acting over a rectangular patch of area. Using this method makes the loads easier to model in structural analyses.

5.2 ISO 19906

Information in this sub-chapter is gathered from ISO:19906 (2010).

The International Organization of Standardization (ISO) is a non-governmental organization and the world's largest developer of voluntary International Standards. The organization has 163 national members which all have the right to be represented on a technical committee of a certain subject, if such a committee has been established. The technical committees prepare the International Standards and the publication of such standards requires that 75 % of the national members that votes on it approves. The overall aim of International Standards is that products and services are safe, reliable and of high quality.

ISO 19906 is the International Standard for Arctic offshore structures and is a part of a series of standards for offshore structures. In addition to provide a vast amount of useful requirements, information, technologies, recommendations and methods for offshore structures in Arctic areas, it also holds the same about ice properties, ice loads, ice-infested areas and more.

The standard is somewhat open in order to not hinder innovation and should therefore be used in combination with sound engineering judgement. In places where there are uncertainties the standard recommends conservative approaches and methods.

All pressures, forces and areas given in this subchapter are in MPa, MN and m^2 respectively.

5.2.1 Global Loads

In this section some methods for calculating global ice loads on vertical structures are given. The reason for including methods for global loads in this thesis is that global pressure is input in formulations considering the combination between global and local loads as in section 5.2.2.3.

Area of a load patch, or *contact area*, is given by (5.1):

$$A = b \times w \qquad (5.1)$$

Where

h is the ice thickness

w is the width of the loaded area

5.2.1.1 Pressure from sea ice acting against vertical structures

This method is based on full-scale measurements of fixed structures and aims to determine the upper bounds of global ice pressures from first- and multi-year ice.

$$p_G = C_R \times (\frac{h}{h_1})^n \times (\frac{w}{h})^m \qquad (5.2)$$

Where

p_G is the ice pressure averaged over the nominal contact area

C_R is the ice strength coefficient, equal to 2.8 MPa for Arctic areas

h_1 is a reference thickness of 1 m

h is the ice thickness

n is a coefficient, equal to -0.5+h/5 for h < 1.0 m, and -0.3 for h > 1.0 m

m is a coefficient equal to -0.16

5.2.1.2 First-year ridges

This section describes a method for calculating the loads from first-year ridges. The motivation for this is that for sea areas with only first-year ice, ridge-structure interaction often represents the governing design scenario.

Horizontal load is determined by (5.3):

$$F_R = F_c + F_k \qquad (5.3)$$

Where

F_c is the action component due to the consolidated part of the ridge

F_k is the keel action component

$$F_c = p_G \times A_N \qquad (5.4)$$

Where

p_G is the ice pressure averaged over the nominal contact area in MPa

$$F_k = \mu_\phi \times h_k \times w \times \left(\frac{h_k \mu_\phi \gamma_e}{2} + 2c\right) \times \left(1 + \frac{h_k}{6w}\right) \tag{5.5}$$

$$\mu_\phi = tan\left(45° + \frac{\phi}{2}\right) \tag{5.6}$$

$$\gamma_e = (1 - e) \times (\rho_w - \rho_i) \times g \tag{5.7}$$

Where

μ_ϕ is the passive pressure coefficient

ϕ is the angle of internal friction

c is the apparent keel cohesion (average value over the keel volume shall be used)

w is the projected width of the structure in meters

γ_e is the effective buoyancy. Units shall be consistent with c

e is the keel porosity

ρ_w is the water density

ρ_i is the ice density

g is the acceleration of gravity

Data on these parameters are available in the standard. Regarding loads from multi-year ridges the procedure given is the same. Multi-year ridges will in general be bigger and stronger, thus representing higher loads, than first-year ridges.

5.2.1.3 Multi-legged structures

An alternative for calculating global loads on multi-legged structures are by use of (5.8). As can be seen, this formula accounts for the effects elaborated on in sub-chapter 3.6. The resulting loads from this approach are smaller than the number of legs multiplied with one leg-load.

$$F_S = k_s \times k_n \times k_j \times F_1 \tag{5.8}$$

Where

F_1 is the ice loads on one leg

k_s accounts for mutual influence and sheltering effects

k_n accounts for non-simultaneous failure

k_j accounts for ice jamming

5.2.2 Local Loads

The local pressures given in this section are the full thickness local pressures and local pressures for large ice features.

Area of a local load patch, or *local contact area*, is given by (5.9):

$$A = a \times w_L \tag{5.9}$$

Where

a is the height of the loaded area

w_L is the width of the loaded area

5.2.2.1 Thin first-year ice

The formulas described in this section are for determining local pressure from level ice, rafted ice and consolidated layers of first-year ridges and are valid for ice thicknesses for up to approximately 1 meter. (5.10) and (5.11) are based on data from the Gulf of Bothnia, while (5.12) is to be used in cases where ice thickness is an unknown.

$$p_F = 2.35 \times h^{-0.5} \qquad for\ h > 0.35m \tag{5.10}$$

$$p_F = 4 \qquad for\ h \leq 0.35m \tag{5.11}$$

Where

p_F is the full thickness pressure in MPa

h is the ice thickness

$$p_L = \gamma_L \times p_F \tag{5.12}$$

Where

p_L is the local full thickness pressure

p_F is the full thickness pressure in MPa

γ_L is a coefficient reflecting the vertical pressure distribution of the loaded area, A, and is set to be 2.5

Figure 5.1 is meant to illustrate the loading area, as a part of an ice sheet, and the pressure distribution over the thickness of the ice.

a) Loaded area   b) Pressure distribution
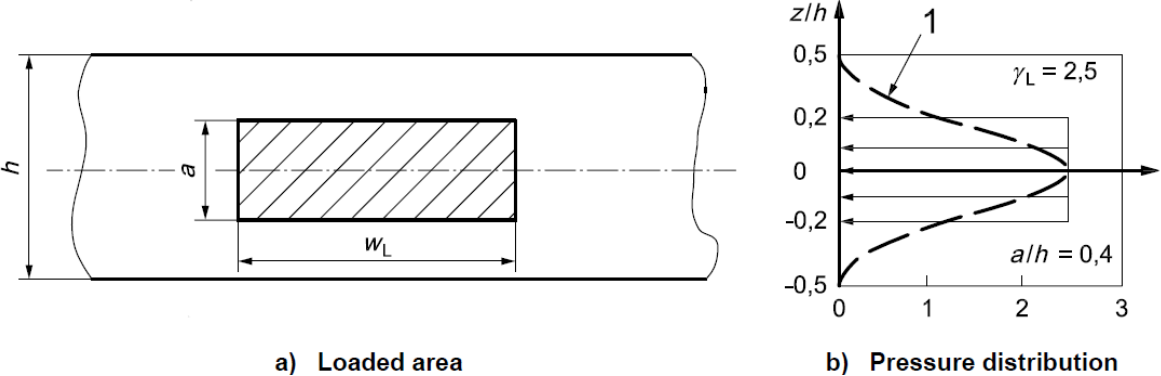
Figure 5.1 – Local pressure distribution on the loaded area. Adapted from ISO:19906 (2010).

5.2.2.2 Local pressure for thick, massive ice features

Local pressure loads due to interaction with ice features with thickness over 1.5 m can be determined by the following equations:

$$p_L = 7.40 \times A^{-0.70} \qquad for\ A \le 10m^2 \qquad\qquad (5.13)$$

$$p_L = 1.48 \qquad\qquad for\ A > 10m^2 \qquad\qquad (5.14)$$

This method is based on full scale measurements from the bottom-founded Molikpaq platform and indentation tests in the Beaufort Sea. Figure 3.1 shows what results these formulas give. Since the method is based on results from fixed structures it may somewhat conservative for floating structures.

5.2.2.3 Ice Pressure Combinations

Local ice loads arise on structures at different locations for different contact areas over time. A way to account for this is to combine local and global pressures. This is done by applying a high local pressure over a small patch of area in combination with a lower background pressure acting over a much larger patch. Such a pressure combination is illustrated by Figure 5.2. The pressure acting over the large area is of course less than the real global pressure and can be found by use of (5.15).

$$p_0^p = \frac{p_0 \times A_0 - p_L \times A_L}{A_0 - A_L}$$

(5.15)

Where

p_0^p is the background pressure

p_0 is the global pressure

p_L is the local pressure

A_0 is the background area

A_L is the local contact area
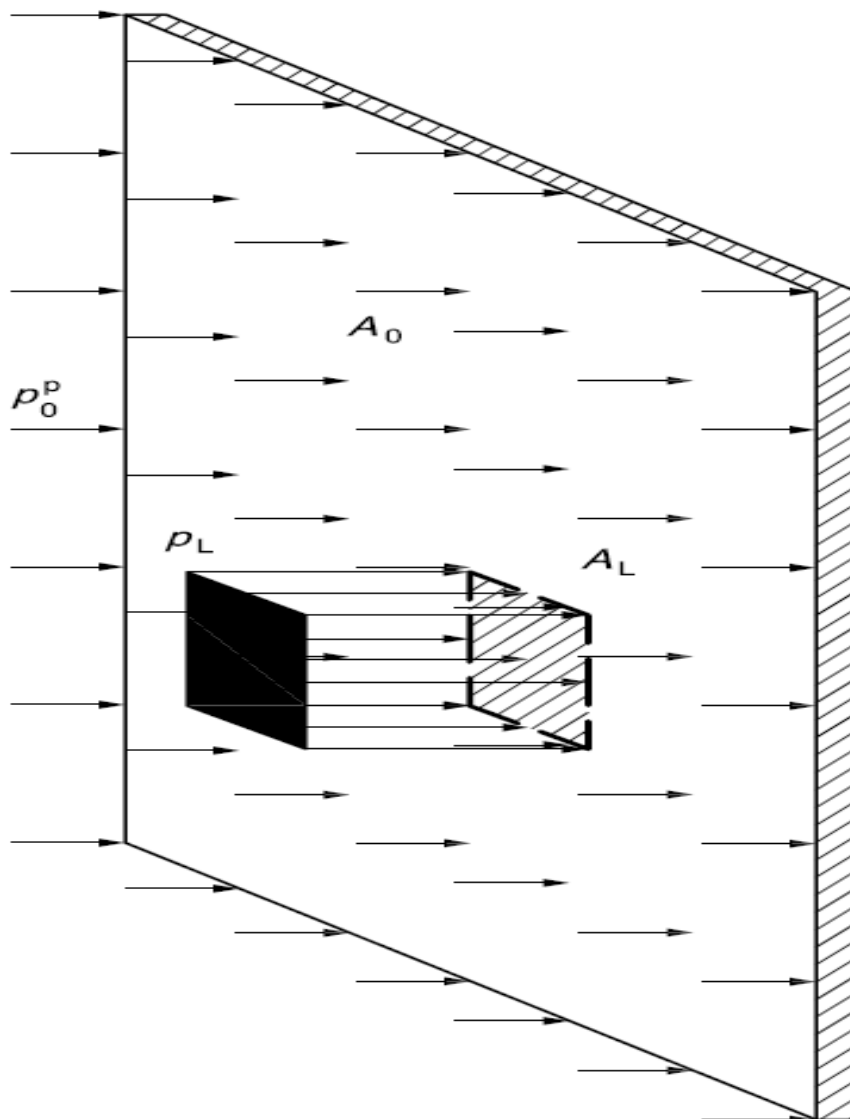
Figure 5.2 – Illustration of pressure combination (ISO:19906, 2010).

5.3 IACS

The International Association of Classification Societies (IACS) is a non-governmental organization. It consists of twelve member classification societies, and has a consultative status with the International Maritime Organization (IMO). IACS was founded in 1968 by seven leading classification societies who wanted to combine their knowledge and experience. Today, IACS develops and applies among other things; rules, recommendations and requirements with the aim of making ships safer while taking care of the environment.

Requirements Concerning POLAR CLASS, hereafter referred to as *Polar Code*, is IACS's unified requirements for steel ships intended to navigate in ice-infested waters. This document contains structural and machinery requirements and has been applied in this thesis due to the lack of any such standards, with structural requirements, for Arctic offshore structures. The dimensioning procedure is covered in Chapter 6, however, the procedure for calculating the design load is shown in this sub-chapter. The calculated design load for the ice belt structure is given in the end of this sub-chapter.

5.3.1 Polar Class

The first thing to do when designing according to the *Polar Code* is to decide which class the structure shall have. Table 5.1 gives a guidance of the different polar classes and their corresponding ice conditions. When choosing class there is a tradeoff made. Higher classes means a heavier and more expensive structure, while lower classes means that the structure may not be fit to operate in certain relevant areas or at certain times of the year. For a floating unit, the class selection also depends on the ice management system. If loads are reduced, the required class is lower. For the structure considered in this thesis Polar Class 4 (PC4) is chosen. The operation area, time of year for operation and ice management system for the structure are not specifically defined and therefore a flexible class is selected.

Table 5.1 – Polar Class Descriptions (IACS, 2011)

Polar Class	Description
PC 1	Year-round operation in all Polar waters
PC 2	Year-round operation in moderate multi-year ice conditions
PC 3	Year-round operation in second-year ice which may include multiyear ice inclusions.
PC 4	Year-round operation in thick first-year ice which may include old ice inclusions
PC 5	Year-round operation in medium first-year ice which may include old ice inclusions
PC 6	Summer/autumn operation in medium first-year ice which may include old ice inclusions
PC 7	Summer/autumn operation in thin first-year ice which may include old ice inclusions

5.3.2 Design Load

The design scenario for ships in ice is an impact to the bow. For a floating offshore unit the potential impact from an ice feature is likely to be of smaller magnitude than the impact design load for a ship, since ships have forward speed. For this reason, it may be that the loads estimated, by use of the procedure given in *Polar Code*, are higher than the corresponding ice loads on a semi-submersible in similar conditions.

The design load itself is characterized by a uniform average pressure acting on a rectangular patch of area. The procedure for determining the design load for the hull scantlings is as follows:

Force, *F* is calculated by:

$$F = fa \times CF_C \times D^{0.64} \text{ [MN]} \tag{5.16}$$

Where

fa is a shape factor for the region considered

CF_C is a crushing failure class factor

D is the displacement [kt] of the structure. The specified minimum value is 5 kt

The load patch ratio is given by:

$$AR = 7.46 \times sin(\beta') \geq 1.3 \tag{5.17}$$

Where

β' is the normal frame angle of the region considered. For a vertical wall the angle is zero.

Line load, Q:

$$Q = \frac{F^{0.64} \times CF_D}{AR^{0.35}} \left[\frac{MN}{m}\right] \tag{5.18}$$

Where

CF_D is a load patch dimension class factor

Pressure, P:

$$P = F^{0.22} \times CF_D^2 \times AR^{0.3} \text{ [}MPa\text{]} \tag{5.19}$$

Design load patch, w and b:

$$w = \frac{F}{Q} \text{ [}m\text{]} \tag{5.20}$$

$$b = \frac{Q}{P} \text{ [}m\text{]} \tag{5.21}$$

Where

w is the width of the load patch

b is the height of the load patch

Average pressure, P_{avg}:

$$P_{avg} = \frac{F}{b \times w} \text{ [MPa]} \tag{5.22}$$

Application of this procedure has resulted in the local design load condition given in Table 5.2. Calculations of the design load can be found in Appendix B. This condition is further used as input in the dimensioning.

Table 5.2 – Calculated Local Design Load Condition

w	1.70 m
b	1.31 m
P_{avg}	3.41 MPa

Unfortunately the design load and load patch, presented in Table 5.2, are smaller than what they should have been. During the calculations the author took the ship displacement, D [kt], for being the ship velocity in knots, instead of the weight of displaced water in kilotons which is the correct input. The consequence of this is that the design load is too low. As a consequence the dimensions calculated, which are based on this design load, are also smaller than they should be. This has led to a structure which is not as strong as it should have been, a fact that one should have in mind when looking at the results from the analyses, presented in Chapter 9. This mistake was discovered in the end of the thesis writing, i.e. after the model was created. Correcting this error in Abaqus was in this case impossible without redoing most of the work that was already done in the model. For this reason it was considered as too late to correct.

5.4 Other Methods

This sub-chapter contains methods for calculating ice loads which are not given in *ISO 19906* or the *Polar Code*. Only local loads are considered here.

5.4.1 CSA code

According to Palmer and Croasdale (2013) the Canadian (CSA) code, which is an Arctic standard, recommend (5.23) and (5.24) for ice crushing for low aspect ratio (h/w). This implies

that the following equation is valid for ice loads, acting over low and wide contact areas, in the Arctic:

$$p_L = 8.5 \times A^{-0.50} \qquad for\ A \leq 10m^2 \qquad (5.23)$$

For Sub-Arctic areas, since the ice there is generally weaker, they recommend a slightly lower load:

$$p_L = 4.2 \times A^{-0.40} \qquad for\ A \leq 10m^2 \qquad (5.24)$$

5.4.2 Palmer & Croasdale

Palmer and Croasdale (2013), on the other hand, recommends combination between of the CSA and ISO approaches when it comes to ice crushing. The following equation is valid for level ice thickness up to 2 m thick and first year ridges:

$$p_L = 4.8 \times A^{-0.50} \qquad for\ A \leq 10m^2 \qquad (5.25)$$

5.5 Design Contact Areas

The design contact areas are the areas of the structure where the loads will have the largest effect. In local structural analysis, these areas are the placement of loading that is critical for the structural components of the structure analyzed. Finding these areas are crucial in order to ensure that the most critical loading conditions are addressed.

For the structure analyzed in this thesis the loads must be placed separately on areas that are critical for the shell plate, the stiffeners, the bulkheads and the stringer plate. *ISO 19906* does not give a specific procedure for determining the critical contact areas, since there exists so many different structural configurations out there. Thus it recommends a trial and error process in order to find the critical conditions. This is where common engineering sense should be used and therefore Figure 5.3 was created. Figure 5.3 is meant to illustrate where the author believes the most critical contact areas are for the different structural components.
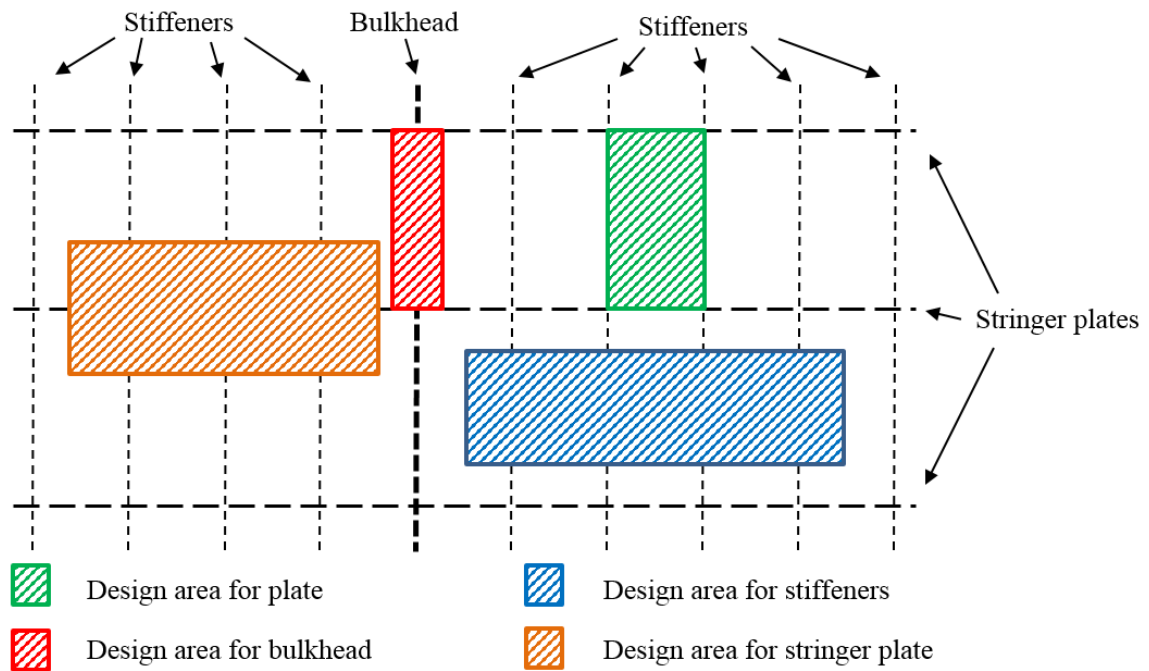
Figure 5.3 - Contact areas addressing critical loading conditions for structural components.

5.6 Discussion, Comparison and Final Selection

Local ice loads are generally hard to predict. There are few methods for calculating such loads, and those methods that are out there, are generally based on full-scale measurements of fixed structures. Global ice loads on fixed structures are generally larger than those on floating structures, but the difference in local loads however, are more uncertain. So, in order to be on the safe side, a conservative load should be applied.

Due to ice management the ice which reaches a floating structure, such as the semi-submersible drilling unit, is normally broken with some larger floes and possibly multi-year or glacial ice. It is then sensible to believe that the design loads will be from multi-year or glacial ice that has slipped through the ice management in some way (ISO:19906, 2010). If the design loads are from multi-year or glacial ice the local pressure from section 5.2.2.2, 5.4.1 and 5.4.2 may be all suitable as local design pressure. These loads are plotted in Figure 5.4 for comparison, while the comparison is given in numbers in Appendix C.
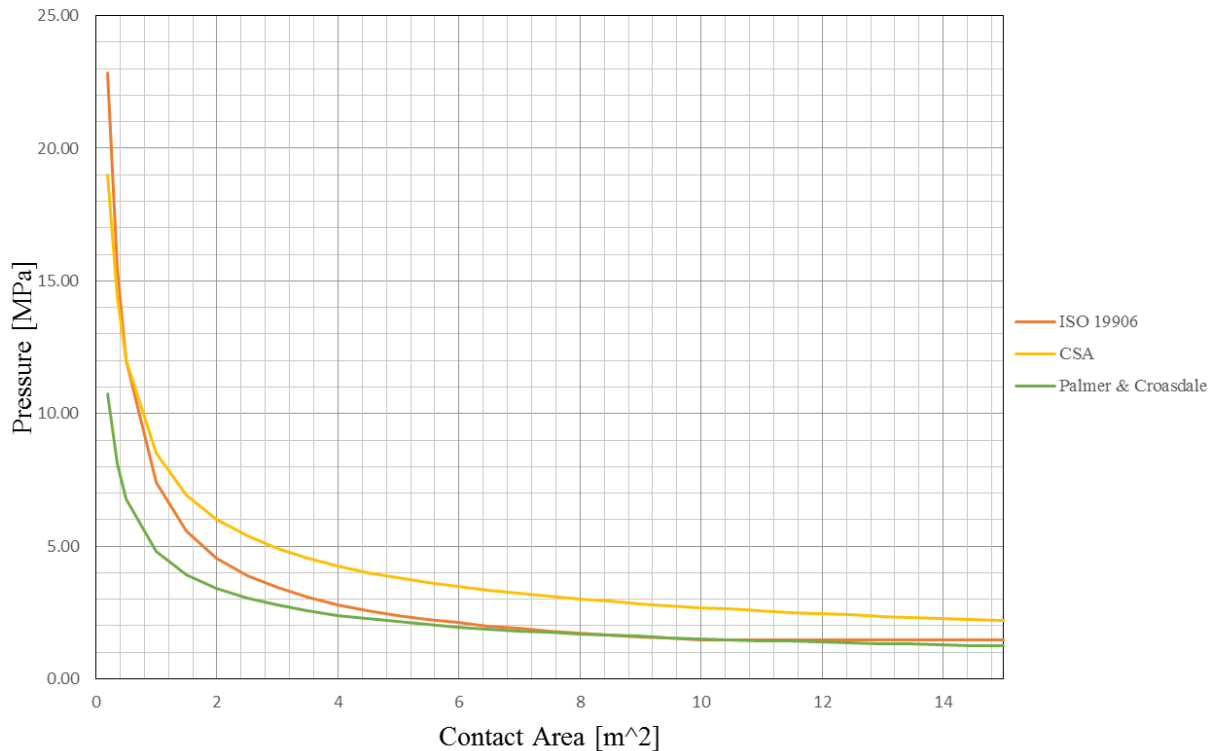
Figure 5.4 – Local pressure using different methods.

Something that is known, is that structures with vertical surfaces interacting with ice will experience larger loads than structures with sloped surfaces. For this reason, according to Palmer and Croasdale (2013), the ISO method for thick, massive ice features may be very conservative for sloped structures. However, the structure in question in this thesis have vertical surfaces and therefore are expected to experience higher loads. As can be seen from Figure 5.4, Palmer and Croasdales's suggested local pressure is the lowest of the three, which makes sense since it is only recommended for level ice up to 2 m and first-year ridges. However, it is not certain that these ice conditions are the design conditions for the structure in question. Therefore a more conservative approach safer to select.

The loads discussed so far in this section are purely local loads, however, a combination between local and global loads is a more realistic loading condition. A method, such as described in 5.2.2.3, is an approach that connects global and local loads. This method will be more conservative than only applying a local pressure, and in fact may be a more realistic load condition. However, in order to find the global pressure one must select several parameters which requires knowledge about the ice conditions of areas where the structure is to operate. For that reason this method is not considered further in this thesis.

Both the ISO method and the CSA method represents large local pressures. For contact areas smaller than 0.5 m^2 the ISO approach gives the largest pressure, but for areas bigger than 0.5 m^2 the CSA approach yields the largest pressures.

All the design contact area are most likely larger than 0.5 m^2 and thus the CSA approach seems like the best load estimation method, in spirit of conservatism. However, the fact that it only applies for low aspect ratios, and that the calculated design load used when dimensioning according to the *Polar Code* was smaller than it should be, cannot be ignored. Therefore ISO's local load from section 5.2.2.2 is used as a design load in the structural analyses presented in this thesis.

6 Local Strength Requirements

Requirements for structural strength of marine structures are very important in order to ensure that the structures built are strong enough to withstand the loads that they are exposed to. When designing a marine structure the designer will try to make the structure just as strong as it has to be, i.e. not over- or under-dimension it. Over-dimensioning will lead to a heavy and more expensive structure, while an under-dimensioned structure will risk being damaged or be directly un-safe. In this chapter a review of some common failure modes for marine structures is given, followed by local requirements for ice strengthening.

6.1 General Failure modes

In order to make sure that a structure can cope with the loads it is exposed to some capacity checks must be performed. These capacity checks must correspond to certain relevant failure modes. In this subchapter a small review over the most important general failure modes with respect to local strength is given.

6.1.1 Yielding

Yielding is important to consider mode for any marine structures. Yielding indicates permanent deformations to the structure and should of course be avoided. Normally it is not allowed, however at some locations of a structure, e.g. at a weld toe, the stress can be higher than yielding. However, the best way to avoid this failure mode is to keep stresses low by designing in a way so that stress concentrations are avoided as much as possible, and ensuring that x-sectional area and section modulus of the structural components are sufficient to withstand the loads.

A common way to check for yielding is the von Mises yield criterion. The criterion is that yielding occurs when the von Mises stress is exceeded. The von Mises equation for plane stress is given by:

$$\sigma_{vM} = \sqrt{\sigma_X^2 - \sigma_X \times \sigma_Y + \sigma_Y^2 + 3 \times \tau_{XY}^2} \qquad (6.1)$$

Where

σ_X is the stress in x-direction

σ_Y is the stress in y-direction

τ_{XY} is the shear stress in the xy-plane

6.1.2 Buckling

For the structure considered in this thesis, which is a part of a larger structure, there will be membrane stresses present. If these stresses are due to compressive loads and are large enough, buckling of the part, or any of its components, may occur. Buckling is an instability problem and a common failure mode for components of marine structures. It is therefore important that a buckling check of the structure is performed. The buckling check should include buckling of the column (global buckling), the plate between the stiffeners, the whole stiffener with attached plate flange as well as the web and flange isolated. In addition, the bulkheads of the structure should also be checked. Requirements with respect to buckling of marine structural components are given in the standards of the classification societies.

6.1.3 Fatigue

Fatigue checks are important for local details. Fatigue is a phenomenon induced by cyclic loads. It starts by a crack initiation due to tensile loads. Then as the loads (of a large enough magnitude) repeat themselves, the crack grows and gets larger and larger. As the crack grows the detail gets weaker and weaker before it finally fractures. There have been a lot of accidents due to fatigue damage which have not been detected, which shows how important it is to design against fatigue. As for buckling there are standards developed by the classification societies that give procedures for doing fatigue checks.

6.2 Ice Strengthening

Ice, as we know by now, represents large loads. And it is important that the structural components which are to be exposed for these large loads are able to withstand them. As of now (Spring 2015) there is no publicly available standard that gives local ice strengthening requirements specifically for floating offshore structures in ice. The standards that cover relevant structures usually refer to rules for ships in ice. Hence the ice strengthening rules for ships must be applied on offshore structures. Inaccuracy in the interpretation of ship rules on offshore structures may lead to slight under- or over dimensioning of the structures considered.

Two of the relevant standards which consider ice strengthening for ships are DNV's *Ships for Navigation in Ice* and IACS's *Requirements concerning POLAR CLASS*. These two documents give local strength requirements for girders, plates and stiffeners which are to comply with a load calculated by a given procedure. The requirements in *Ships for Navigation in Ice* are based on elastic methods while *Requirements concerning POLAR CLASS* are based plastic methods, which might do that they give slightly different requirements.

In this thesis the rules of IACS have been applied. The procedure and results for dimensioning according to these rules are shown in this sub-chapter. It should be noted that it is only the plate thickness and stiffener dimensions of the outer shell that has been dimensioned according to these requirements.

6.2.1 Dimensioning according to IACS

In order to make sure that the hull is sufficiently strengthened for arctic conditions a relevant standard should be consulted. Several standards for dimensioning of ship hulls in ice have been developed by the different classification societies. However, as mentioned earlier, there are no such standards for floating offshore structures. Therefore the dimensioning in this thesis have taken base in ship rules and applied them to the selected structural component of the floating unit.

6.2.2 Plate Thickness

This section covers the estimation of required minimum plate thickness. The plate thickness has two components; t_{net} and t_s. t_{net} is the plate thickness required to resist the design ice loads calculated in the previous section, while t_s is an extra thickness accounting for corrosion and abrasion due to ice interaction.

$$t_{net} = 500 \times s \times \frac{\sqrt{\dfrac{AF \times PFF_P \times P_{avg}}{\sigma_Y}}}{1 + \dfrac{s}{2b}} \ [mm] \tag{6.2}$$

Where

s is the stiffener spacing [m]

AF is the hull area factor

PFF_P is the peak pressure factor

σ_Y is the yield stress [MPa] of the material. The yield stress is taken be of high strength 355 MPa because of the high pressure loads.

t_s is a tabulated value. The structure is assumed to have effective protection against corrosion and abrasion, since IACS recommends it for all ships.

The final minimum required plate thickness is given by

$$t = t_{net} + t_s \ [mm] \tag{6.3}$$

6.2.3 Beam Stiffeners

Dimensioning of the beam stiffeners is here divided into four parts; calculation of structural capacity, calculation of load effects induced by the design loads, comparison of capacity and load effects, and a structural stability check.

The procedure to find acceptable stiffener dimensions is a trial and error procedure. Dimensions must first be selected before one can check that they are in agreement with the requirements. The dimensions shown in Figure 6.1 were assumed values before calculations started. The plate thickness and stiffener spacing have to be in agreement with the values in section 6.2.2.

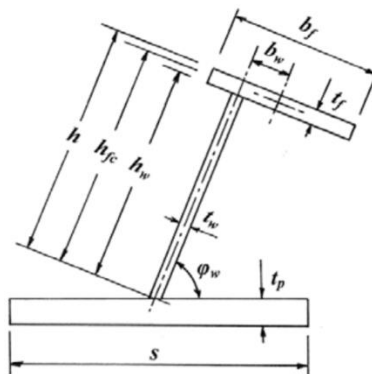**Figure 6.1 – Stiffener geometry (IACS, 2011).**

6.2.4 Capacity

The structural capacity of the beam stiffeners has to be determined. In *Polar Class* the capacity is determined by the actual net effective shear area of the stiffener and effective plate flange, A_w, and actual net effective plastic section modulus, *Zp*. This means that the capacity is determined by use of plastic methods.

The actual net effective shear area of the beam stiffener is given by (6.4) and the actual net effective plastic section modulus is given by (6.5).

$$A_w = \frac{h \times t_{wn} \times sin(\varphi_w)}{100} \; [cm^2] \tag{6.4}$$

Where

h is the height of the stiffener [mm]

t_{wn} the net web thickness [mm]. $t_{wn} = t_w - t_c$

t_c is a corrosion deduction [mm]

φ_w is the angle [deg] between web and the plate, which is 90 degrees in this case

$$Z_p = A_{pn} \times {t_{pn}}/{20} + \frac{h_w^2 \times t_{wn} \times sin(\varphi_w)}{2000}$$
$$+ \frac{A_{fn} \times (h_{fn} \times sin(\varphi_w) - b_w \times cos(\varphi_w))}{10} \; [cm^3] \tag{6.5}$$

Where

A_{pn} is the net cross-sectional area of the local frame $[cm^2]$

A_{fn} is the net cross-sectional area of the flange $[cm^2]$

t_{pn}, h_w, h_{fn} and b_w are as described in Figure 6.1

6.2.5 Load Effects and Corresponding Requirements

The load effects gives an shear area, A_t, and an plastic section, Z_{pt}, that the calculated A_w and Z_p are to comply with. The requirements are $A_w \geq A_t$ and $Z_p \geq Z_{pt}$.

A_t and Z_{pt} are given the following equations:

$$A_t = \frac{100^2 \times 0.5 \times LL \times s \times (AF \times PPF_t \times P_{avg})}{0.577 \times \sigma_Y} \; [cm^2] \tag{6.6}$$

Where

LL is the length of the loaded portion of the span

s is the stiffener spacing

AF, PPF_t, P_{avg} and σ_Y are as previously defined

$$Z_{pt} = \frac{100^3 \times LL \times Y \times s \times (AF \times PPF_t \times P_{avg}) \times a \times A_1}{4 \times \sigma_Y} \ [cm^3] \qquad (6.7)$$

Where

a is span length [m]

Y and A_1 are coefficients. For more information see [Equation 23] in the *Polar Code*

All other parameters are as previously defined.

6.2.6 Structural Stability

In order to prevent local buckling in the web and flange, (6.8), (6.9) and (6.10) are required to be satisfied.

$$\frac{h_w}{t_{wn}} \leq \frac{805}{\sqrt{\sigma_Y}} \qquad (6.8)$$

$$t_{wn} \geq 0.35 \times t_{pn} \times \sqrt{\frac{\sigma_Y}{235}} \qquad (6.9)$$

$$b_f \geq 5 \times t_w \qquad (6.10)$$

6.2.7 Final Dimensions

The dimensioning has given the results presented in Table 6.1, while detailed calculations are given in Appendix D. The dimensions satisfies the requirements given in *Polar Code*.

Table 6.1 – Hull Scantling Dimensions

Polar Class	PC 4
Plate thickness	40 mm
Web height	375 mm
Web thickness	32 mm
Flange width	150 mm
Flange thickness	35 mm

The stiffener spacing of the outer hull varies from approximately 0.8 m down to approximately 0.58 m, while 0.8 m is used input in the calculations. If the correct design load had been used in the dimensioning calculations the dimensions obtained had been likely to be conservative for parts of the structure. However, the dimensions in Table 6.1 is now likely to be non-conservative, due to the wrong input in terms of the design load.

The some of the dimensions of other components than outer shell plating and corresponding stiffeners have been altered somewhat from the drawings provided due to the need of ice strengthening, and for simplicity's sake. These changes are not done according to any standard and mostly involve increasing material thicknesses. Further reasoning for these changes are given in sub-chapter 8.1, while all thicknesses are shown in Figure 8.3.

7 The Finite Element Method

This chapter gives a review of the Finite Element Method, which in this thesis is applied as a tool for calculating load-effects and structural resistance for the ice belt structure. The chapter includes concepts and theories relevant for the problem in this thesis, in addition to information of how these are implemented in the computer software Abaqus.

All information given about Abaqus are obtained from ABAQUS (2014), while most of the rest of the chapter based on Moan (2003). All other sources are specified in the text.

7.1 Introduction

There are many different methods for computation of load-effects and structural resistance. Methods of structural analysis can be divided into two different types; analytical methods and numerical methods.

Analytical methods are methods which yield exact solutions, but are often based on simplifications of the model which is analyzed. Analytical methods can be easy to solve and are therefore often used for simple hand calculations. Example of an analytical method is the matrix method. The matrix method can among others be used for frameworks and truss structures.

When a structure is too complex to solve analytical, numerical methods are used. The most important numerical method for analysis of marine structures is the Finite Element Method (FEM). The FEM does not yield exact solutions, but if performed correctly it will give solutions of a sufficient degree of accuracy.

7.2 FEM in General

As stated in the introduction the Finite Element Method is a numerical method for analyzing structures. The method models a structure as a collection of small elements. These elements have shapes that make the analysis of them much easier than an analysis based on the actual shape of the structure. This makes FE results approximate solutions which are composed by piecewise simple solutions.

In order to achieve accurate results from the method one must use sound engineering judgement and experience to select good input such as geometry, boundary conditions, elements, mesh. It also requires knowledge to interpret the output.

The advantage of the FEM is that it can be used for all kinds of problems; one can model any shape, load and boundary conditions. The main disadvantage of the method is that it can be hard to achieve accurate results.

7.2.1 Steps of the Method

To get an overview of the Finite Element Method the various steps of the method is given in this section.

1) Discretization – Dividing the geometry of the structure into elements
2) Element analysis – Obtaining the element stiffness relation

$$S = k \times v + S^0 \tag{7.1}$$

Where

S   is generalized nodal point forces

k   is element stiffness matrix

v   is nodal point displacements

S^0 is nodal point forces for external load

3) System analysis – Obtaining the relationship between load and nodal point displacements by demanding equilibrium for all nodal points in the structure

$$R = K \times r + R^0 \tag{7.2}$$

$$K = \sum_j a_j^T \times k_j \times a_j \tag{7.3}$$

$$R^0 = \sum_j a_j^T \times S_j^0 \tag{7.4}$$

Where

R   is the system load vector

K   is the system stiffness matrix

r is the global displacements

R^0 is the external loads on the system

a_j is the topology matrix for element j

4) Boundary conditions – Introducing boundary conditions by inserting known displacements into v

5) Finding global displacements – Finding the global displacements by solving the equations given in 3)

6) Calculation of stresses – Using Hooke's law to determine the stresses. Strains are derived from the element displacement functions.

7.3   Shell Element Theory

When doing Finite Element Analyses (FEA) on marine structures it is common to use shell elements to model components like columns and stiffened panels. The reason for this is that shell elements carry loads in a combination between bending moments, like plate elements, and in-plane forces, like membrane elements.

If we look at a stiffened panel we can see that the panel itself really consists of plane plates. But when the plate of the panel is exposed to a lateral load it will bend to some degree. The stiffeners will also bend, acting like beams with the plate as effective flange. It is this overall bending which causes membrane stresses in the plate and make the shell element relevant for the problem.

Shell theories are based on the same theories as plates regarding bending. These theories are the Kirchhoff theory and the Mindlin-Reissner theory, and will be explained in section 7.3.1 and 7.3.2. Which theory that is applicable is depending on the material thickness relative to the in plane dimensions. ABAQUS (2014) defines the shell problems the following way:

Thin shell problem: $\frac{thickness}{span} < \frac{1}{15}$

Thick shell problem: $\frac{thickness}{span} > \frac{1}{15}$

7.3.1 Kirchhoff Theory

Kirchhoff theory, also known as thin-plate theory, is based on these two assumptions:

- The lateral stress component in the plate, σ_z, is negligible.

- A line that is straight and perpendicular to the mid surface before loading is still straight and perpendicular to the mid surface after loading.

The latter assumption basically means that transverse shear deformation is zero i.e. transverse shear stress is not accounted for. The stress-strain relationship is then:

$$\boldsymbol{\sigma} = \begin{bmatrix} \sigma_x \\ \sigma_y \\ \tau_{xy} \end{bmatrix} = \boldsymbol{D} \times \boldsymbol{\varepsilon} = \frac{E}{1 - v^2} \times \begin{bmatrix} 1 & v & 0 \\ v & 1 & 0 \\ 0 & 0 & \frac{(1 - v)}{2} \end{bmatrix} \begin{bmatrix} \varepsilon_x \\ \varepsilon_y \\ \gamma_{xy} \end{bmatrix} \qquad (7.5)$$

Where

$\boldsymbol{\sigma}$ is the stress vector containing the normal stresses and the shear stress

$\boldsymbol{D}$ is the plate stiffness containing the Young's modulus and the Poisson ratio

$\boldsymbol{\varepsilon}$ is the strain vector containing the strains in the plane

It is important to be aware of the fact that transverse stresses will be present in a plate exposed to transverse loads in reality, even though they are not included in this formulation.

7.3.2 Mindlin-Reissner Theory

Mindlin-Reissner theory is also known as thick-plate theory. The assumptions of this theory are:

- The lateral stress component in the plate, σ_z, is negligible.

- A line that is straight and perpendicular to the mid surface before loading is still straight, but not perpendicular to the mid surface after loading.

The latter assumption in this case means that transverse shear deformations are allowed. Thus there will be transverse shear strains and stresses. This yields the following stress-strain relationship:

$$\boldsymbol{\sigma} = \begin{bmatrix} \sigma_x \\ \sigma_y \\ \tau_{xy} \\ \tau_{xz} \\ \tau_{yz} \end{bmatrix} = \boldsymbol{D_{MI}} \times \boldsymbol{\varepsilon} = \frac{E}{1-v^2} \times \begin{bmatrix} 1 & v & 0 & 0 & 0 \\ v & 1 & 0 & 0 & 0 \\ 0 & 0 & \dfrac{1-v}{2k} & 0 & 0 \\ 0 & 0 & 0 & \dfrac{1-v}{2k} & 0 \\ 0 & 0 & 0 & 0 & \dfrac{1-v}{2k} \end{bmatrix} \begin{bmatrix} \varepsilon_x \\ \varepsilon_y \\ \gamma_{xy} \\ \gamma_{xz} \\ \gamma_{yz} \end{bmatrix} \quad (7.6)$$

Where

k is a correction factor of 1.2 which accounts for the fact that the shear strain is not constant over the thickness

Elements that are based on the thick plate theory perform better for shear stresses and should therefore be used when these types of load effects cannot be neglected, namely in thick plates. However, as the thickness decreases, thick plate elements may prove to be less accurate than thin plate elements. The reason for this is a phenomenon called *shear locking*. Shear locking is when spurious shear strains appear in the elements. These strains are stealing energy from the bending deformation process. The consequence of shear locking is that the deflection of the plate, or shell, becomes more and more inaccurate as the domination of bending deformation over shear deformation increases. This results in a solution that is too stiff. The effects of shear locking can be reduced by selective integration.

7.3.3 Shell Elements in Abaqus

Abaqus has a large shell element library, but the general-purpose, conventional elements, as well as elements specifically suitable for thick and thin shell, are those which are considered in this thesis. This section gives a small review of these elements. All information in this section are gathered from ABAQUS (2014).

The general-purpose conventional elements are elements that are valid for thick and thin shell problem. They use thick shell theory when shells are thick and thin shell theory when shells are thin. As stated in 7.3, Abaqus defines the limit for thick shell problems at a thickness/span ratio of 1/15, but this is dealt with by the software. The element types S4 and S4R are common examples of such general purpose elements.

When the problem is a thick shell problem, transverse shear deformation have to be accounted for. In such cases thick conventional shell elements, like S8R or S8RT, should be used.

However, the two should only be used for thick shell problems according to ABAQUS (2014). If they are used for thin shell problems they will give too stiff solutions.

Regarding thin conventional shell elements Abaqus has two types; elements that solves thin shell theory and elements that impose the Kirchhoff constraint numerically. These elements will always give thin shell solutions. Some of those elements are the STRI3, S4R5 and S8R5 elements.
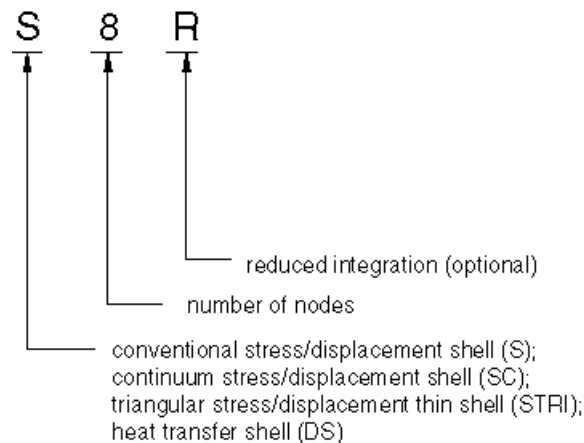

Figure 7.1 – Naming convention for 3D shell elements. Adapted from ABAQUS (2014).

Figure 7.1 shows the general naming convention of shell elements. This means that e.g. S4R is a four-node shell element with reduced integration with hourglass control and finite membrane strains, while S8R is an eight-node doubly curved shell element with reduced integration. S8R5 is the same as S8R only that it has five active degrees of freedom instead of six, i.e. it is a thin shell element. The S4R, S8R and S8R5 element all support buckling.

7.4   Numerical Integration

This sub-chapter is based on Bell (2013) and Mathisen (2013).

When establishing the element stiffness matrix, some sort of integration is necessary. For simple elements like 1D bar elements and 2D rectangle elements analytical integration may be applied. However, when establishing the element stiffness matrix for more advanced elements, numerical integration has to be applied. The reason is that their corresponding analytical expressions are very difficult to derive. In fact, it can also be proven that use of numerical

integration can improve the finite element solution. Though, it should be noted that numerical integration for evaluating the element stiffness matrix is an approximate method.

The integral of the stiffness matrix for a 2D element will have the form:

$$I = \int_A f(x, y) dx dy = \int_{-1}^{1} \int_{-1}^{1} f(\xi, \eta) d\xi d\eta \tag{7.7}$$

If the problem of calculating (7.7) is considered to be finding the volume under the under the curve one could use *quadrature rules* to solve the problem. Quadrature rules consider the integrals as the sum of the products between the function $f(\xi, \eta)$ and a weight w as shown in (7.8).

$$I = \int_{-1}^{1} \int_{-1}^{1} f(\xi, \eta) d\xi d\eta = \sum_{i=1}^{n} \sum_{j=1}^{n} w_i w_j (\xi_i, \eta_j) f(\xi_i, \eta_j) \tag{7.8}$$

There are different quadrature approaches (rules), but the most common one is the Gauss quadrature rule.

7.4.1 Gauss Quadrature

Gauss quadrature is a method that locates the sampling points and gives them a weight w to minimize the error in integration. It is a very convenient quadrature rule since it uses fewer sampling points to achieve the same accuracy as other quadrature rules.

In Abaqus one can select both Gauss quadrature and Simpson quadrature. However, the Gauss quadrature is according to theory the best option to use.

7.4.2 Full and Reduced Integration

Full integration means a quadrature rule of that accuracy that is necessary to exactly integrate all components of the element stiffness matrix of an undistorted element. An undistorted element is an element where the edges are straight and the side nodes are uniformly distributed along the edges. For a four cornered (quadrilateral) element, a corresponding undistorted element have to be of quadratic, rectangular or parallelogram shape.

In numerical integration, adding more integration points will increase the accuracy of the integral itself. However, it will not necessarily integrate the accuracy of the finite element solution.

Reduced integration of an element means a quadrature rule that is less than full order. By using this approach, one can actually improve the results of the finite element analysis. This is because it reduces the shear locking effect mentioned in section 7.3.2. In addition, reduced integration will lower the computational time, which is very convenient in general.

A downside with reduced integration is that it may lead to false deformation modes, called "hourglassing". As shown in Figure 7.2, the integration point (center) of the element remains unchanged after the deformation. This indicates that all the stress and strain components in that point are zero. Thus the element has no stiffness in the mode that it deforms in. This effect is large for coarse meshes and decreases as the mesh is refined (ABAQUS, 2014). Also, the accuracy provided by reduced integration drops significantly when elements are distorted or loaded in in-plane bending.

Figure 7.2 – Bending of linear element with reduced integration subjected to bending moment M.

In Abaqus the hourglassing is dealt with by introduction of artificial stiffness which limits the effect of the phenomenon. The problem is most severe for linear elements, while for quadratic elements the hourglass modes have a hard time to propagate in the mesh.

7.5 Nonlinear FE Theory

Until this point only linear FE theory have been discussed, where small displacements and linear stress-strain relationship is assumed. However, when ultimate strength of structures is to be considered these assumptions are no longer valid without modifications.

In this subchapter different non-linear behaviors and their corresponding solution methods are highlighted.

7.5.1 Linear versus Nonlinear FE theory

When considering nonlinear FE theory one still uses the same basic principles as for other structural analyses. This means that force equilibrium, kinematic compatibility and a stress-strain relationship is still used. The main difference between linear and nonlinear FE theory is the stiffness of the structure considered. This can be illustrated by the static equilibrium equation for a structure:

$$R = K \times r \tag{7.9}$$

Where

R   is the external load

K is the system stiffness

r is the displacement

The static equilibrium equation is just the same for a linear problem as for a nonlinear problem. In addition the load and displacement terms are also the same. The stiffness term, however, is not the same. As we know, the stiffness characterizes the response of the structure to the applied load. In nonlinear theory the stiffness changes from the ordinary linear stiffness to a more complex type of stiffness. The change is due to one or more of the following three effects; change in geometry, change in the material properties and change of boundary conditions.

7.5.2 Geometry

In linear theory, the assumption of small displacements allows for equilibrium equations to be established for the initial structural configuration. But as the displacements are getting larger the change of geometry must be accounted for in order to obtain the correct results. If this is done, geometric non-linearity has been taken into account.

The feature characterizing changing stiffness due to change of structural shape is that the stiffness is a direct function of displacements. This means that the stiffness must be recalculated continuously as the structure deforms, and as a consequence calculation time is increased.

An example of the effect of changing stiffness due to geometrical effects can be seen from Figure 7.3. In the first step, the member has not deformed and the load is carried by bending. In the second step, the member has deformed and now carry the load by deforming both in-plane and in bending. This means that the deformation of the member has changed how it carries the load.
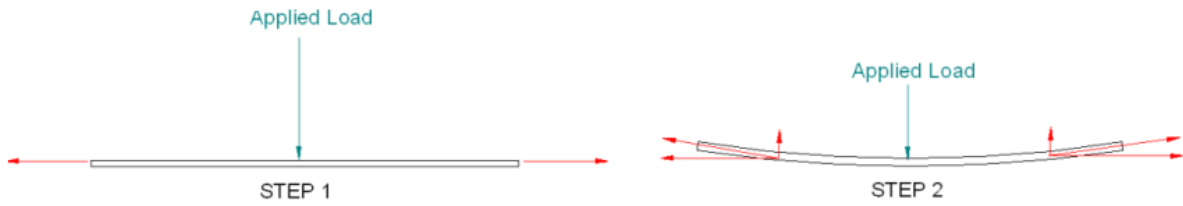
Figure 7.3 – Changing stiffness due to large deformations. Adapted from Motovated Design & Analysis .

In Abaqus, nonlinear geometry is accounted for by allowing large deformations. This is simply done by ticking a box in the step module in the program.

7.5.3 Material

When stresses in e.g. metals exceeds a certain magnitude the linear stress-strain relationship is no longer applicable. The stress-strain relationship then needs to be modified from linear to non-linear, in order to capture the response accurately. If this is done non-linear material behavior is accounted for. A typical stress-strain curve for mild steel is shown in Figure 7.4.
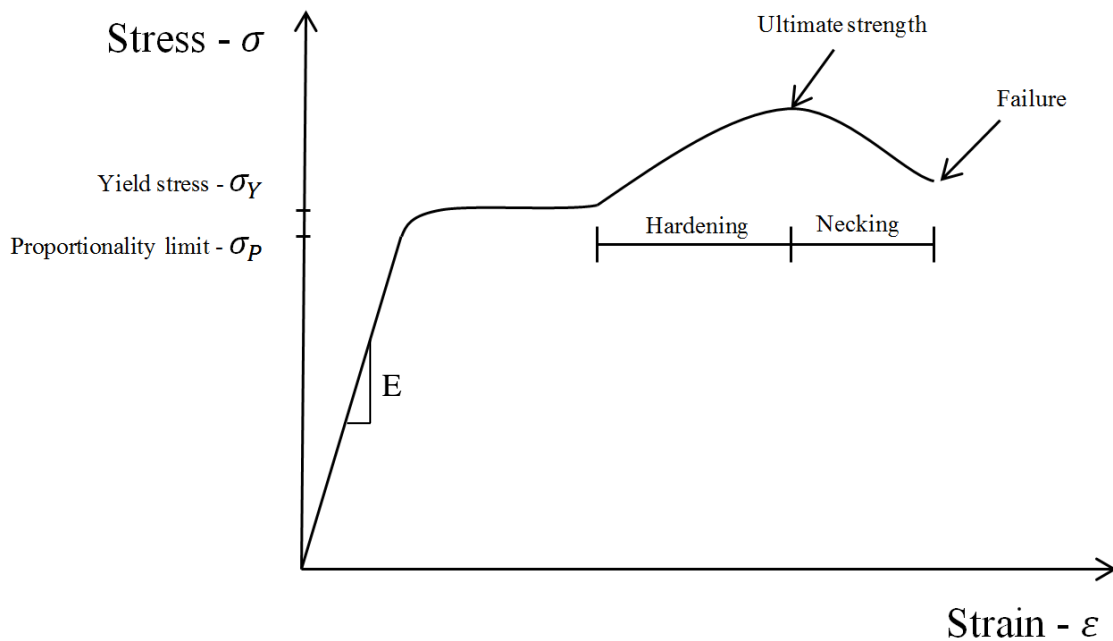
Figure 7.4 – Typical stress-strain curve for mild steel.

The stress-strain curve is crucial to understand in order to get what material nonlinearity is all about. As seen in Figure 7.4, the stress-strain relationship is linear up to the proportionality

stress. After that the relationship goes over to be nonlinear. The strains corresponding to stresses up to yield magnitude are elastic, i.e. not permanent. After the material yields the plastic strain starts, i.e. the material gets permanent deformations. The rise in the non-linear curve is due to a phenomenon called hardening. Due to hardening the stresses required for further deformations in the material are higher. The ultimate strength represents the highest stress the material can have. After the point of ultimate strength is reached, the stress decrease after in a phase called necking before it ultimately fails.

In Abaqus nonlinear properties can be given to materials by defining their plastic behavior, in addition to their elastic one. When defining plastic material behavior one can choose which type of hardening the materials are to have, and define stresses with corresponding plastic strains.

7.5.4 Boundary Conditions

If deformations are large in a structure, contact between structural members may occur. This implies a change in boundary conditions from the initial configuration to the deformed configuration. Nonlinear boundary conditions mean that the boundary conditions of a structure changes and that the change in boundaries is not a linear function of the loads.

7.5.5 Choice of Reference System

When having large deformations, selection of a suitable reference system must be performed so that the geometry of the structure can be properly described. The common reference system in structural mechanics is the Lagragian approach. In this approach the motion at a material particle is described. However, there are two different formulations for the Lagrangian approach; the total formulation and the updated formulation. The difference between the two formulations is that the total formulation refers the geometry under a certain load condition to the initial geometry of the structure. The updated formulation refers to the *current* geometry, which means that the coordinates of the reference system is updated as the geometry changes.

7.5.6 Solution Methods

In order to solve nonlinear problems special solution methods are required. There are plenty of different solution methods, each with their pros and cons. In this section, some load-displacement curves are shown before three types of solution methods are described briefly.

In study of nonlinear static behavior of structures the load-displacement diagram is a very important tool. By using such a diagram one can really capture the different nonlinear features of the problem. Three different load-displacement curves are shown in Figure 7.5.
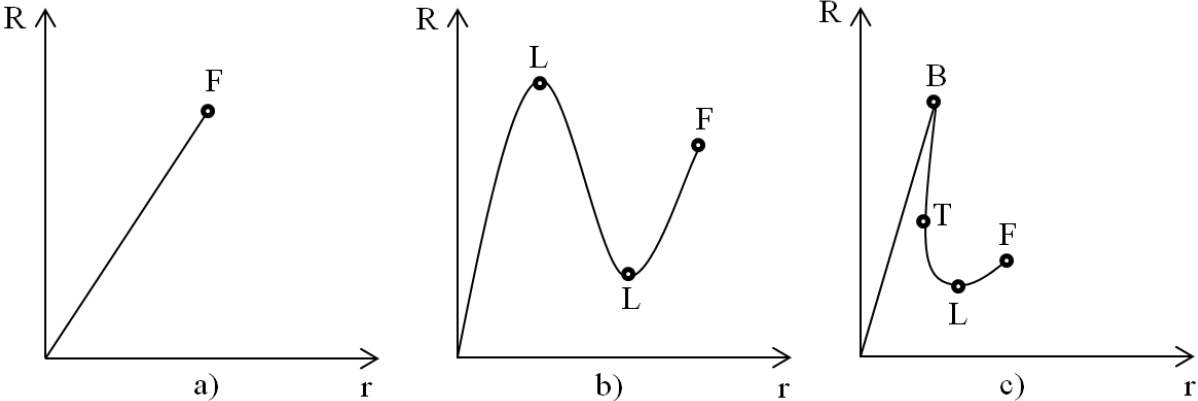

Figure 7.5 – Load-displacement diagrams.

Diagram a) corresponds to brittle material with no plastic deformations before the failure (F). Diagram b) shows a typical snap-through response where softening and hardening are combined. The limit points (L) are where the slopes of the curves are zero. Diagram c) shows a buckling case, where the behavior is linear until buckling (B) occurs. Post buckling behavior involves a snap-back before hardening and ultimately failure occurs. The turning point of the snap-back behavior is shown by T. The curves are also called equilibrium paths since each point along the paths represents equilibrium between load and structural resistance.

7.5.6.1 Incremental methods

Incremental methods are methods for finding the nonlinear structural behavior by applying the external load stepwise. For each load increment applied equilibrium equations are solved, and thereby the equilibrium path of the load-displacement diagram is found.

Procedure of incremental methods:

1. Applying a load increment ΔR
2. For each load step the displacement increment Δr is found by the incremental equilibrium (7.10):

$$\boldsymbol{K}_I(\boldsymbol{r}) \times d\boldsymbol{r} = d\boldsymbol{R} \tag{7.10}$$

Where

$K_I(r)$ is the incremental system stiffness

3. The total displacement for each step is found by summation of the displacement increments.

4. For calculating the next displacement *Δr* the total displacement is used in the expression for the incremental stiffness.
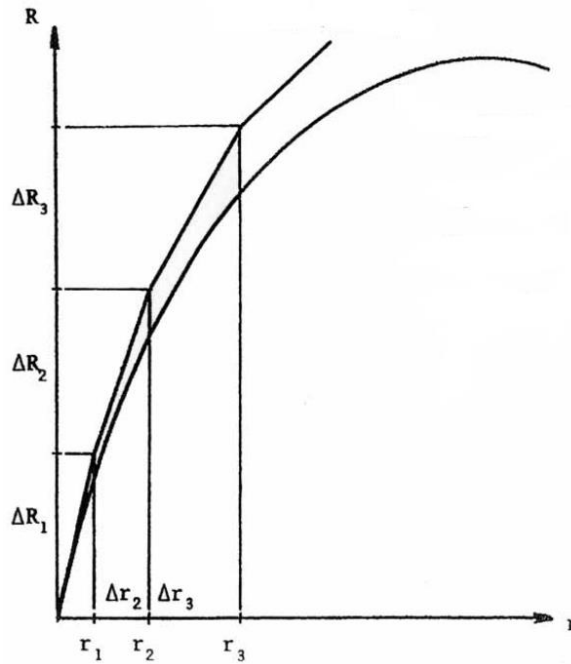

Figure 7.6 – Euler-Cauchy incrementation (Moan, 2003)

The incrementation methods generally become more accurate as the increment sizes decrease. It should also be noted that they generally overestimate the incremental stiffness in softening and underestimates the incremental stiffness in hardening.

7.5.6.2 Iterative methods

Iterative methods are methods that apply numerical iterations to solve equilibrium equations. For nonlinear FE analysis the most applied iterative method is the Newton-Raphson method. Newton-Raphson method is a method used to calculate roots by the following formula:

$$x_{n+1} = x_n - \frac{f(x_n)}{f'(x_n)} \tag{7.11}$$

The results from the iteration for a general load-displacement relationship is shown by Figure 7.7.
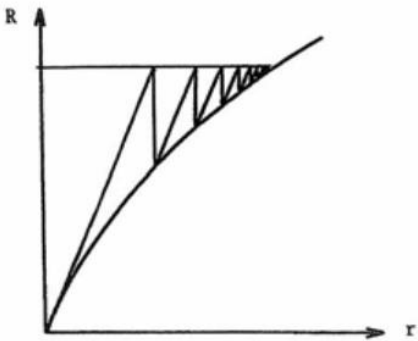

Figure 7.7 – Newton-Raphson iteration (Moan, 2003).

As we can see from Figure 7.7 the iteration procedure requires a lot of iterations when performed in this way, especially when the iteration is closing in on the correct solution. When a lot of iterations are required, a lot of computational time is required. This is of course not wanted. However, by updating the incremental stiffness during the iteration process, time can be saved with no loss in accuracy worth mentioning. By updating the incremental stiffness in the Newton-Raphson iteration we use the so-called *modified Newton-Raphson iteration*. An example of how this works is shown in Figure 7.8.
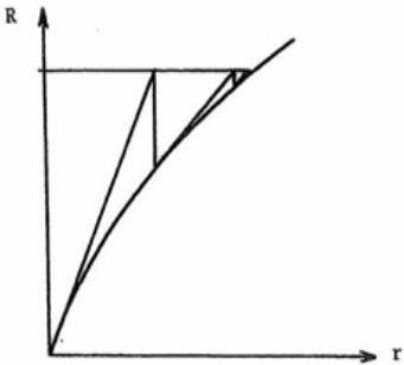
Figure 7.8 – Modified Newton-Raphson iteration (Moan, 2003).

7.5.6.3 Arc-length methods

When encountering limit points of the equilibrium path, snap-back or snap-through behavior, the methods described in section 7.5.6.1 and 7.5.6.2 does not suffice. The methods of incrementation and Newton-Raphson have trouble describing what happens at these points, and then arc-length methods have to be applied. While the two previous methods are load controlled

methods, the arc-length methods are a combination between load and displacement control. This can be seen from the global equilibrium equation, (7.12), of the arc-length methods:

$$\mathbf{g}(\mathbf{r}, \lambda) = \mathbf{R}_{\text{int}} - \mathbf{R}_{\text{ref}} = \mathbf{0} \qquad (7.12)$$

Where

$\mathbf{R}_{\text{ref}}$ is the fixed external load vector

λ is the loading parameter

$\mathbf{R}_{\text{int}}$ is the internal reaction to the load

$\mathbf{r}$ is the displacement vector

By using a combination of load and displacement control it is possible to overcome e.g. limit points by using displacement control and e.g. snap-back by switching over to displacement control. There are some different arc-length methods, but ABAQUS uses Riks-Wempner's method which is shown in Figure 7.9.
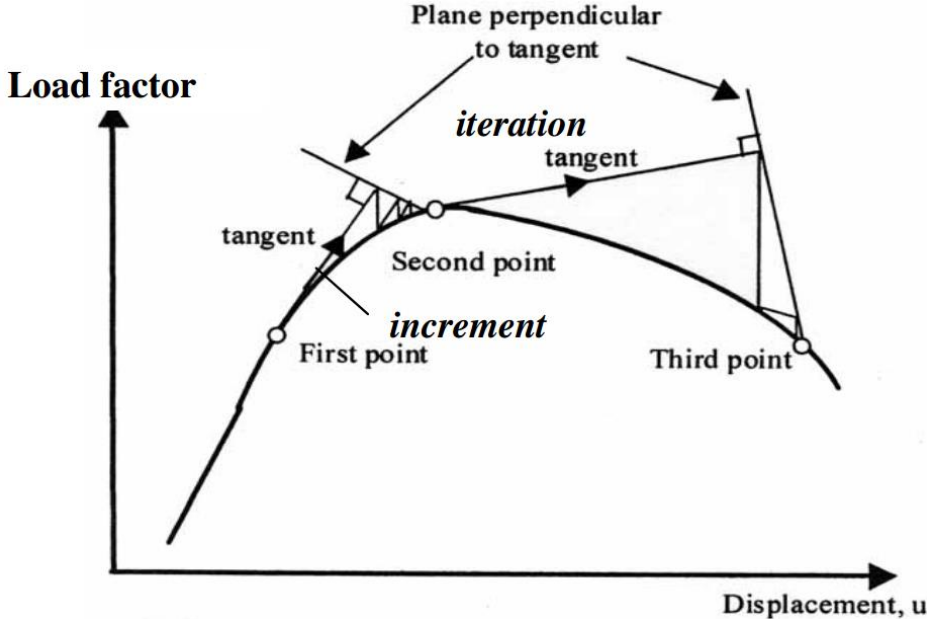
Figure 7.9 – Riks-Wempner's arc-length method (Moan, 2003).

8 Computer Model

In order to do an analysis considering local ice loads on a floating offshore structure a local model is required. This chapter describes the ice belt model, which is analyzed itself, and the corresponding setup of the of the applied FE analysis software Abaqus. It includes modelling and geometry information, material selection, elements and mesh, loads, boundary conditions and the setup of the analysis steps.

8.1 Modelling in Abaqus

Abaqus does not only solve FE problem, it can also be used for modelling purposes. The model created in this thesis was created in Abaqus/CAE, which is the interface of the software of the Abaqus software. Abaqus uses a feature-based part modelling. This means that a part is built up of several features, which are the components of the part. Examples of such features are the stiffeners and brackets of the stringer plate.

The model is created as a shell structure which is the common choice for marine structures. The author has selected to make the model as detailed as possible in order to capture the effects of small details like cut-outs and local reinforcements. This has consequences for the mesh, as can be seen in sub-chapter 8.3. Figure 8.1 and Figure 8.2 can be compared with the provided stringer drawing (Figure A.1) for verification of the model.
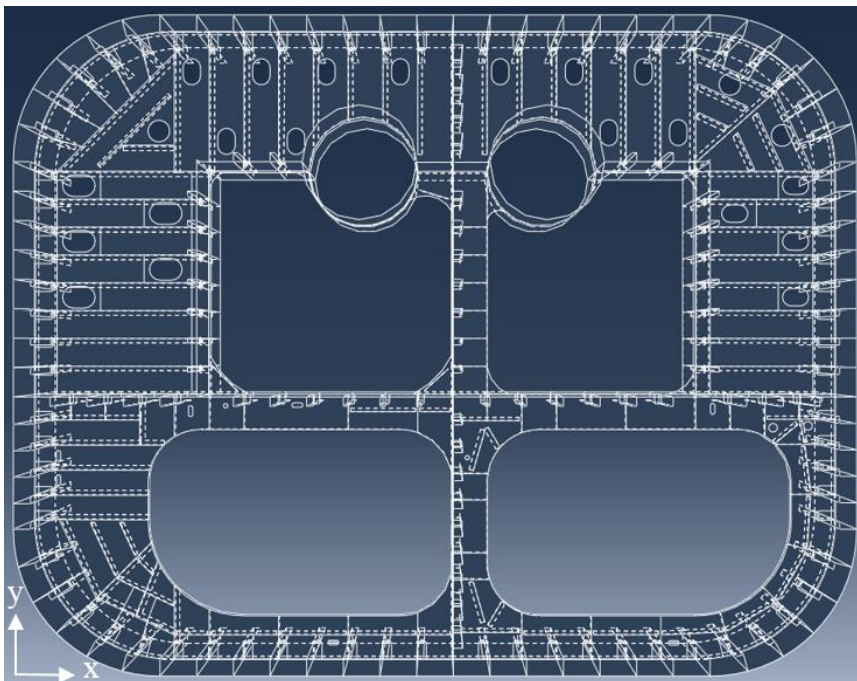

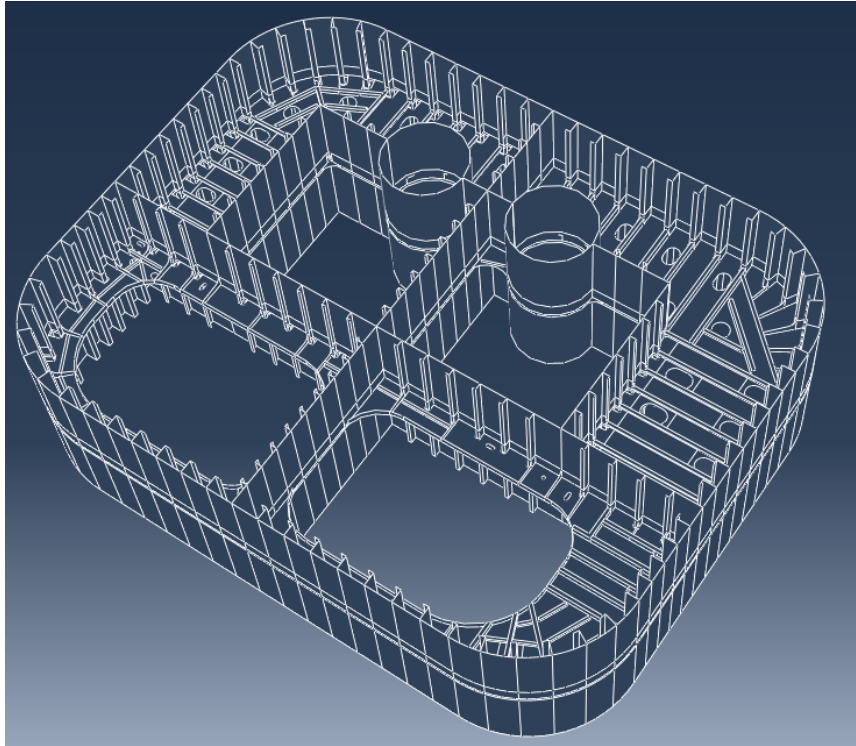**Figure 8.1 – The model seen from above (xy-plane).**

Figure 8.2 – Iso-view of the model.

The author has modelled all structural components of the model in the same, or approximately the same, locations as on the drawings provided. However, assumptions regarding structural thickness and dimensions have been made. Most of the components, except from the outer shell and its stiffeners, which are dimensioned according to the *Polar Code*, have been given thicknesses and dimensions that are assumed. The reason why these assumptions have been made is tripartite;

- information on the complete column structure is not provided
- the author feels that strengthening of inner structure is also required
- having less dimensions to deal with when modelling

Figure 8.3 gives an overview of what thicknesses are used where. As mentioned in Chapter 4, there is some structure connected to the mooring system present on the relevant stringer. This feature is not included in the ice belt model, since it are located in an unlikely place for an ice classed semi-submersible.
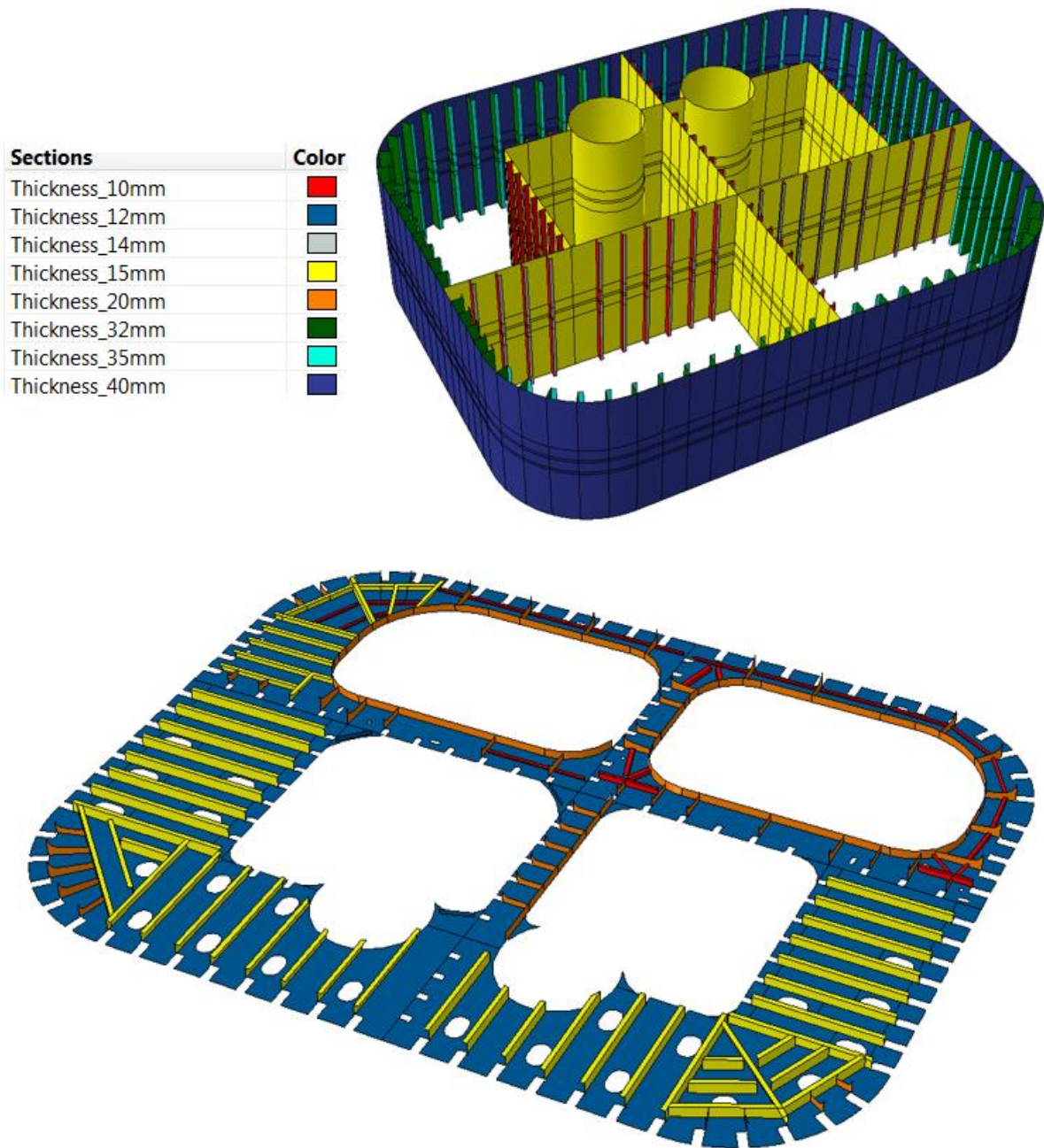
Sections	Color
Thickness_10mm	🟥
Thickness_12mm	🟦
Thickness_14mm	⬜
Thickness_15mm	🟨
Thickness_20mm	🟧
Thickness_32mm	🟩
Thickness_35mm	🟦
Thickness_40mm	🟦

Figure 8.3 – Color-coded model based on structural thickness.

Although the modelling turned out to be successful, the author recommends to use a more specialized modelling software for large marine structures. Modelling of large structures in Abaqus requires a lot of repetitive work, especially in the creation of features that can cannot be copied and moved easily to the desired location. Also, complex geometries are found to be challenging to create in Abaqus/CAE.

8.2 Material

Due to the high loads that ice represents S355 steel has been chosen as material. In Abaqus the material properties must be implemented manually.

Density of the material is defined for the purpose of accounting for gravitational loads due to material weight. The density of the steel is set to be 7850 kg/m^3.

In order to run an analysis in Abaqus one must also define some elastic properties. These are the modulus of elasticity and the Poisson's ratio. For structural steel these are generally, and in this thesis, set to be 210 GPa and 0.3 respectively. In addition the material is defined as isotropic, i.e. it has the same strength in all directions.

Since the analyses in this thesis are nonlinear, a stress-strain curve of the material, such as described in section 7.5.3, also has to be defined. In general, material properties given in relevant standards should be used. DNV (2013) suggests using European Standards (EN) for steel S355, consequently these standards are used in this thesis. Figure 8.4 gives meaning to the parameters for S355 steel which are listed in Table 8.1. The properties for material thickness between 16 mm and 40 mm are used since the maximum material thickness in the model is 40 mm. This is conservative for thicknesses less than 16 mm.
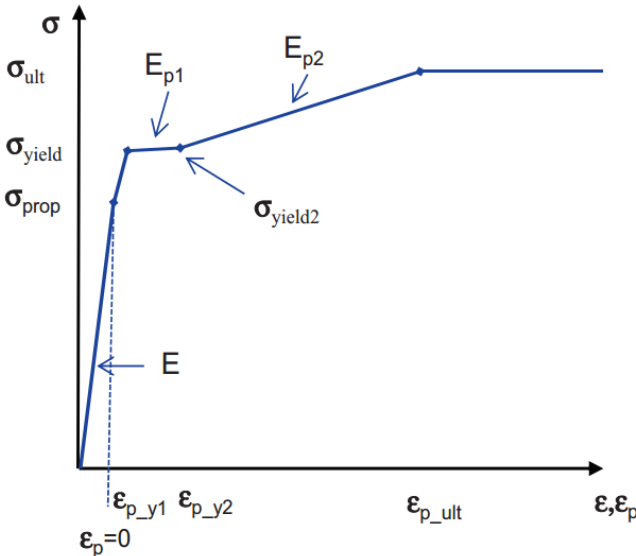

Figure 8.4 – Parameters to define stress-strain curves (DNV, 2013).

Table 8.1 – Nonlinear properties of S355 steel, adapted from DNV (2013).

σ_{prop}	310.5 MPa	ε_{p_prop}	0
σ_{yield}	345 MPa	ε_{p_y1}	0.004
σ_{yield2}	348.5 MPa	ε_{p_y2}	0.02
σ_{ult}	470 MPa	ε_{p_ult}	0.15

It is important to be aware that the material data given here are in engineering form, while Abaqus requires the true (Cauchy) stress and logarithmic strain as material input. This is obtained by following the procedure given in Zareh (2011). Table 8.2 gives the values which are used as input in Abaqus.

Table 8.2 – True nonlinear properties of S355 steel.

σ_{prop} [MPa]	310.5	ε_{p_prop}	0
σ_{yield} [MPa]	346.4	ε_{p_y1}	0.004
σ_{yield2} [MPa]	355.5	ε_{p_y2}	0.02
σ_{ult} [MPa]	540.5	ε_{p_ult}	0.14

8.3 Elements and Mesh

Elements and mesh basically determines the accuracy of results obtained from FE analyses. Different elements are suitable for different problems and should be selected thereafter. When it comes to mesh, it generally should be sufficiently fine to represent conditions in potential failure areas in a detailed way. This section is largely based on DNV (2013).

When selecting what element to use, one must first of all select which element family it shall come from. For analysis of marine structures in general, shell elements are the common choice and thus selected in this thesis as well. The second selection to be made is related to what kind of features the element shall have. Depending on the problem one must decide what kind of shape functions and integration formulas that represents the desired quantities, like stress or displacements, in the best possible way. For example it is known that elements with higher

order shape functions generally gives more detailed stress estimates than elements with linear shape functions.

When it comes to mesh size it is a matter of accuracy versus computational time. In general a fine mesh gives more accurate estimates than a coarse mesh, however, computational time increases drastically with the number of elements. The trick is to find a mesh size which gives adequate results, while at the same time keep the computational time to a level that the user can live with. One way of doing this is by have a fine mesh in areas of interest and a coarse mesh in areas of less importance.

8.3.1 The Model

Meshing the model considered in this thesis involves a lot of work. The complex geometry of the stringer plate, with its stiffeners and brackets, makes it impossible to use the built-in structured meshing technique in many locations, without partitioning the model. Partitioning the model means dividing its surfaces into several smaller surfaces. The aim of partitioning is to isolate areas with complex geometry, such as cut-outs, where achieving an ideal mesh (quadratic or rectangular elements) is impossible. In such areas the free meshing technique have to be used. Figure 8.5 shows the difference between an un-partitioned model and a partitioned model in terms of available meshing technique. In both cases structured meshing of the complete model has been attempted, while free meshing has been chosen on surfaces where structured meshing are not available. The difference between structured and free mesh is illustrated by Figure 8.6.
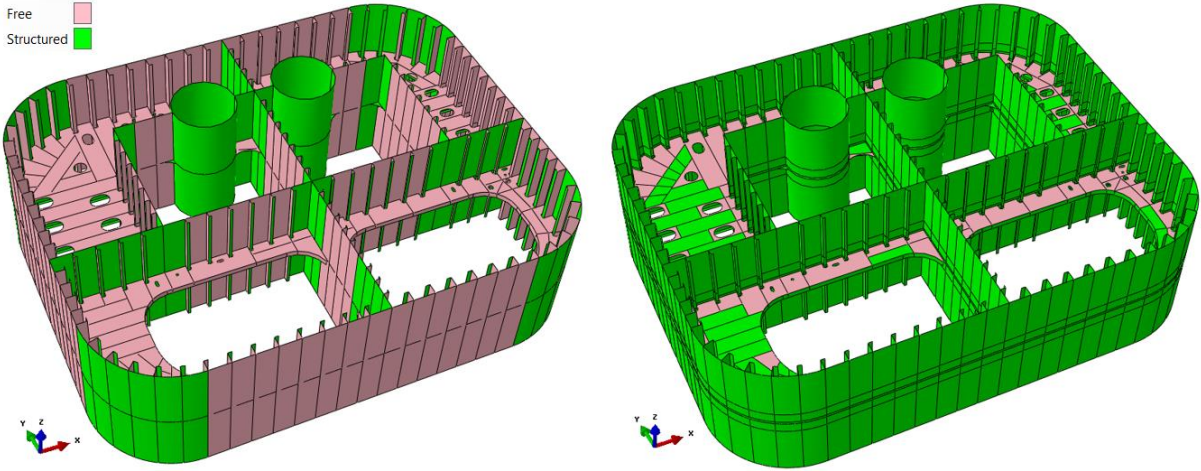

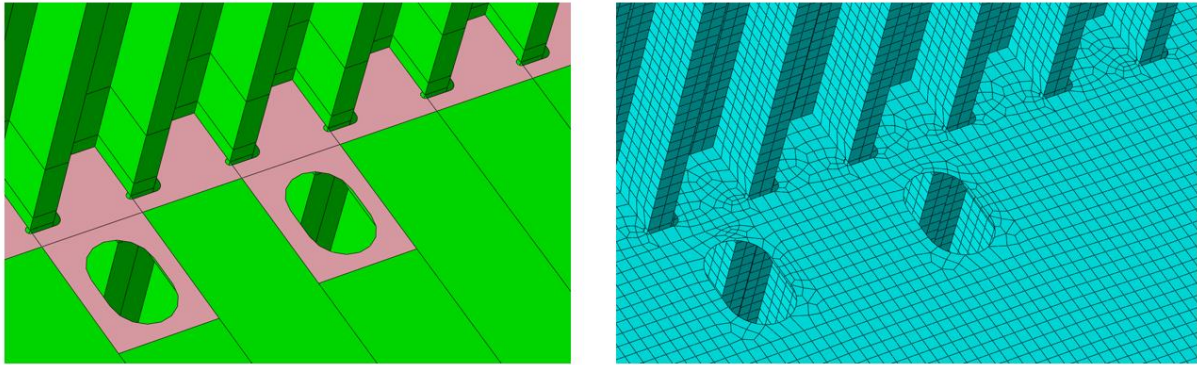
Figure 8.5 – The model before and after partitioning.

Figure 8.6 - Difference between free and structured meshing (mesh size 75 mm).

8.3.2 Convergence check

In order to select the best possible element and mesh for the main analyses, a convergence check has been conducted. The structure considered in the check is only a part of the main structure, due to saving of computational time and in order to have a structured mesh. The part selected is a stiffened panel as part of the main structure. Of course this means that stiffener span, plate thickness and stiffener dimensions are the same as stated in section 6.2.7. The stiffener spacing used is 0.8 m. The convergence structure are loaded by a uniform pressure of 0.67 MPa over a contact area with height 1.4 m and width 1.6 m with center in the middle of the model. It is also fixed against all translations and rotations along the stiffener and plate ends. The model is displayed in Figure 8.7.

The results that the convergence check gives may not be suitable for the entire main structure because only a certain part of it is considered. However, since the convergence structure is of rather simple geometry, where stress is assumed to converge faster than for more complex geometries, it is assumed that the results give an expected maximum mesh size in order to achieve results of a sufficient accuracy for the main structure.
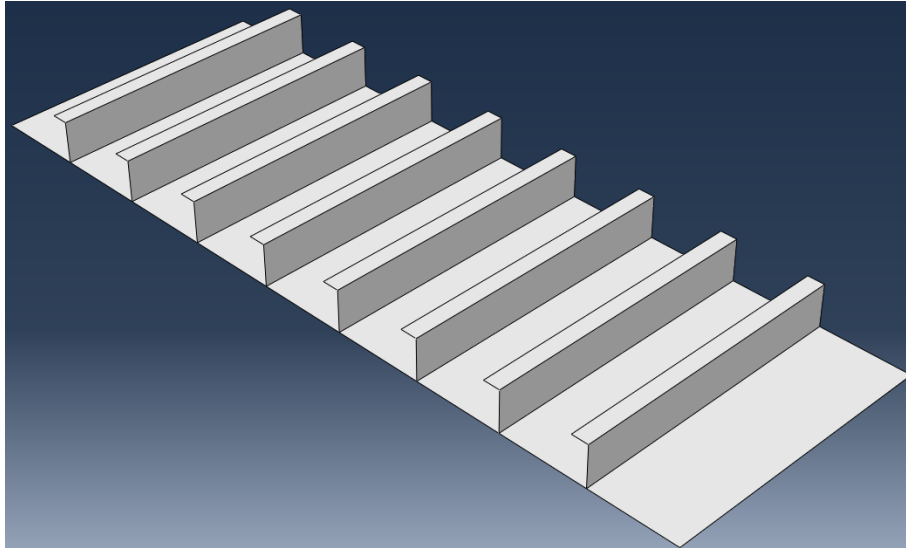
Figure 8.7 - Convergence model.

The elements considered in the convergence check is S4R, S8R and S8R5. These are general-purpose, thick and thin shell elements, as described in section 7.3.3. The only element shape considered is quadrilateral and the only mesh technique considered is structured technique. The mesh size ranges from 200 mm to 20 mm (half of plate thickness). The quantities considered for convergence are maximum longitudinal stress of the plate, the maximum transverse stress in the stiffener flange and the maximum plate deflection. Longitudinal direction in this context is the stiffener direction. Maximum von Mises stress is not considered here since the maximum stress will occur in singularity points, i.e. it will not converge.
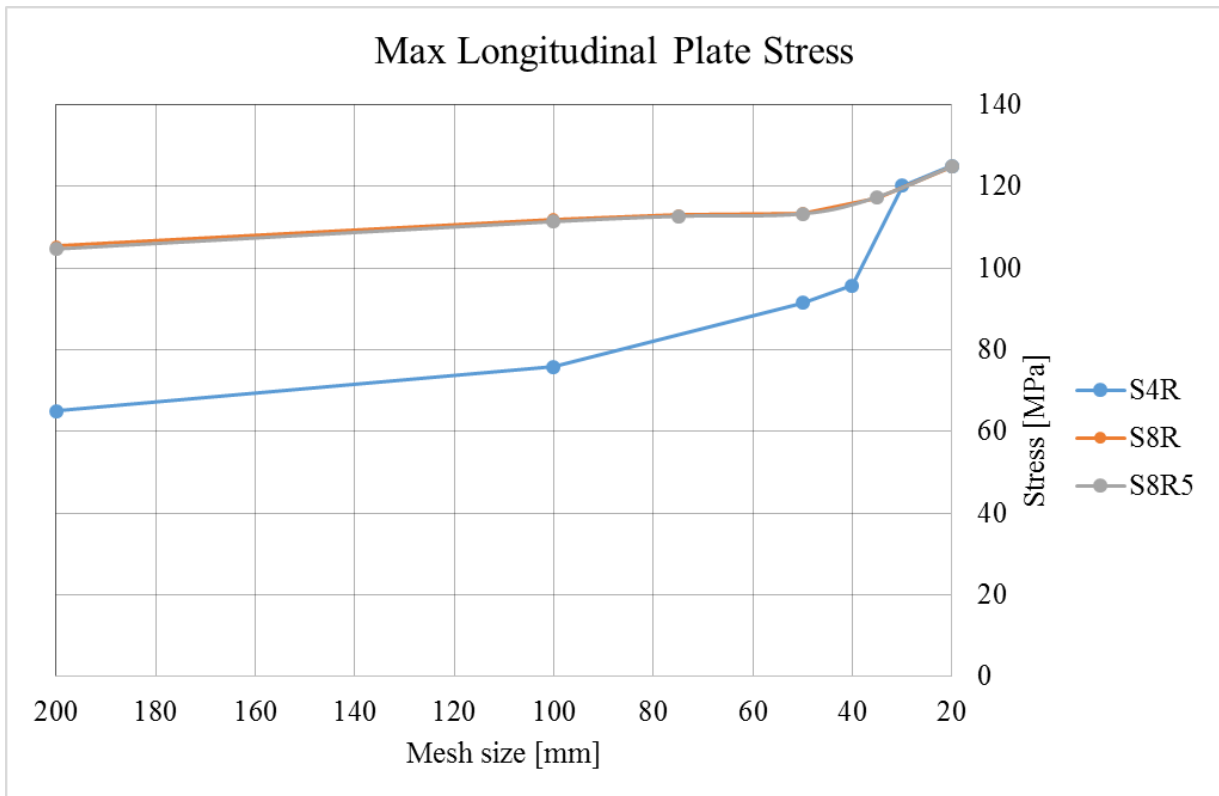
Figure 8.8 - Maximum longitudinal plate stress.
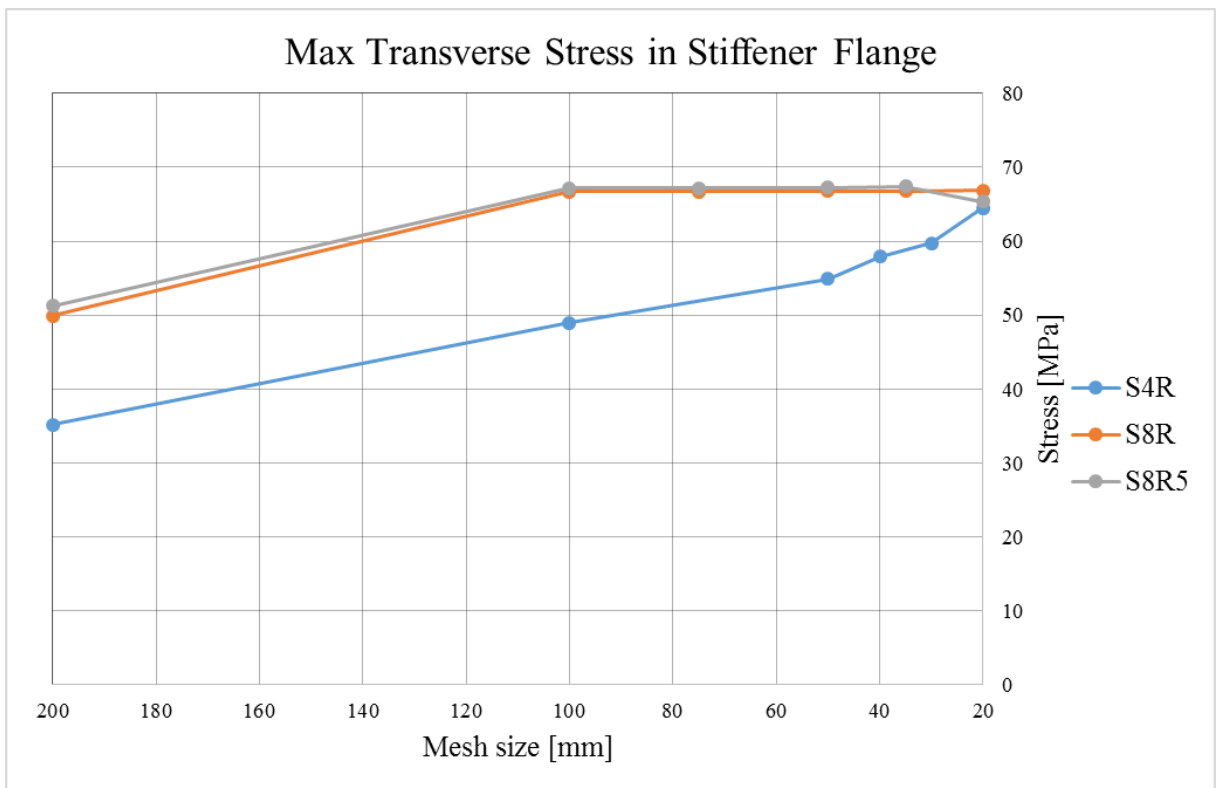
Figure 8.9 - Maximum transverse stress in stiffener flange.

66
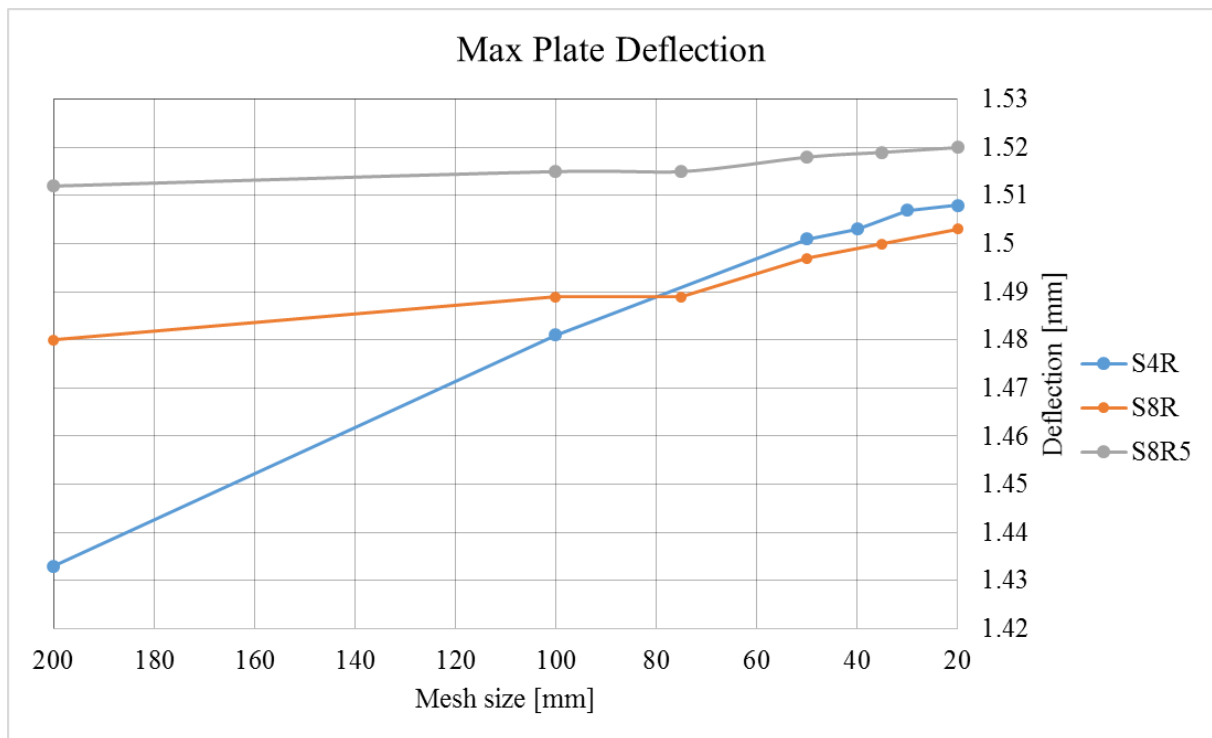
Figure 8.10 - Maximum plate deflection.

As can be seen from Figure 8.8 and Figure 8.9 the quadratic S8R and S8R5 elements gives higher and more even stresses than the S4R element, which coincides with DNV (2013). The mesh must be much finer for S4R than for S8R and S8R5 in order to get stresses of similar magnitude. However, the S8R element requires significantly more computational time than the two others and is only applicable for thick shell problems. Figure 8.10 shows that the differences in calculated displacements, between the three element types, are small when the mesh size is around 80 mm or less.

The convergence check model have a plate thickness of 40 mm and stiffener spacing of 0.8 m which means that the thickness/span ratio is 1/20. Thus S8R elements are not applicable to this problem, according to ABAQUS (2014). The smallest stiffener spacing in the main model is approximately 0.58 m. In those areas the thickness/span ratio is 2/29, barely a thick shell problem. As a consequence S8R elements are found not applicable on the main model.

Based on the results from the convergence check the optimal element for these analyses seems to be S8R5, however when using this element for the ice belt model the analyses crashes. The author has not been successful in determining the source of these crashes, but has a feeling that it probably has to do with either the geometry of the model, the mesh or the boundary conditions applied. Therefore the analyses given in this thesis have been performed by use of the S4R

element with a global mesh size of 100 mm. If the results from the convergence check is taken as a standard the chosen element with corresponding mesh size may give non-conservative stresses. This is given some attention in the parameter study in section 9.1.5.

8.4 Loads

There are three loads applied to the structure in this thesis; a hydrostatic load, an axial load due to platform weight and buoyancy, and a local ice load.

8.4.1 Hydrostatic

Although the hydrostatic load is much lower than the two other loads, it is still present and thus applied to the structure in the analyses. The pressure varies linearly from maximum at the bottom of the model to zero at the waterline, which is 3 m above. The pressure is calculated from (7.1) which gives a maximum pressure of 30.166 kPa. Figure 8.11 shows the hydrostatic load acting on the structure.

$$p_{HS} = \rho_{sw} \times g \times h \tag{7.1}$$

Where

p_{HS} is the hydrostatic pressure in Pa

ρ_{sw} is the density of sea water, equal to 1025 kg/m^3

g is the acceleration of gravity, equal to 9.81 m/s^2

h is the depth, at maximum equal to 3 m
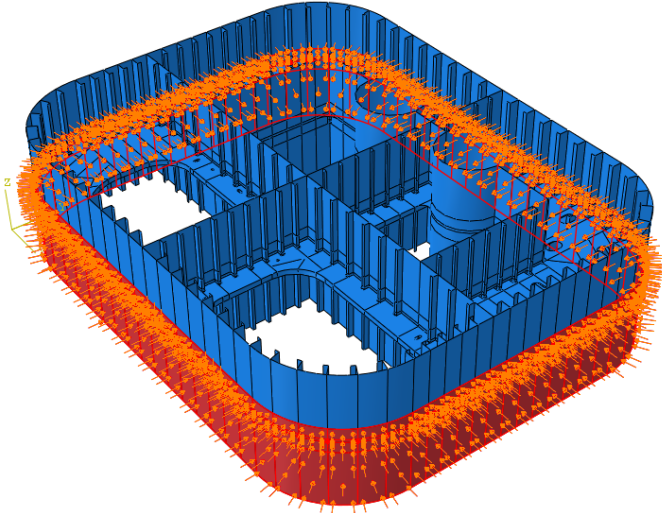
Figure 8.11 - Hydrostatic load.

8.4.2 Axial

Deepsea Stavanger has a displacement of 51742 tons at operational draught. This weight is of course carried by the four columns and is, in still water, presumably divided equally between the columns. However, as the platform moves so does its center of gravity, this causes the columns to carry different weights. In this thesis it is assumed that the column in question carries half of the platform weight, in order to be on the safe side. This load is applied as an edge load on the top edge of the model and has a magnitude of 1.48 MN/m. Figure 8.12 shows the axial load acting on the structure.
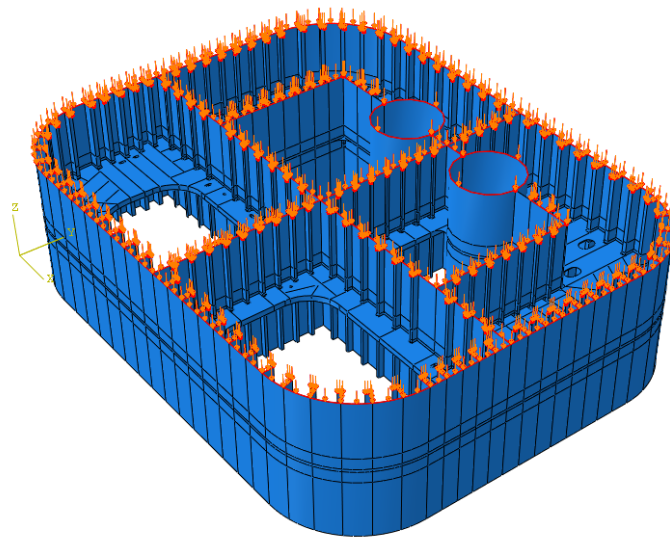
Figure 8.12 - Edge load accounting for platform weight.

8.4.3 Local Ice load

The local ice load applied in the analyses presented in sub-chapter 9.1 is the load from ISO which is discussed in sub-chapter 5.6. Due to the size effect, which is included in the load calculation method from *ISO 19906*, it is not given what the design load areas for the different components are. Thus, some assumptions regarding the design load areas, which are given in this section, have been made. In sub-chapter 9.2, increasing ice loads are applied to the structure in order check capacity with respect to yielding and ultimate stress. The design load areas used in the capacity check (sub-chapter 9.2) are the same as used in the analyses in sub-chapter 9.1.

The design load area for the plates are assumed to be a plate component between two stiffeners and two stringer plates. Since there is only one stringer plate in the model the design area of the plate will be close to a boundary. This enhances the importance of realistic boundary conditions.

Considering the stiffeners, the author has done some experiments in order to find the design load area. The same model as for the convergence check was used and two cases was examined; loads on one stiffener and loads on two stiffeners. Cases with more than two stiffeners was not studied due to the results obtained from the initial experiments. For the case with loads on one stiffener the load width was set to be equal to the stiffener spacing while the load height was varied. For the case with loads on two stiffeners the load width was set to be twice the stiffener spacing, also with varying load height. The results shows that the stiffener stresses was largest when only one stiffener was loaded, as shown in Figure 8.13. Thus it is assumed that the design area for the stiffeners has a height of 1.2 m and a width equal to the stiffener spacing.
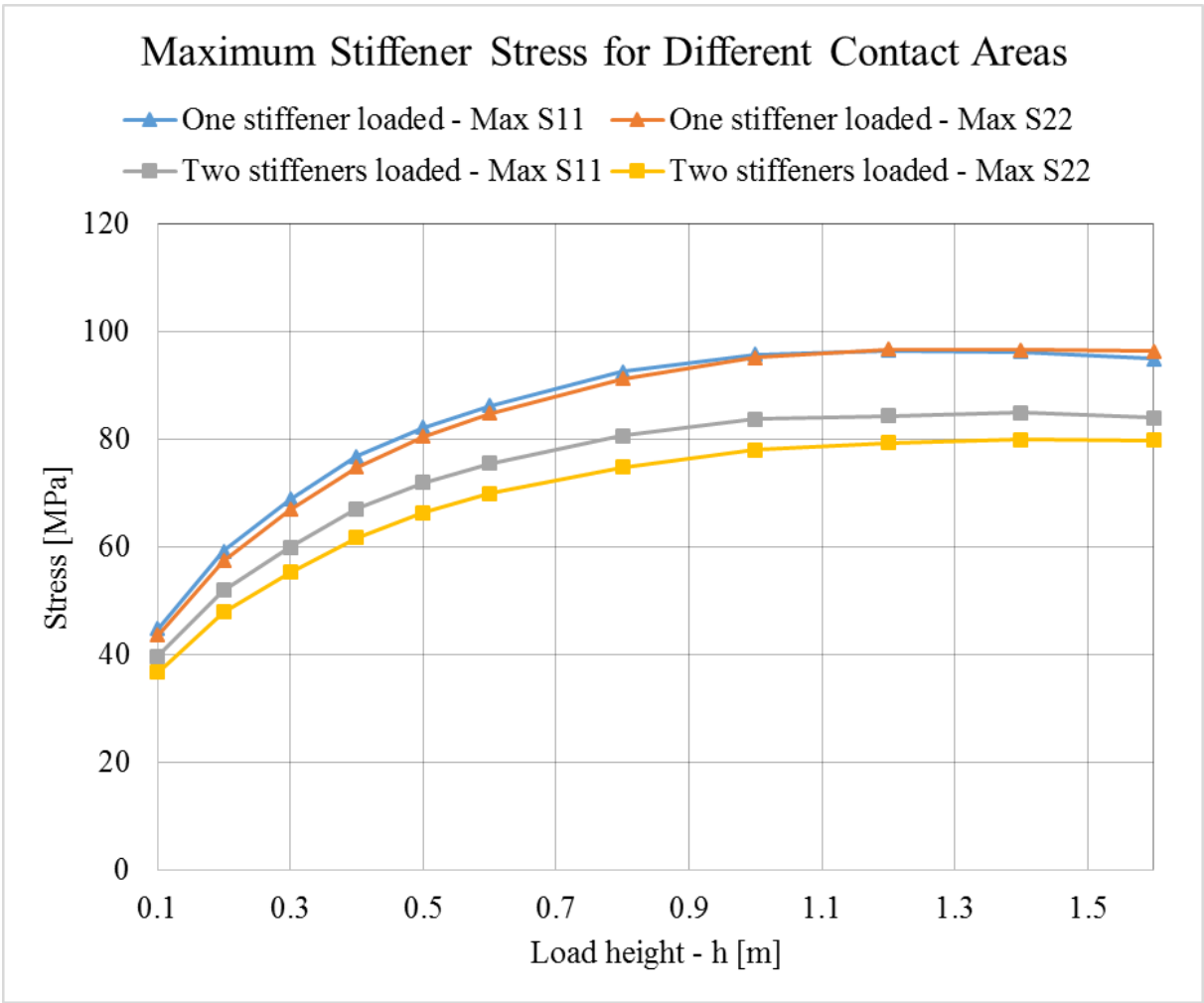
Figure 8.13 - Maximum stiffener stress for different contact areas.

Considering design load for bulkheads it is assumed the largest load effects will come from a loaded area that is 2.5 m high and has a width equal to the stiffener spacing.

The stringer has a geometry that varies from location to location on the structure. This makes it highly challenging to find the most critical loading area. In the simulations it has been assumed that the design load area is 1 m high and has a width equal to four times the stiffener spacing of the location where it is loaded.

Figure 8.14, Figure 8.15, Figure 8.16 and Figure 8.17 show a design contact for a plate, stiffener, stringer and a bulkhead, respectively.
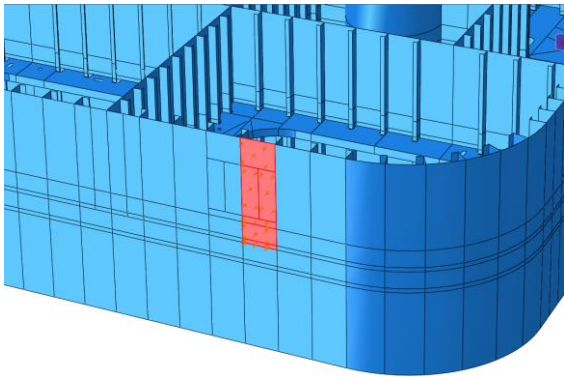

Figure 8.14 – A design load area for plate.
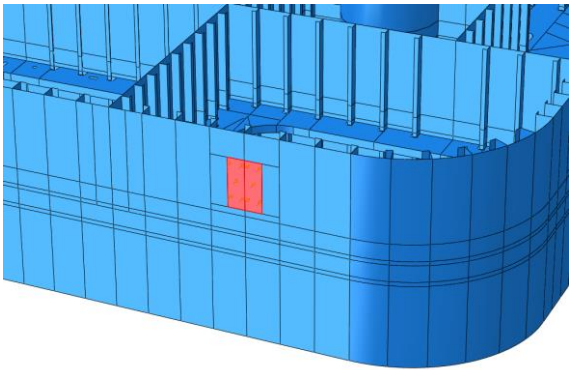
Figure 8.15 – A design load area for a stiffener.
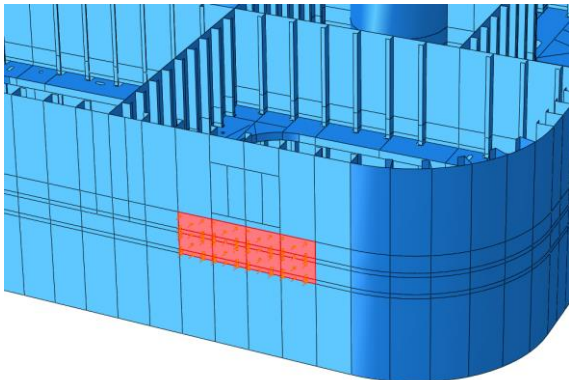
Figure 8.16 – A design load area for the stringer.
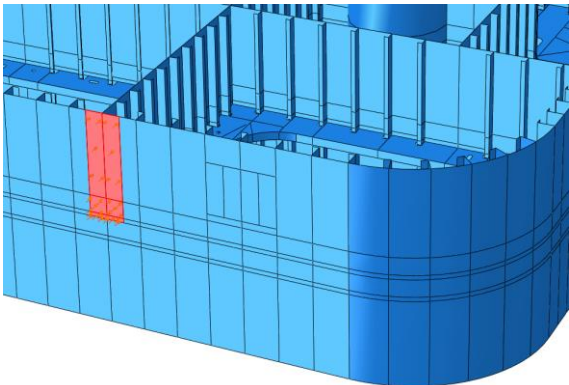
Figure 8.17 – A design load area for a bulkhead.

8.5 Boundary Conditions

Boundary conditions are in general very important FE analyses. In order to get the best possible results realistic boundary conditions are required. However, if realistic boundaries cannot be defined, the boundaries should always be defined in a way that gives conservative results.

For the ice belt model two alternative boundary conditions are considered;

- Fixed against all translations and rotations along bottom and top edges of the model.

- Fixed against all translations along the bottom edges and fixed against horizontal translations along the top edges of the model.

If the model is fixed against all translations and rotations along the top and bottom edges of the outer shell and stiffeners, there will be unnaturally high stresses in the boundaries close to the ice loads. However, out in the field, the consequence of this boundary condition is smaller deformations and lower stresses.

By only fixing the top and bottom edges against horizontal translation, one allows for the structure to deform more than it probably would in reality. The consequences of this boundary condition are larger deformations and higher stresses in the field that it would be in the reality. For the problem in this thesis, it is necessary to fix the bottom edges against vertical translation in order for the structure to be able to carry the axial load. When the bottom edges of the stiffeners are not able to move vertically, they are basically not free to rotate there either.

In general the boundaries will translate and rotate if the loads are high enough. By fixing the boundaries completely, one creates stiffer boundaries than the adjacent structure will provide in reality. By letting the boundaries rotate freely, one will give the structure a freedom which it does not in reality have.

Since the adjacent structure are expected to be less stiff than the ice belt, and due to the conservative stresses that is expected to be the consequence, the chosen boundary condition for the ice belt model is the boundary condition which enables rotation. The design loads for the plate, stiffeners and bulkheads are then to be applied on the top part (above the stringer) of the model, since the bottom edges are fixed against translation in the vertical direction. Figure 8.18 shows the boundary conditions of the model.
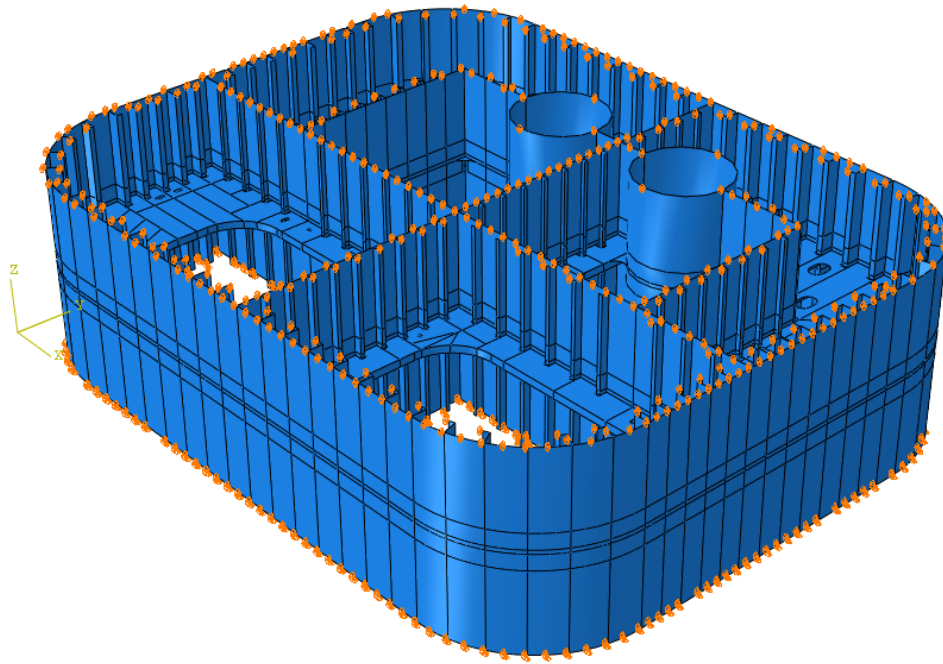
Figure 8.18 – Boundary conditions of the ice belt model.

8.6   Analysis Step

The step module in Abaqus is where the type of analysis and its properties are chosen. It is possible to solve many different types of problems by use of Abaqus and thus there are several different types of analyses to choose from. When an analysis type is chosen one must decide what properties it is to have. Examples of such properties are the time period, linear or nonlinear geometry, damping factors and incrementation.

The types of analysis used in this thesis are the static, general type and static, Riks type. Nonlinear geometry is switched on in both types, enabling for large deformations. For the static, general analyses the time period is set to 1 second. The incrementation type is set to automatic and the default increments of the analysis are used. The solution technique is set to full Newton. For the static, Riks analyses the default settings for incrementation and equation solving are used. These analyses stop when the defined maximum increment is reached. For this case, the maximum set to be 100.

9 Nonlinear Static Analyses

This chapter presents the different structural analyses that are performed of the model and their corresponding results. The structural response due to design loads on plates, stiffeners, bulkheads and stringer have all been analyzed separately. In all analyses axial and hydrostatic loads are applied, in addition to ice loads. The chapter consists of the following two parts;

- A check of how the PC4-classed structure responds to the local loads that *ISO 19906* give for the different design contact areas.
- A capacity study of the structure with steadily increasing loads.

The local ice loads are applied to the structure without considering which areas that are most probable to interact with ice, but rather what areas that are critical with respect to structural response. This means that the ice loads are, to large extent, applied in areas where the structure is expected to be weakest. However, some areas which are assumed to be stronger are also loaded with ice loads, but this is more for the sake of comparison. For readers to easily understand which areas that are examined in the different analyses the different parts of the ice belt has been given names. Figure 9.1 shows the naming of these parts.
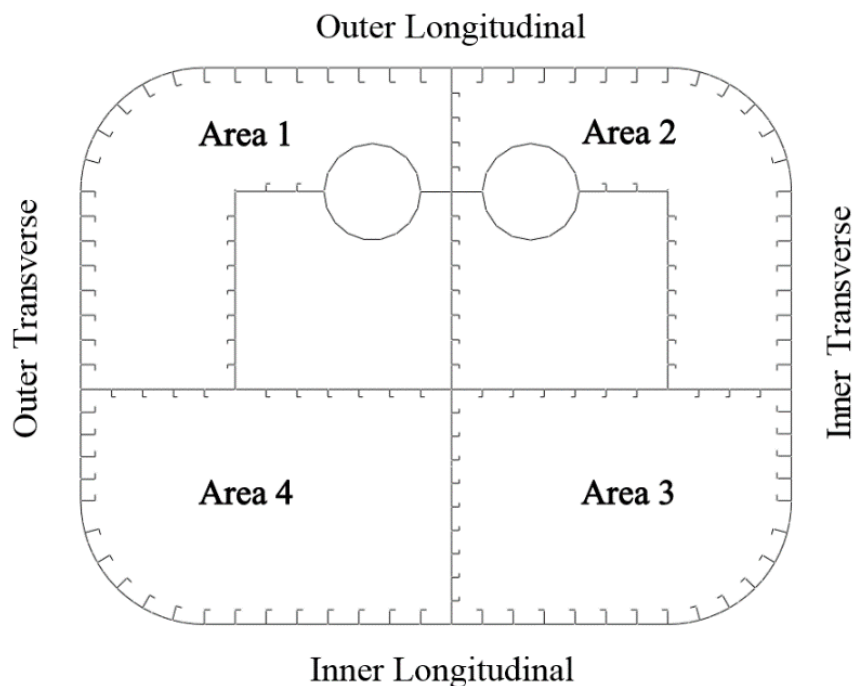

Figure 9.1 – Naming of the different parts of the ice belt.

9.1 Structural Response due to ISO Design Load

The analyses presented in this section are conducted in order to see how the local load from *ISO 19906* affect a structure dimensioned after the *Polar Code's* PC4 class. While studying the results from these analyses it is important to be aware of that the loads applied do not account for ice classes, but rather for extreme-level ice events (ELIE) in general. ELIE-loads are according to ISO:19906 (2010) to be used for Ultimate Limit State (ULS) design conditions.

For the analyses in this section, the ULS design criterion is chosen to be governed by a maximum allowable stress equal to the yield stress, i.e. 346.4 MPa. Ideally the maximum allowable design stress should be lower than the yield stress, but the mistake made in the dimensioning makes the structure weaker than intended. Therefore the yield stress may be of a more suitable magnitude, as a maximum allowable stress, than a lower stress would be.

Since the model is fairly large, only certain areas of it is examined. As mentioned in start of Chapter 9, the selection of areas examined are based on where the author thinks the structure is weakest and where it is strongest. For example Area 3 are examined in a large number of the analyses since it is the area with the least internal structure of the four main areas, and thus it is expected to be the weakest part of the ice belt.

9.1.1 Plate

This section presents the results from analyses where the ice belt has been exposed to design load cases for the plates. Six different analyses have been performed; two for plates on the longitudinal sides, two for corner plates, one for the large plates on the transverse sides and one for the small plates on transverse sides. The results are presented in 9.1.1.1 and 9.1.1.2. There are four different sizes of the design plate areas. These areas, along with their respective ISO load are given in Table 9.1.

Table 9.1 – Design loadcases for plates.

Design Plate Area [m^2]		ISO Design Pressure [MPa]
Plates on longitudinal sides	2.00	4.56
Corner plates	2.09	4.42
Small plates on transverse sides	1.44	5.73
Big plates on transverse sides	1.60	5.33

9.1.1.1 Results from the different cases

The plates that have been checked on the longitudinal sides are in Area 2 and Area 3. These plates have different surrounding structure and therefore give different response, although they are loaded with the same load. Area 3 is the area where the stringer structure is expected to be weakest, while the stringer structure is relatively strong in Area 2. As can be seen from Figure 9.2 and Figure 9.4, the stresses due to plate design load in Area 3 are higher than the ones in Area 2 (grey areas are areas with stress equal to, or higher than, yield stress). This implies that the stringer geometry have a significant influence on the stresses in plate and stiffeners. Figure 9.3 and Figure 9.5 show that the maximum plate deflection is twice as high in Area 3 as in Area 2. The large difference in deflection between the two areas is assumed to be the result of plastic deformation in Area 3.
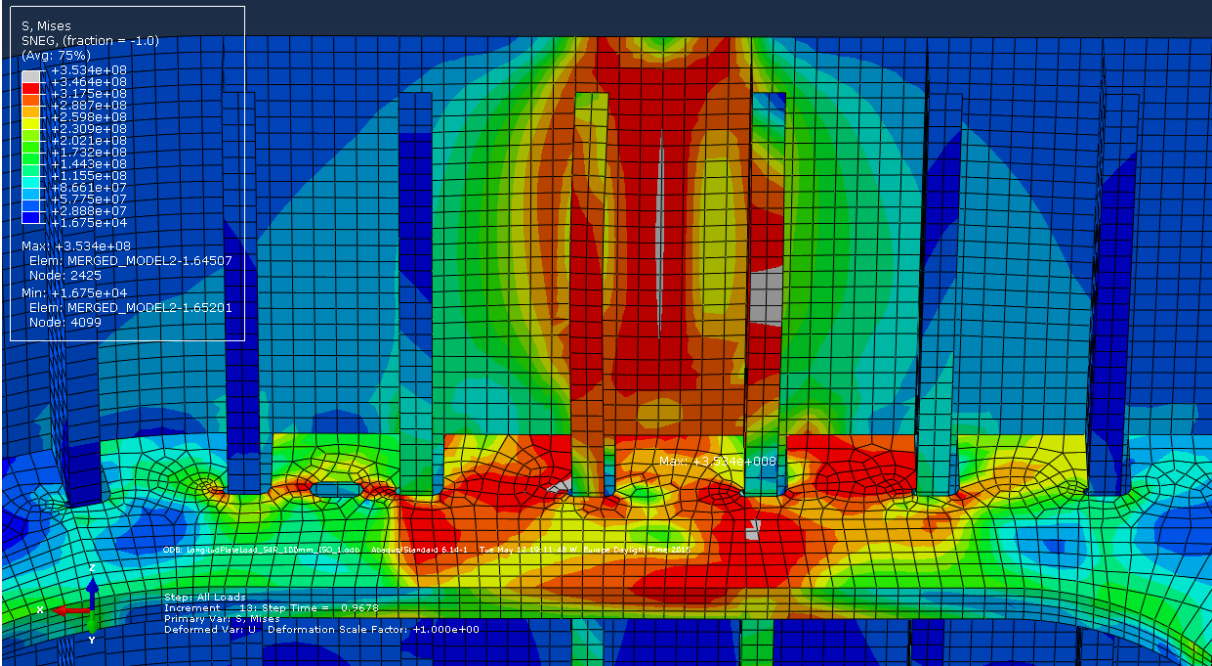
Figure 9.2 – Response in von Mises stress due to design plate load at longitudinal side in area 3.
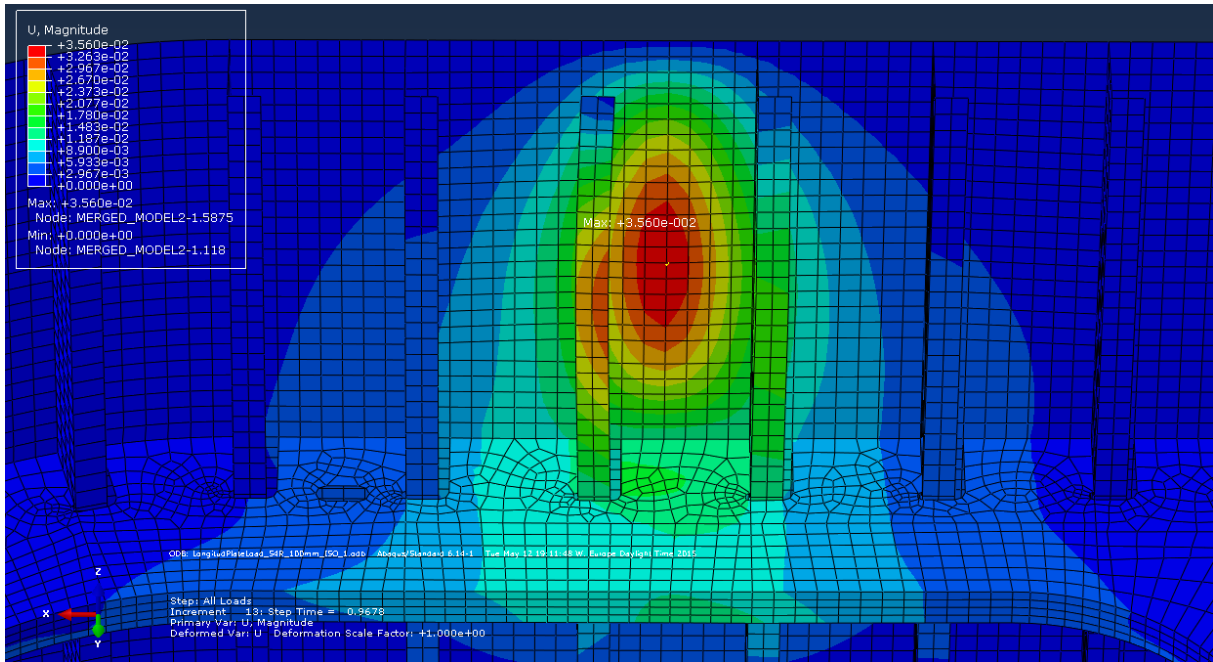
Figure 9.3 – Response in displacement due to design plate load at longitudinal side in area 3.
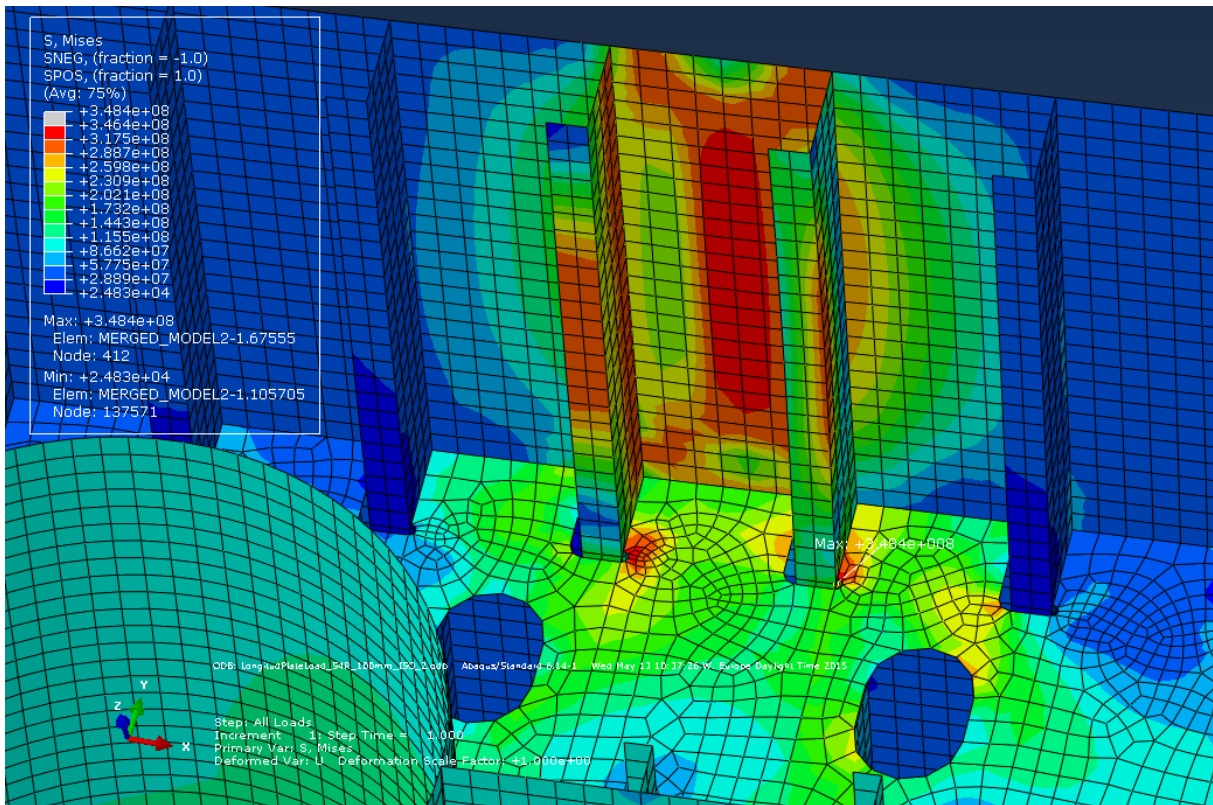

Figure 9.4 - Response in von Mises stress due to design plate load at longitudinal side in area 2.
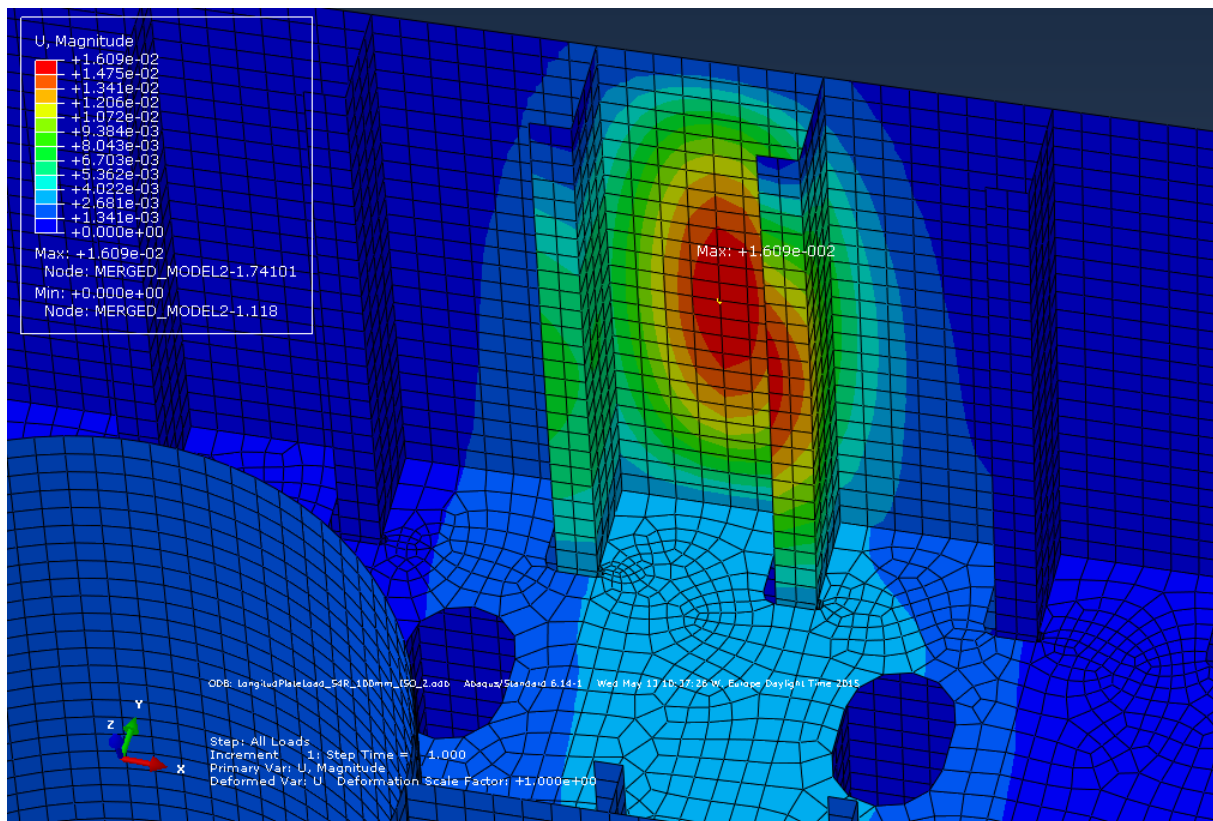
Figure 9.5 – Response in displacement due to design plate load at longitudinal side in area 2.

The corner plates examined are in Area 1 and Area 3. The results from the analysis of the corner plates in Area 3 shows that yielding occurs both in the plate and in the stringer, while for Area 1 there is only yielding in the plate. It should be noted that stresses, in Area 1, are generally close to yield in an area of approximately the same size as the load area, i.e. around 2 m². Maximum plate deflection are in both cases larger than 3 cm. The two stiffeners that forms the boundaries of the plates deform asymmetrically due to their cross sectional shape (L-bars). The stiffener to the left deforms almost as much as the center of the plate, only in the sideways direction. The stiffener to the right shows a significantly smaller deformation in the sideways direction. Figure E.1 and Figure E.3 show the stress distribution for the two cases, while Figure E.2 and Figure E.4 show the displacements.

The small plate in the transverse direction that is examined is also located in Area 3. As shown in Table 9.1, this is the load case with the highest applied pressure. The maximum stress in the plate is lower than yield, however, in large parts of it, the stress level is close to yield magnitude. This applies for the stiffeners as well. The maximum stress in the analysis is found in the stringer where several areas yield. In addition, the largest deflection is also found in the stringer

plate, something which might imply buckling. Figure E.5 and Figure E.6 give the stress distribution and displacements, respectively, for this case.

The examined large plate in the transverse direction are located in Area 2. The analysis gives similar results as the analysis for the small plate does. As can be seen from Figure E.7, there is no yielding in plate or stiffeners although stresses are close to yield stress. The difference between the two analyses lies in the stringer. Stresses are generally lower in the stringer, which makes sense since it is larger and has stiffeners going in the same direction as the load. Still, there is some yielding in the stringer plate. Maximum displacement for this case is found to be in the flange of the stiffener to the left of the plate (seen from Figure E.8), at the middle of the stiffener span, where it is 2.24 cm.

9.1.1.2 Summary

The stresses obtained from the analyses are generally high. Maximum stress in all the analyses exceed the yield stress to some degree. Even though the analyses are conducted with respect to design conditions for the plates, there are high stresses both in the stringer and stiffeners. In fact maximum von Mises stress are often located in the stringer.

The stress in plates and stiffeners in areas with the largest stiffener spacing, i.e. in corners and on longitudinal sides, are generally higher than in areas with smaller stiffener spacing. In areas with small stiffener spacing the highest stresses are found in the stringer, while they are lower than yield in plate and stiffeners. It can also be seen that the stringer structure influences the stresses in stiffeners and plates. The plates and stiffeners in areas with massive stringer structure have lower stresses and deformations than in areas where stringer structure is more modest. Thus the most critical area in terms of structural response, when a plate is loaded, is the on the longitudinal side of Area 3 (Figure 9.2).

9.1.2 Stiffeners

In this section the results from the analyses with design loadcases for the stiffeners are presented. Two different analyses has been conducted considering design stiffener loads. These are on the longitudinal and transverse sides in Area 3. Table 9.2 gives the design loadcases for the stiffeners, while the results follow in 9.1.2.1 and 9.1.2.2.

Table 9.2 – Design loadcases for stiffeners.

Design Stiffener Area [m^2]		ISO Design Pressure [MPa]
Stiffeners on longitudinal sides	0.96	7.61
Stiffeners on transverse sides	0.69	9.56

9.1.2.1 Results from the different cases

For the case with design load on a stiffener on the longitudinal side in Area 3, the results show yielding in the two adjacent plates and the stringer, in addition to both in the web and flange of the stiffener itself. The bracket beneath the stringer also show significant yielding in the connection to the stiffener. The maximum stress occurs in the stringer plate, in a cut-out near the stiffener web. The maximum stress is approximately 400 MPa. The maximum deflection is 5.6 cm and occurs at the middle of the stiffener span in the flange. The stiffener is loaded so that the center of the load patch is located at the middle of the stiffener web, and since the stiffener has an L-shape, this cause sideways deformation. In fact, the sideways deflection in the at the point of maximum deflection is around 5 cm, while in the load direction it is only around 2 cm. Figure 9.6 and Figure 9.7 show the results in terms of von Mises stress and displacements respectively.
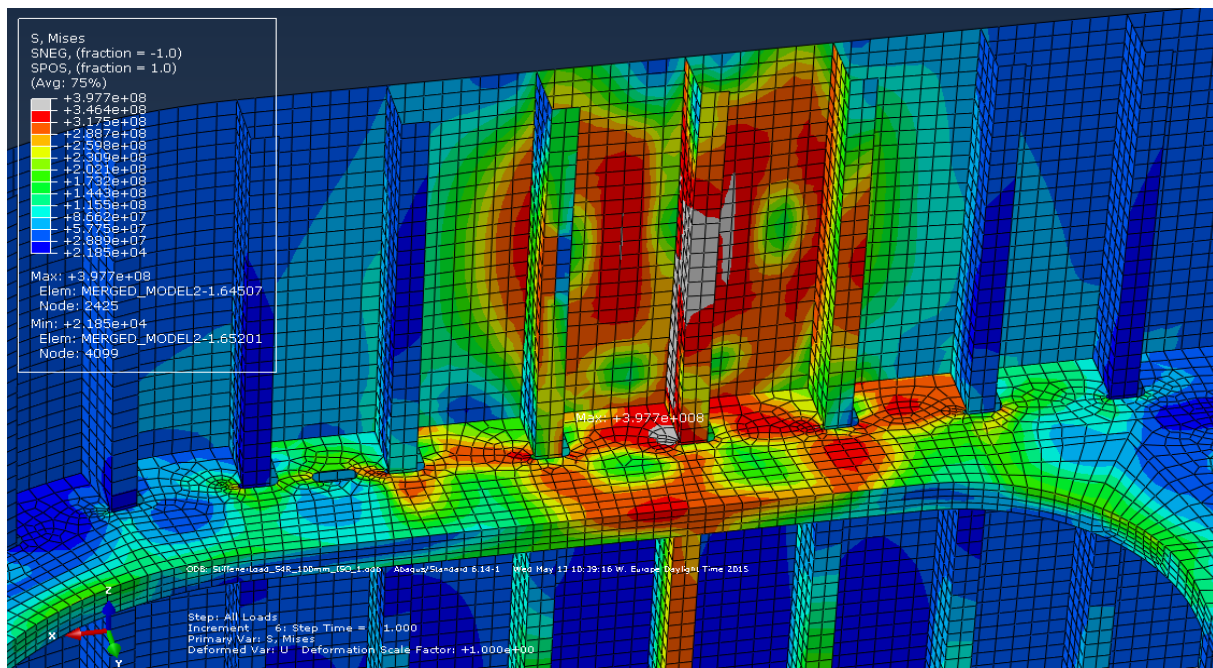

Figure 9.6 – Response in von Mises stress due to design stiffener load at longitudinal side in area 3.
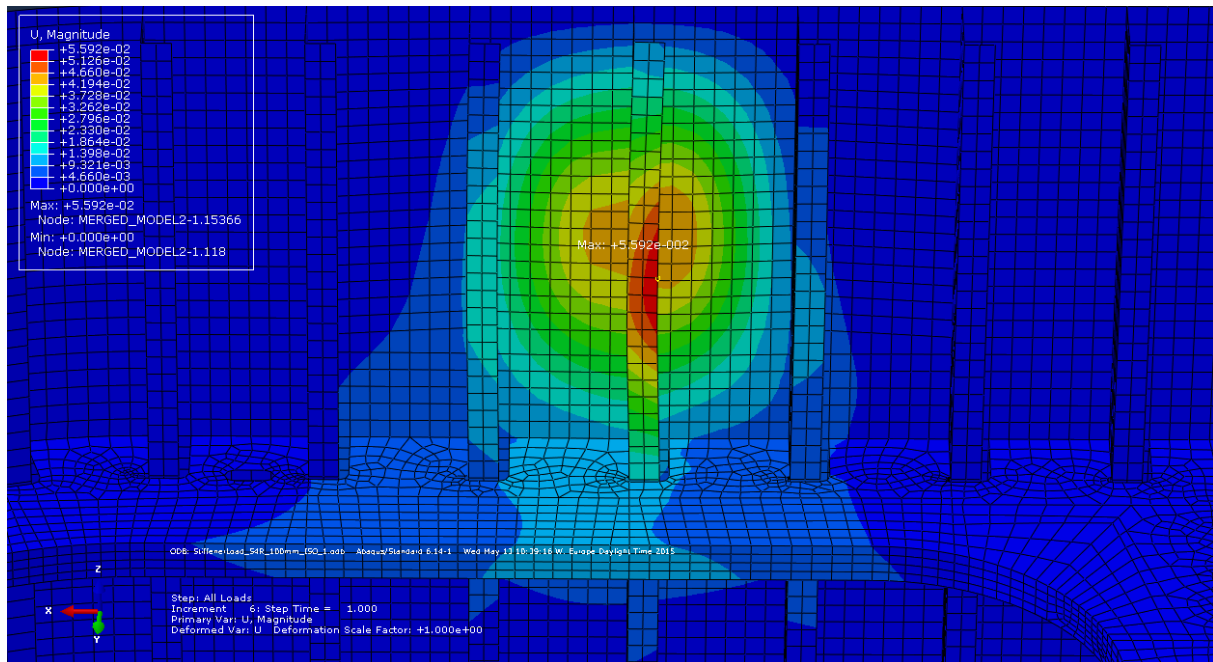
Figure 9.7 – Response in displacement due to design stress load at longitudinal side in area 3.

The stiffener loaded on the transverse side is also located in Area 3. This is where the lowest stiffener spacing on the ice belt is. Results show yielding in the stiffener, in a small part of the stringer and in the bracket connected to the stiffener. The maximum von Mises stress is 357 MPa and is located in the stringer. The maximum deflection is 2.9 cm in the flange at the middle of the stiffener span. Generally the response in this analysis follows a similar pattern, while being lower than in the previous. Figure E.9 and Figure E.10 gives plots of stress and displacements for this case.

9.1.2.2 Summary

The stresses exceed yield stress in both analyses. Where the stiffener spacing is largest, so is the response. This goes for all the components influenced by the loads. A significant difference between the two analyses in terms of response is that both the adjacent plates yield in the first analysis, while they do not yield in the second.

9.1.3 Bulkheads

In this section the results from the analyses with the design loadcases for bulkheads are presented. Table 9.3 gives the design loadcases while the results are presented in 9.1.3.1 and

9.1.3.2. Four analyses have been performed; one analysis for each bulkhead end. In Appendix E.3 stress and displacement plots are given for the performed analyses.

Table 9.3 – Design loadcases for bulkheads.

Design Bulkhead Area [m^2]		ISO Design Pressure [MPa]
Transverse bulkhead	2.00	4.56
Longitudinal bulkhead	1.44	5.85

9.1.3.1 Results from the different cases

From the analyses where the transverse bulkhead (the one going in the transverse direction through the ice belt) are loaded, acceptable results with respect to the design criterion are found. The maximum stress on each of the longitudinal sides are 317 MPa which is below the yield stress. The stress maxima are located in the outer plating close to their connection to the bulkhead. Even though theses stresses are lower the yield stress they are slightly higher than the proportionality stress which is 310.5 MPa. Therefore some plastic deformation occurs. This can be seen by looking at, Figure 9.8, which a plot of the equivalent plastic strain on the inner longitudinal side. The largest deformations occur in the middle of the two plates on each side of the bulkhead. The maximum deflection is, on both sides, 4.7 mm and located in the plates adjacent to the bulkheads, as shown by Figure E.12 and Figure E.14.
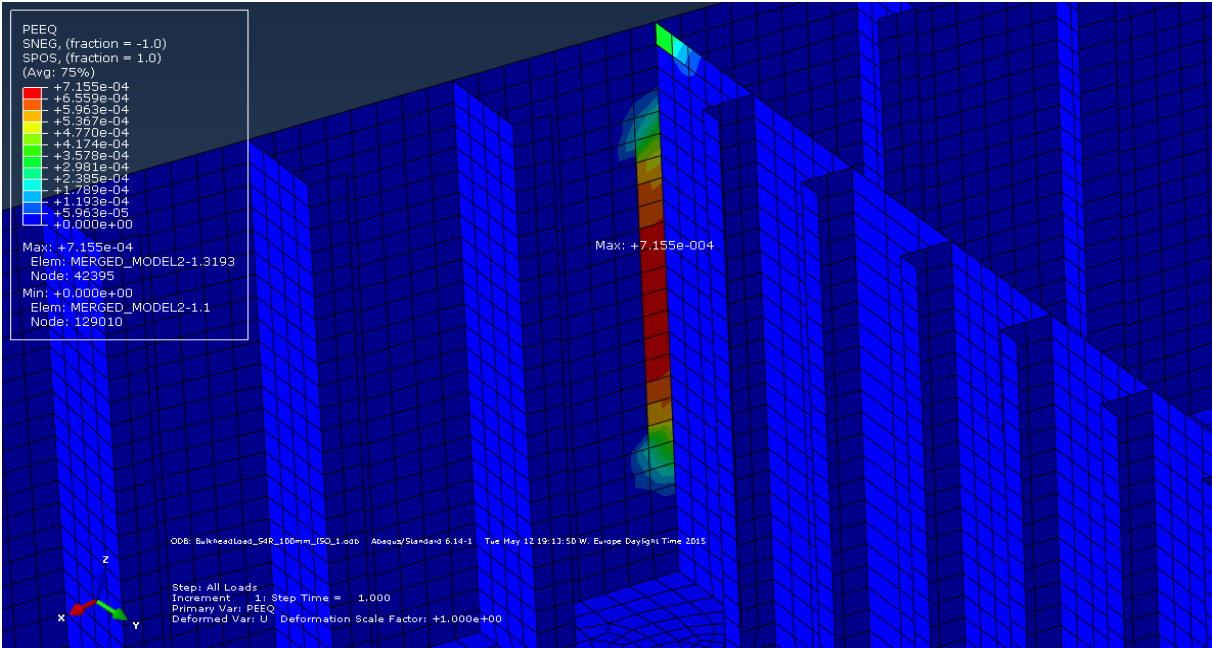

Figure 9.8 – Equivalent plastic strain due to design bulkhead load on bulkhead between Area 3 and 4.

82

The results from the analyses considering the longitudinal bulkhead are at first glance similar to those from the transverse bulkhead analyses. For these cases the stresses are slightly higher in the bulkhead itself, while it is lower in the adjacent plates. The maximum von Mises stress is still lower yield stress and higher than the proportionality stress, indicating plastic deformations of a small extent. However, when looking at the displacements it clear that there are big differences in the deformation pattern. The largest displacements found in these analyses are 8.1 mm and, as shown by Figure 9.9, located in the center of a plate component in the bulkhead. The magnitude of this displacement, and the deformation pattern in general, implies that it is the buckling effect that is seen here.
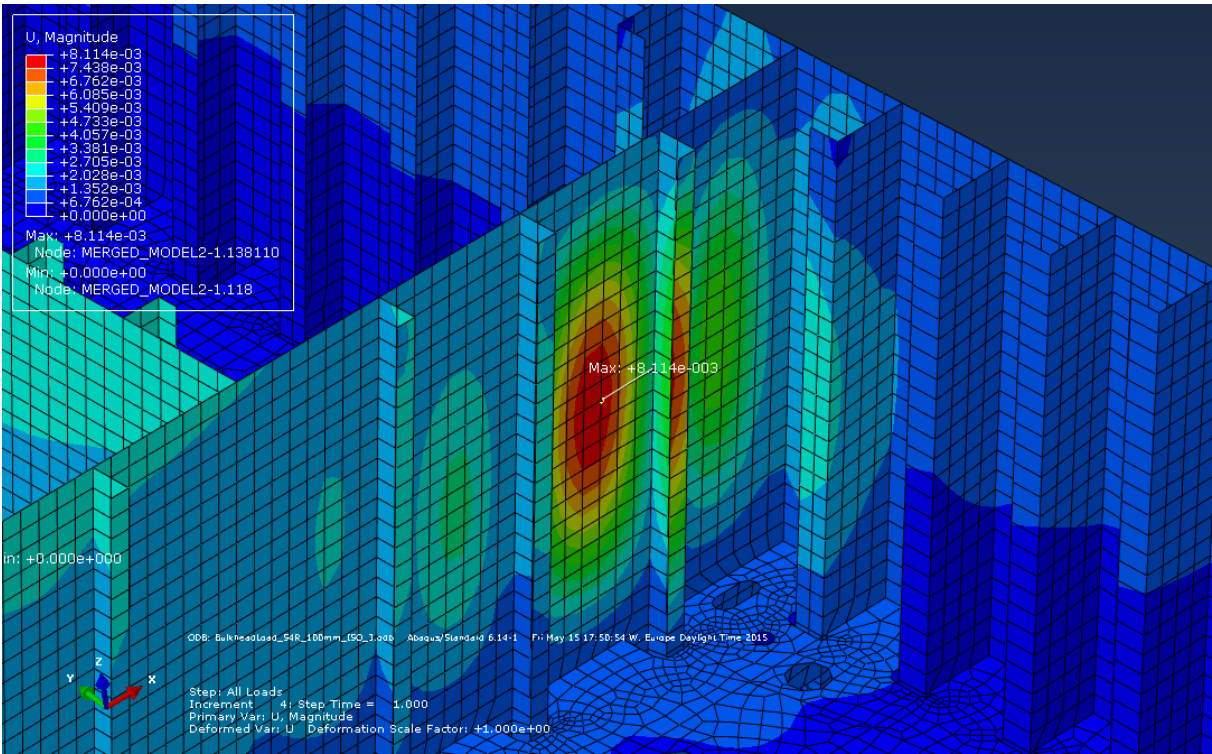
Figure 9.9 – The displacements due to design loadcase for the longitudinal bulkhead between Area 2 and 3.

9.1.3.2 Summary

The maximum stresses are lower yield, but higher than the proportionality stress for all analyses. This means that plastic deformations occur, but to a small extent. The deformation patterns of the analyses, where the longitudinal and transverse bulkhead are loaded, differs from each other. When the transverse bulkhead is loaded the largest deformations occur in the outer shell plating, while when the longitudinal bulkhead is loaded they occur in the bulkhead itself. The cause for this difference may perhaps have do with the loadcases. The main difference

between the loadcases on two different bulkhead are that for the transverse bulkhead the pressure is lower and the area is larger. Perhaps since the load is more distributed for the cases where the transverse bulkhead is analyzed, the outer shell carries more of the total load than the bulkhead.

9.1.4 Stringer

This section the presents the results from the analyses where the design loadcases for the stringer are applied to the structure. Table 9.4 gives the design load cases while the results are presented in 9.1.4.1 and 9.1.4.2. Four analyses have been performed; one in Area 4, two in Area 1 and one in Area 3. Plots of stress distributions and displacements, additional to those in the main report, for the different cases are given in Appendix E.4.

Table 9.4 – Design loadcases for stringer.

Design Stringer Area [m^2]		ISO Design Pressure [MPa]
Longitudinal sides	3.20	3.28
Transverse sides	2.56	3.83

9.1.4.1 Results from the different cases

The results from the analysis, where the stringer located along the longitudinal side of Area 4 is loaded, show yielding in a small area of the stringer. The maximum von Mises stress is 357 MPa occurs in the area that yields. Some larger areas have stresses higher than the proportionality stress, this includes two of the stiffeners. The maximum displacement is located in the outer shell plate and has a magnitude of 1.5 cm.

Regarding the stringer on the transverse side, of Area 1, the maximum von Mises stress is just lower than the yield stress. However, it occurs in a singularity point, where it in reality should be a cut-out. This point is shown by Figure 9.10. If the singularity point is overlooked stresses are quite low in this analysis compared to the one from Area 4. The largest displacements are in the outer shell plate and have a magnitude of around 5.5 mm.

When the stringer is loaded on the longitudinal side of Area 1 its response is quite similar to when it is loaded on the transverse side. The stringer structure is at its strongest in Area 1, so stresses are more modest than in Area 3 and 4. The maximum response in terms of von Mises

stress is 328 MPa and occurs in the stringer in the area between two cut-outs which are relatively close to each other (Figure 9.11). Deformations are close to identical to the other stringer analysis in Area 1, both in terms of location and magnitude.
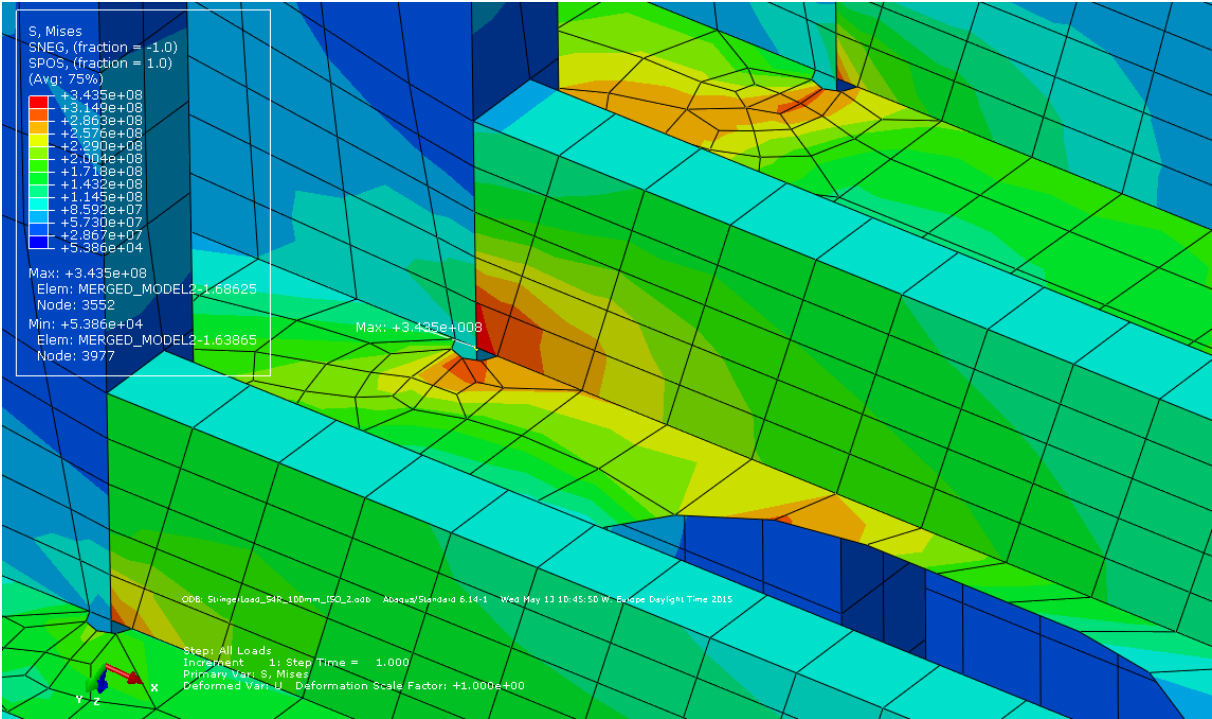

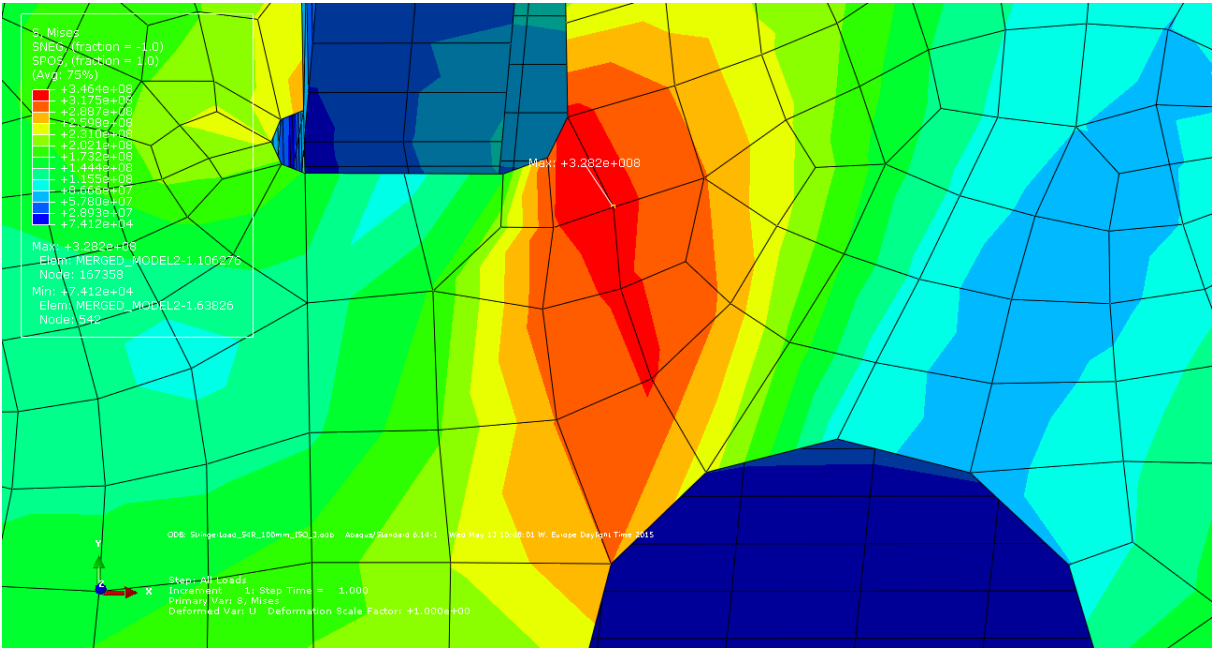**Figure 9.10 – Maximum von Mises stress occurring in a singularity point along the transverse side of Area 1.**

Figure 9.11 – Maximum von Mises stress occurring between two cut-outs in the stringer on the longitudinal side of Area 1.

As seen from the analyses both for plate and stiffener loads; Area 3 is the area where structural response is highest. This is also the case when the stringer is loaded. Yielding occurs four places in the stringer going along the longitudinal side. All these places are located near the cut-outs for the stiffeners. The deformations are almost exactly the same as for the analysis of Area 4.

9.1.4.2 Summary

Results show that it goes a clear line along the longitudinal bulkhead in terms of stringer strength. While the two analyses of Area 1 give acceptable stresses, considering the criterion defined in sub-chapter 9.1, the two analyses of stringer in Area 3 and 4 does not.

9.1.5 Parameter study

This part presents a small parameter study where the effects of nonlinear versus linear geometry, and mesh refinement have been investigated. The analyses that forms the basis for the parameter study has been performed on the longitudinal side of Area 3 where the stiffener is loaded with the design loadcase from Table 9.2.

9.1.5.1 Nonlinear versus linear geometry

The way that the effects of nonlinear geometry are checked is by running two analyses; one where small displacements is assumed, i.e. linear geometry, and one that uses the actual displacements, i.e. nonlinear geometry. The results from these analyses, in terms of von Mises stress and displacements, can be seen by comparing Figure 9.6 versus Figure 9.12, and Figure 9.7 versus Figure 9.13.

Based on the results of this check it seems like the effects are small in terms of deformation pattern. By that it is meant that the structure deforms in the same way. However, the magnitude of the displacements are not the same. When linear geometry is used the displacements are almost twice as high as when nonlinear geometry is applied. This has of course consequence for the stresses. Larger parts of the structure yields when nonlinear geometry are turned off, and in that respect it is a more conservative approach than its counterpart. However, it is more realistic to account for changing geometry and therefore it should be used when performing nonlinear FE analyses, as done in this thesis. The reason for the large difference in results is that the structure carries a larger parts of the loads by membrane (in-plane) action when nonlinear geometry is applied, than when only linear geometry is applied.
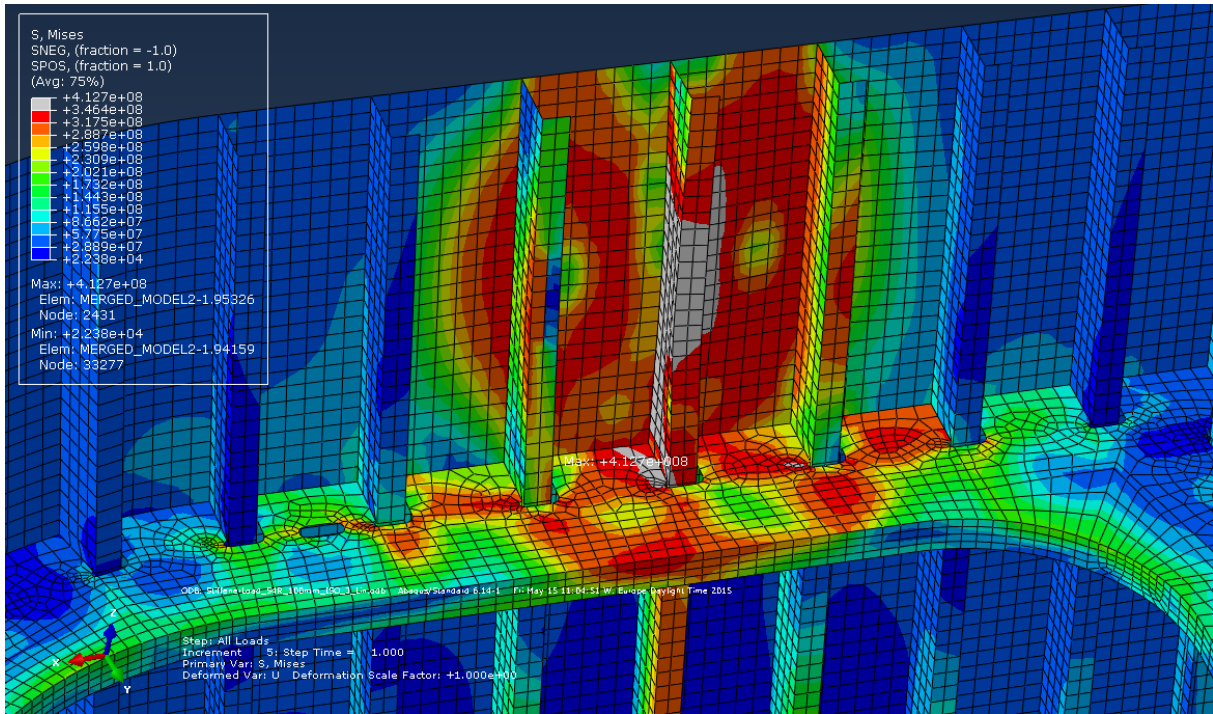
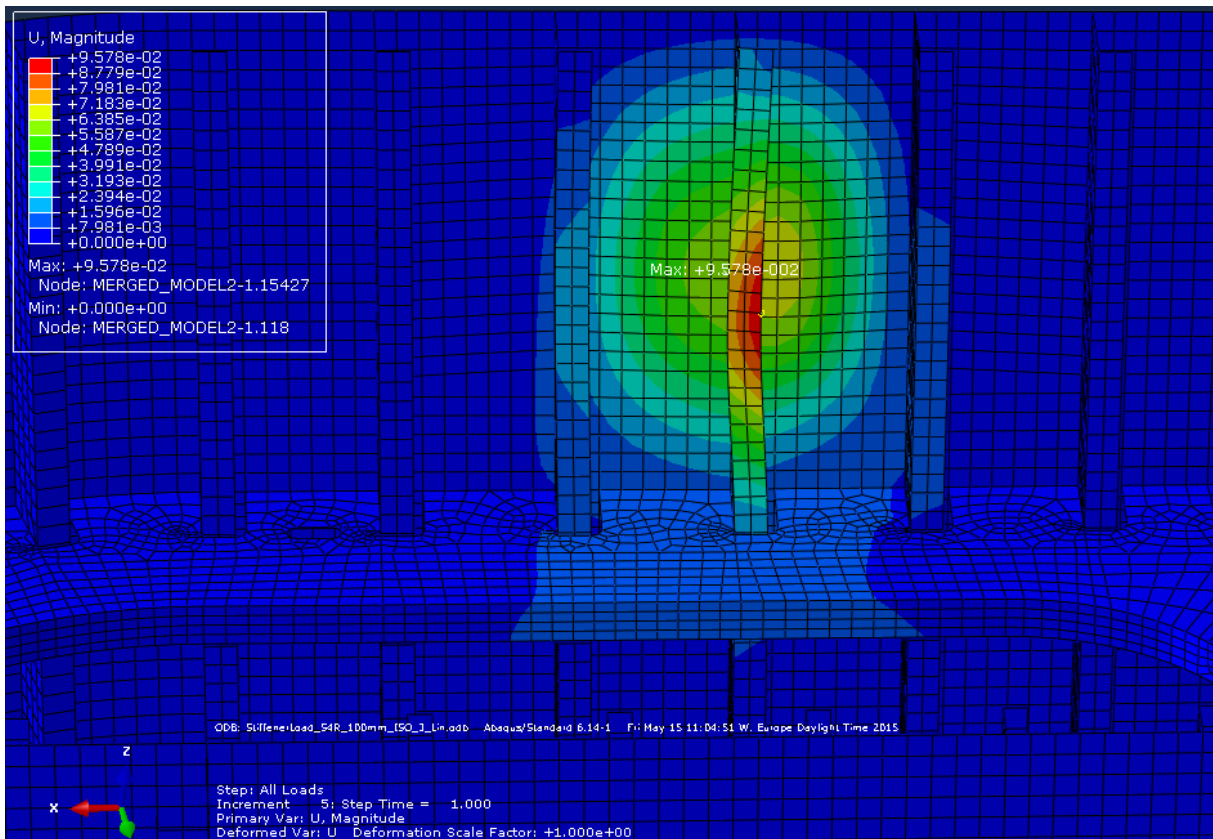**Figure 9.12 – Response in von Mises stress with nonlinear geometry switched off.**

Figure 9.13 – Displacements whit nonlinear geometry switched off.

9.1.5.2 The effects of mesh refinement

The effects of mesh refinement was studied in the convergence check in section 8.3.2. However the convergence model was only a stiffened panel. In this study the effects of the mesh size has been examined for the ice belt structure. The mesh sizes used are 100 mm, which have been used in all analyses, and 50 mm. Results can be seen by comparing Figure 9.6 versus Figure 9.14, and Figure 9.7 versus Figure 9.15, for von Mises stress and displacements, respectively.

The convergence check showed that stresses increased as the mesh became finer when using the S4R element. This is also the case for the mesh refinement study carried out here. The analysis, where 50 mm mesh size is used, gives higher stresses in general, than the one where 100 mm mesh size is used. In terms of displacements the difference is quite small. The results from this study substantiates the results from the convergence check.
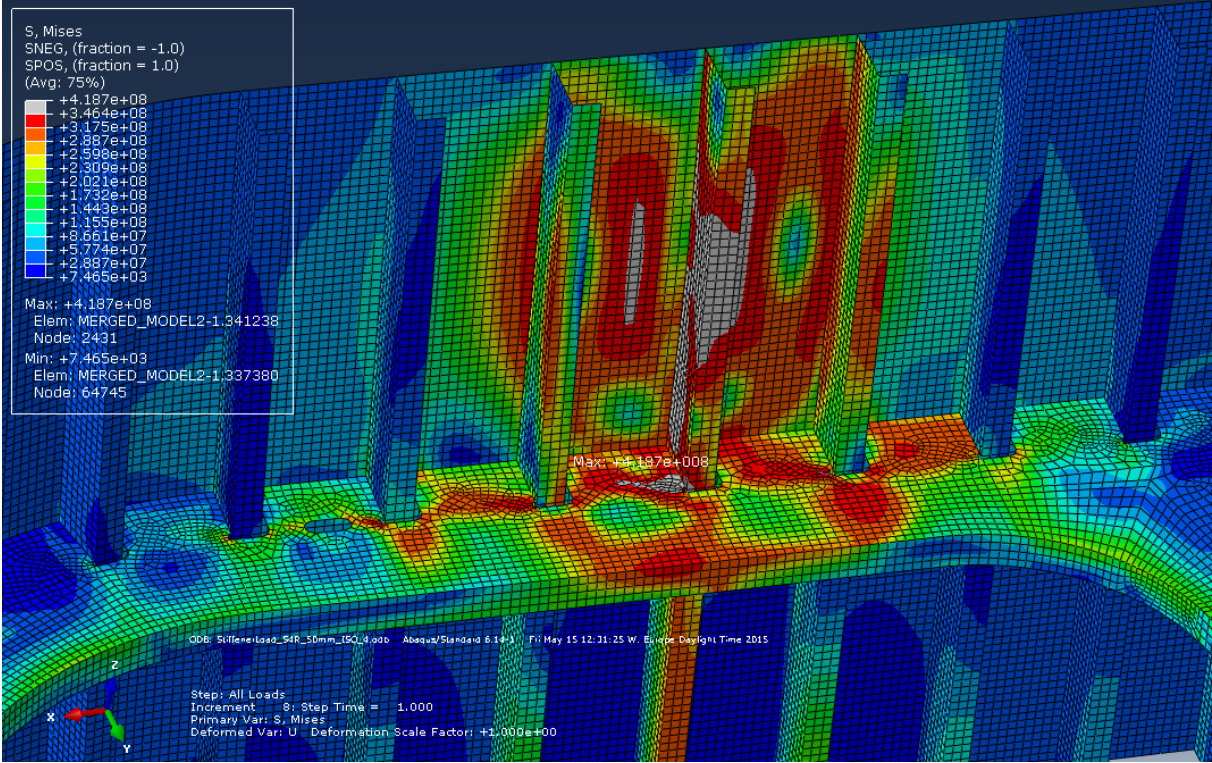
Figure 9.14 – Von Mises stress for mesh size 50 mm.
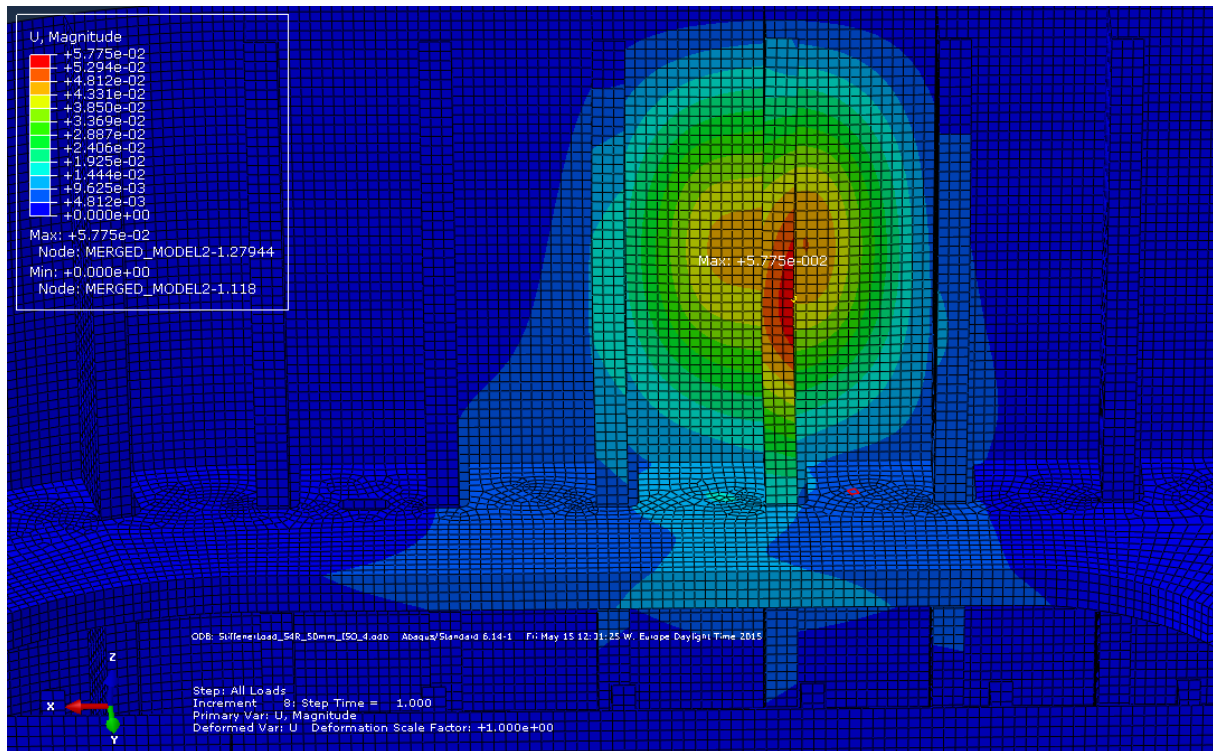
Figure 9.15 – Displacements with mesh size 50 mm.

9.1.6 Main Findings and Discussion

The results of these analyses shows that the ice belt is generally not able to cope with the loads in an adequate way, i.e. it does not comply with the design criterion of maximum allowable stress equal to the yield stress.

From the analyses with plate loads it can be seen that something has to be altered in order for the structure to comply with the design criterion. Stiffener type, stiffener spacing and configuration are all influencing factors that should be studied. Since the current stiffener type is L-bars, the plate loads are not distributed evenly between the two stiffeners on each side of the loaded plates. This is not only affecting the stiffeners, but also how loads are distributed into the stringer. By using T-bars instead of L-bars the loads would be distributed more evenly from the plate to larger parts the structure, and thus decrease the maximum stress. The plate stress is largest where stiffener spacing is largest. To avoid yielding in the plates the stiffener spacing could be reduced instead of increasing the plate thickness further. Increasing the plate thickness will make the structure heavier than increasing the number of stiffeners will. From the results it is also clear that the stringer structure has a significant influence on load effects both in the plate and the stiffeners. Strengthening the stringer in the load direction, especially

in Area 3 and 4 where the stringer is weakest, would be favorable in terms of reducing load effects.

The analyses where design stiffener loadings are applied are the ones that gives the highest stresses. Also here effects from stiffener type, stiffener spacing and stringer stiffness are seen. The stiffeners considered deforms sideways due to the stiffener type, in addition to the expected deformation in the load direction. This cause the flange to have high stress in the sideways direction and thus higher von Mises stress than it would have had if it was symmetric. The plates on each side of the stiffeners considered also yield, this effect is reduced when stiffener spacing is reduced. Also, increasing the stringer stiffness would contribute to decrease the largest stresses.

The results from the analyses where the bulkheads are loaded with their respective design loads are the ones with lowest stresses in general. This is expected due to the boundaries of the bulkheads and their orientation towards the loads. From the analyses of the longitudinal bulkhead the buckling effects can be seen. This behavior was also expected to be prominent for the transverse bulkheads as well. However, it is not. The reason why they do not behave as expected may lie in the size of the design load area, as mentioned in section 9.1.3, or it may be the result of an error in the model.

In the results from the stringer analyses there is no surprises. Response is unacceptable high in Area 3 and 4, while more modest, and adequate to comply with the design criterion, in Area 1. This has of course to do with the stringer configuration. It is generally larger and has more members stiffening itself in Area 1 than in 3 and 4. A point of concern from these analyses is the asymmetric stress distribution due to the boundary conditions. Since the boundary conditions are not exactly the same on the top and bottom of the model (written about in sub-chapter 8.5) the results are not as realistic as they would have been they had been the same.

From the parameter study it is seen that the effects from using nonlinear geometry are large. The structure becomes stiffer as it deforms and this is accounted for by this approach. It requires more computational power, since the stiffness has to be updated each step of the load, but it gives more realistic results. Regarding the mesh refinement study the results from the convergence check gained credibility since the results from the mesh refinement showed the same tendency; the stresses increase as the mesh becomes finer for the S4R element. This means that S4R element, with the mesh size 100 mm, may be giving too low stresses.

9.2 Local Capacity Study

In this section the capacity study of the model, considering local ice loads, is given. The analyses are performed by use of both the general and Riks method, and the subjects investigated for each analysis are;

- At what points and loads does the stresses reach yield first.
- At what points and loads does the stress and strain reach the capacity of the material first.

The model is subsequently loaded in the capacity study; first the axial load and the hydrostatic pressure are applied, since they are considered permanent loads, then the local ice load is applied gradually. There are four analyses in total; one for the plates, one for the stiffeners, one for the bulkheads and one for the stringer, in Area 3, 3, 2/3 and 4 respectively.

It should be noted that material imperfections, residual stresses, flaws in welds and etc. are not included in the model. Fracture is nor accounted for in the analyses, which might be unrealistic.

Additional plots, of stress and displacements, to those given in this sub-chapter can be found in Appendix F.

9.2.1 Plate

The results from the analysis with increasing plate load shows that yield stress is reached first in the bracket connected to one of the stiffeners which forms the boundaries of the plate field. The point that reaches yield is just below the cut-out in the bracket where it is connected to the stiffener as can be seen in Figure 9.16. This happens at the third increment where the load applied is 3.33 MPa. At the next increment the load is 4.05 MPa, and by then two other areas have yielded; in the stringer close to the stiffener on the other side of the plate, and in the plate itself.

The ultimate von Mises stress occurs at the same place as the first yield. In other words it is a detail that collapses first. The bracket gets pulled by the buckling stringer plate and because of

that it twists in addition to the in-plane load it gets from the stiffener. The ultimate stress occurs at the 24th increment. At this time the load is 5.25 MPa. However, even though the ultimate stress is reached in the stringer at this point, the stresses in the outer plates and stiffeners are not near reaching this magnitude. This can be seen from Figure 9.17. It should be noted that the color-scaling of the stress are different from Figure 9.16 to Figure 9.17.
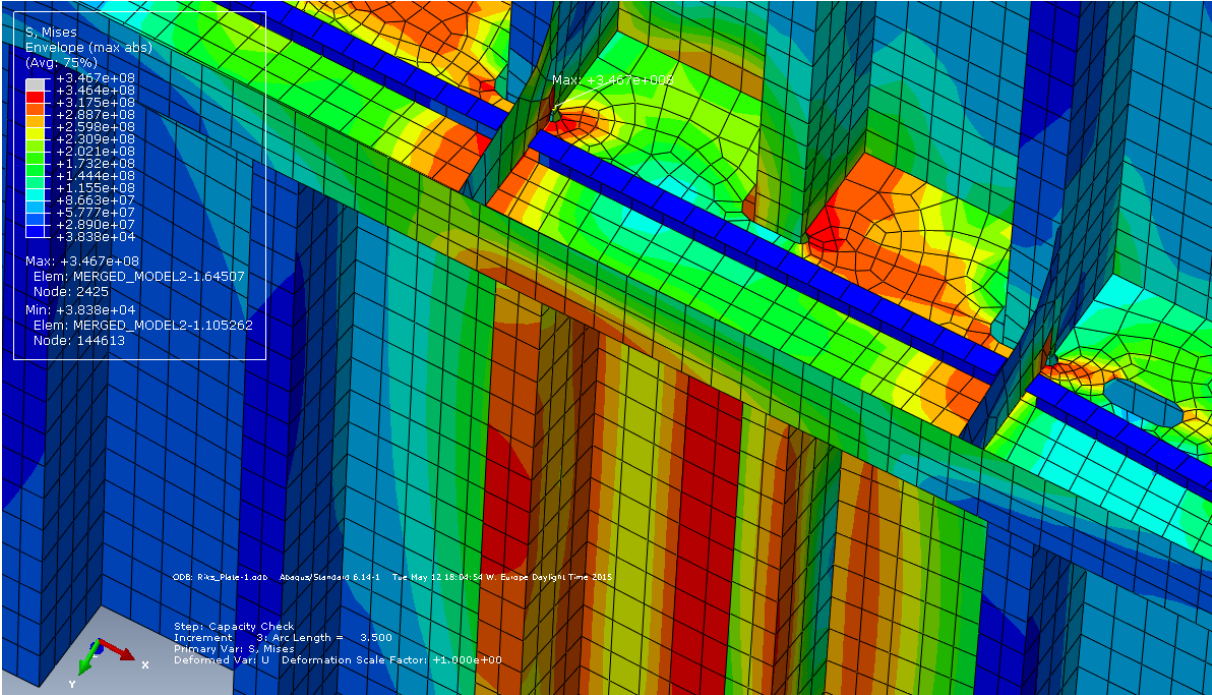

Figure 9.16 – Response in von Mises stress at first yield due to plate load.
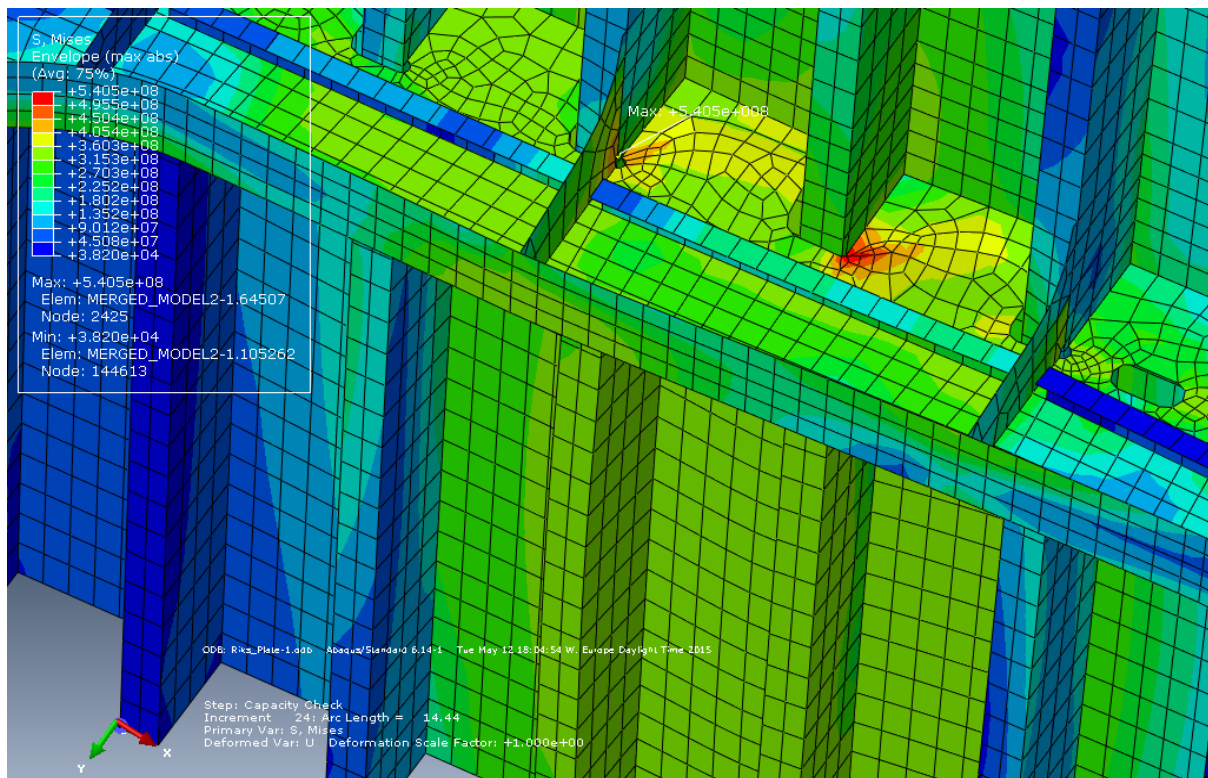
Figure 9.17 – Response in von Mises stress when ultimate stress is reached.

9.2.2 Stiffener

In the stiffener load analysis it is also the bracket that yields first, just as in the plate load analysis. The bracket is closely followed by the stringer plate in the same area, and the stiffener itself. First yield is reached at increment 4, where the load is 5.05 MPa. Figure 9.18 gives a close-up of the point of first yield.

Ultimate von Mises stress is also reached first in the bracket. This at increment 16 where the load is 10.62 MPa. By then large areas of the stiffener, outer plates, stringer plating and the bracket has yielded (Figure 9.19). Also in this case, the von Mises stress in and around the point of ultimate stress is much higher than in the rest of the stringer, stiffeners and outer plates. This implies that it is a weak point in the ice belt. The stress in the stiffener does not reach ultimate stress before increment 35. By then the load is 17.60 MPa.
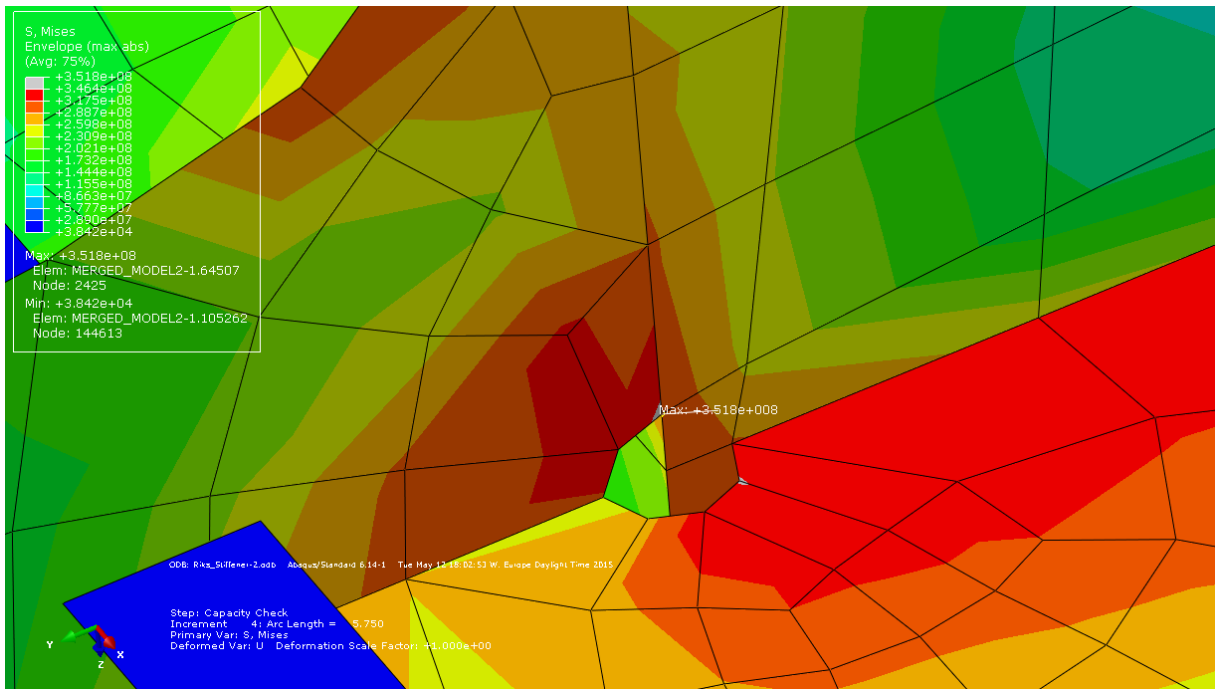
Figure 9.18 – Close-up showing point of first yield due to stiffener load.
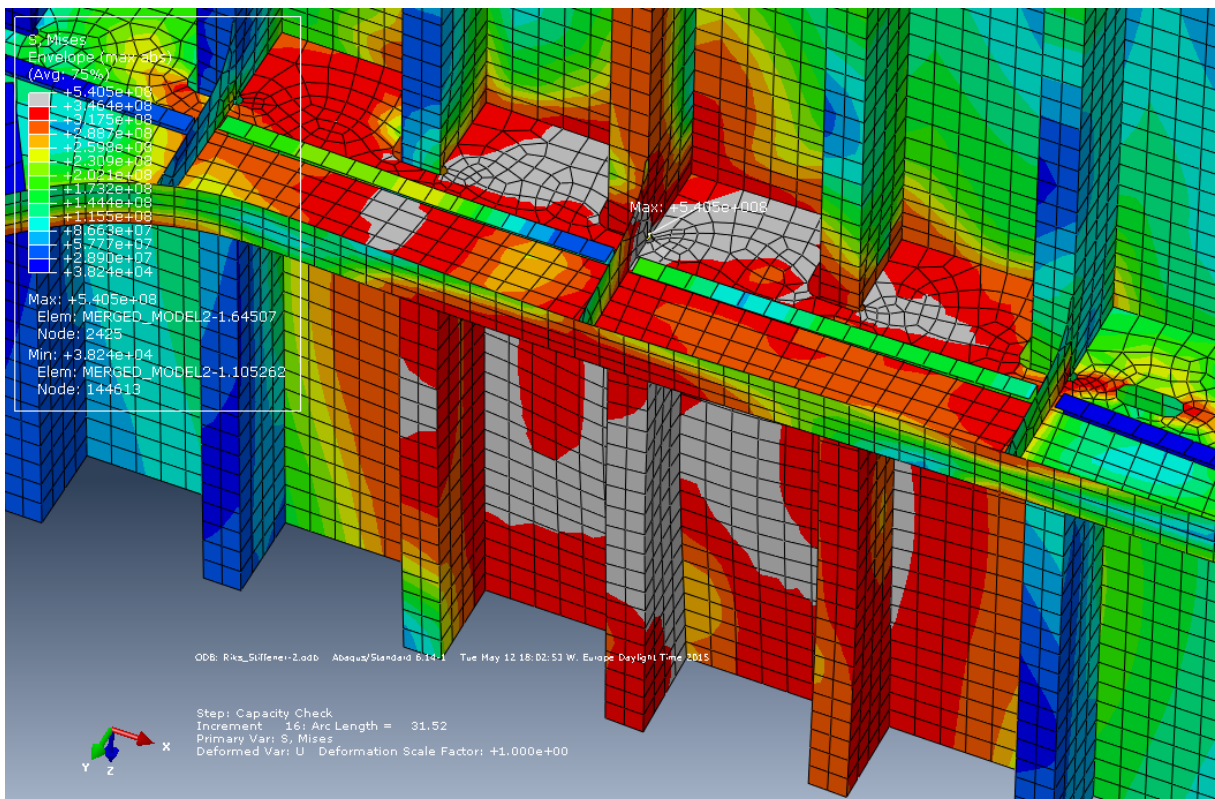
Figure 9.19 – Response in von Mises stress at ultimate stress increment. Grey color means yielding.

9.2.3 Bulkhead

First yield occurs in a similar position in the bulkhead analysis as in the two previous. It occurs in the web a stiffener on the stringer in the connection between the stringer stiffener and a stiffener from the outer hull (Figure 9.20). The von Mises stress reaches the yield stress in increment 4, where the applied bulkhead load is 4.68 MPa. Strictly speaking, this point should not have existed since there should be a cut-out at that location, and then the point of first yield probably would have been on the bottom of that cut-out, as for the brackets. In the top corner of the bulkhead there is a singularity point. Also in this point stresses are relatively large compared to the rest of the structure. The singularity point occurs at that location because of the boundary conditions, which influence this analysis significantly. The point of largest displacement is in the flange of one of the stiffeners of the outer hull. The magnitude of the displacement is approximately 1 cm, which can be seen from Figure F.4.
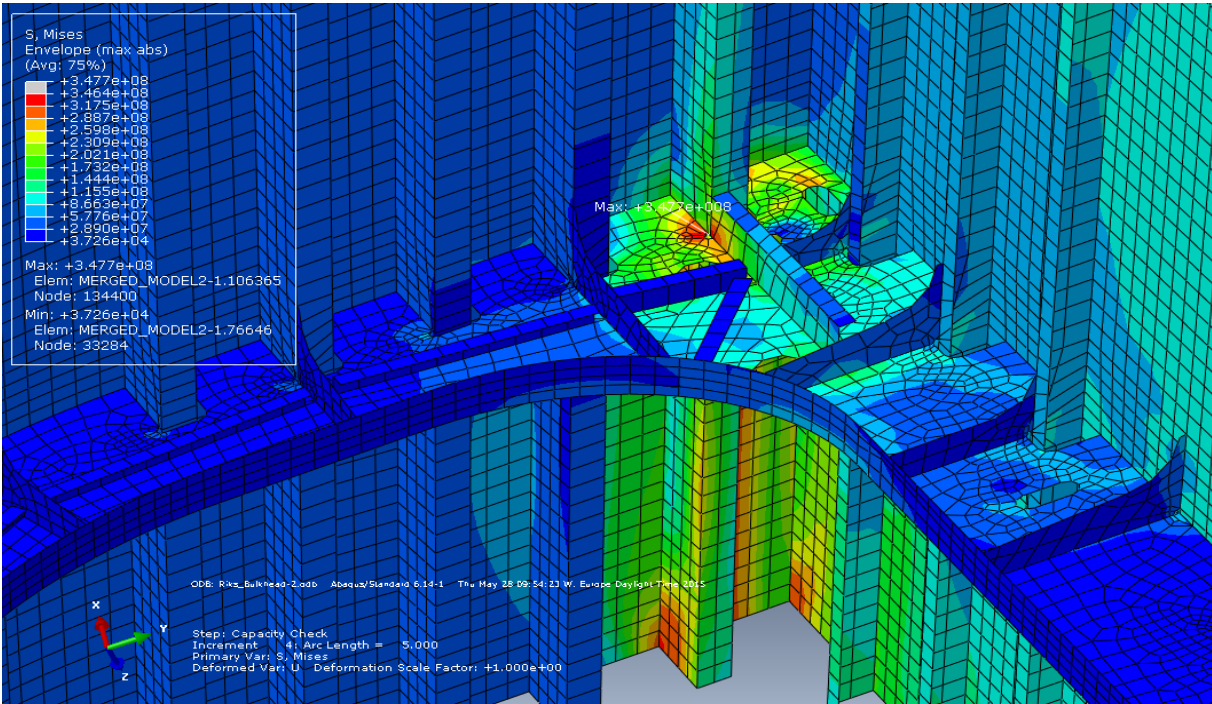
Figure 9.20 – Response in von Mises due to bulkhead load at first yield.

The ultimate stress is reached in increment 26, where the load is 9.89 MPa. It is reached in the same location that yields first. This can be seen from Figure 9.21. The next point that reach 540.5 MPa is the singularity point at the top of the bulkhead edge. The largest displacement at increment 26 is approximately 15 cm and located in the middle of the first plate area of the bulkhead.
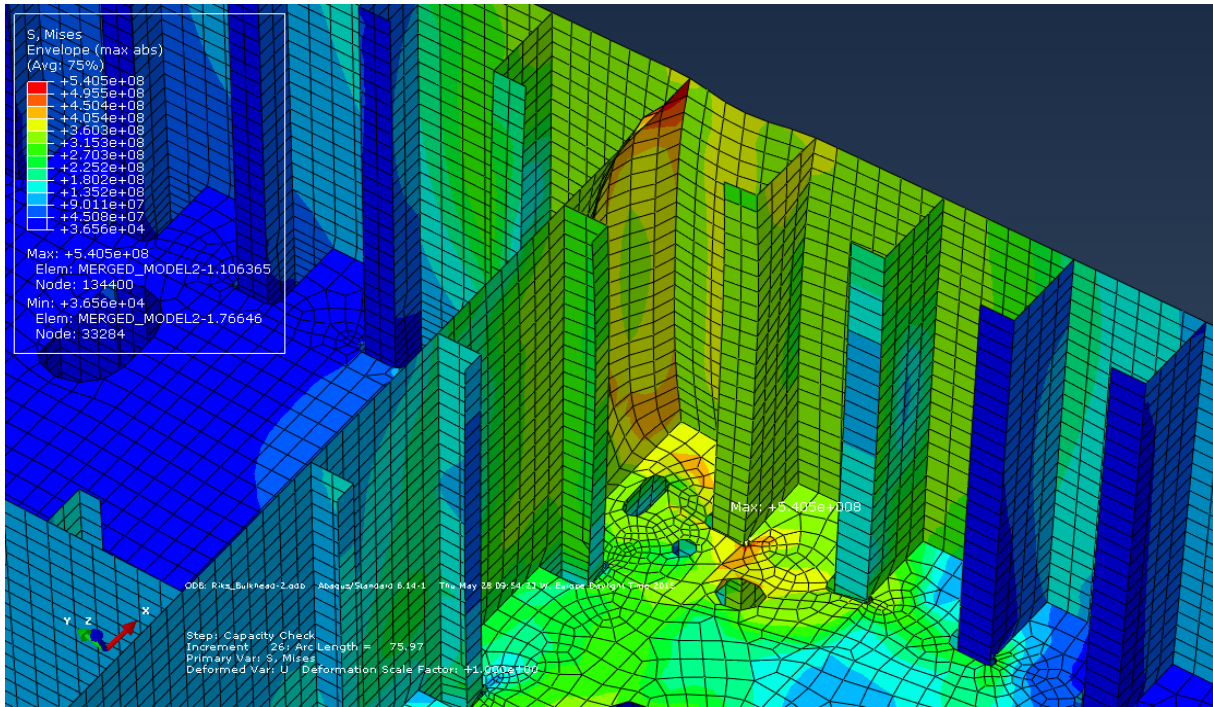
Figure 9.21 – Response in von Mises due to bulkhead load at first ultimate stress.

9.2.4 Stringer

For the analysis with stringer load first yield occurs at a stiffener cut-out (Figure 9.22) in the stringer plate at increment 3, i.e. first yield occurs in another detail. At this increment the load applied is 2.80 MPa.
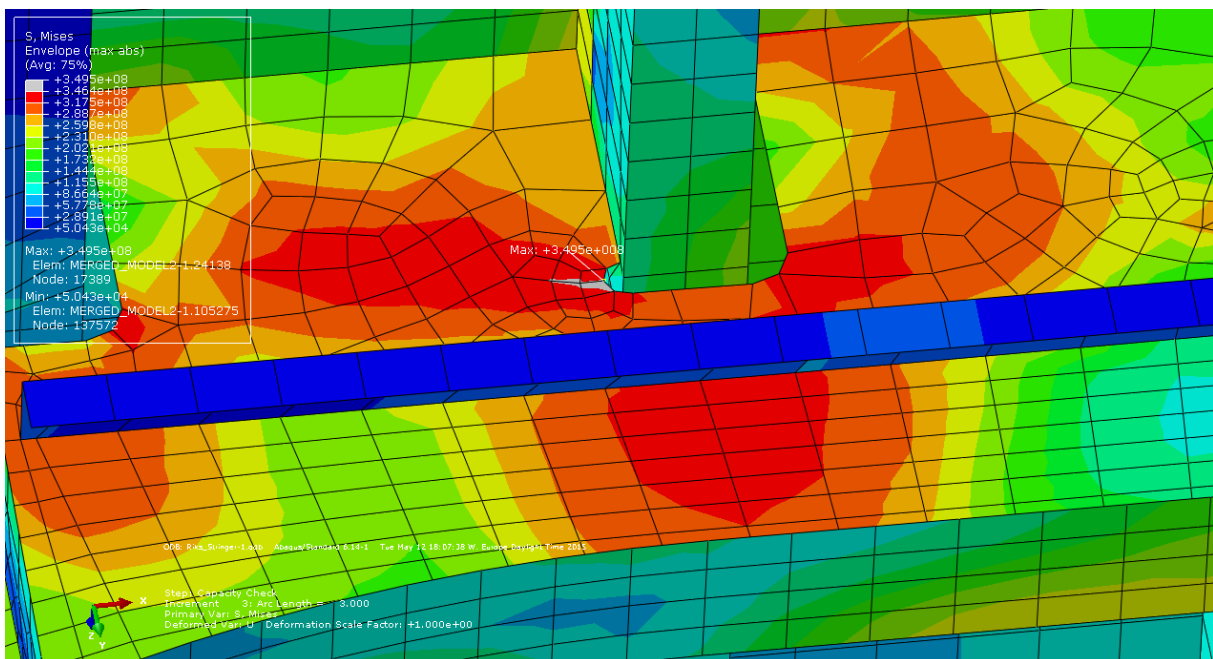

Figure 9.22 – Close-up showing point of first yield due to stringer load.

Ultimate von Mises stress occurs first in the same spot that yields first. This happens at increment 14, and at that time the applied load is 4.45 MPa and large parts of the stringer have yielded. In this analysis, as well as in the others, the stress is much higher in some small details than in the rest of the area studied. This can be seen from Figure 9.23. The maximum displacement of the stringer in the load direction is around 10 cm, while the vertical displacement of the stringer plate is around 8 cm at the largest.
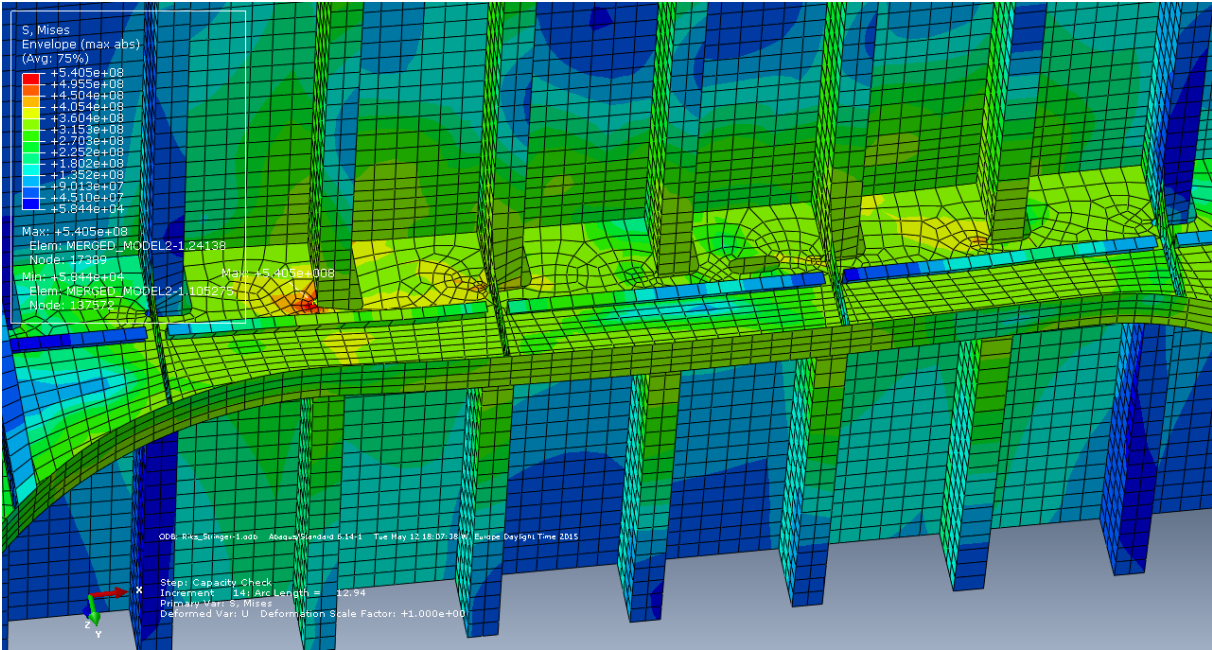
Figure 9.23 – Plot of von Mises stress when first ultimate stress is reached.

9.2.5 Main findings and discussion

The results from these analyses shows that the weak spots of the ice belt lies in the stringer. Even though loads, specifically created for plates, stiffeners and bulkheads are applied, it is still in the stringer that stresses are highest. In details such as brackets, stringer stiffener and cut-outs, where stress concentrations occur, the stress reaches both yield stress and ultimate stress first. The effects of the stress concentrations get enhanced by the fact that the stringer is not designed to withstand loads of such magnitudes that local ice loads may represent.

In the cases where plate, stiffeners and the stringer are loaded the stringer plate struggles. As the loads increase the stringer plate appears to be buckling by displacing significantly in the vertical direction before it yields. Thicker stringer plate would help avoiding this, in addition to help lowering the stresses near the cut-outs. Another action to avoid the buckling effect could

be to introduce extra stiffening to the stringer plate by having more stiffeners or brackets in the load direction.

The brackets that are connected to the outer stiffeners and stringer plate have high stresses just above their cut-out. This is due to the stress concentrations that occur because of sudden change of geometry. The brackets and stiffeners on the stringer are not dimensioned for the large loads that the outer stiffener transmits to them.

So, what can be seen here is that dimensioning the outer structure against ice loads alone is not sufficient for such a structure to be able to cope with the loads in a reasonable way. Also the inner structure should be configured and dimensioned for such conditions.

10 Discussion

The main findings in this thesis are; the structural response of the ice belt when exposed to the local load from *ISO 19906,* and the capacity of the structure, with respect to yielding and ultimate material stress. In this chapter several factors that influence the results are discussed. The discussion includes sections on dimensioning, the model, boundary conditions, loads, mesh and elements.

10.1 Dimensioning

Local structural configurations for ships and floating offshore structures are not necessarily that different from each other. The application of a ship design standard like the *Polar Code* for dimensioning parts of a floating offshore structure hull, as conducted here, is a recommended practice since it does not exist any relevant standard for the subject. However, the fact that there are differences between the design loads from ice on ships and floating offshore structures cannot be disregarded. The load dimensioned for, by use of the *Polar Code*, is an impact to the bow of a ship in transit. Calculation of the design load for a given polar class involves some parameters that are not suitable for a semi-submersible column. There are also several parameters in the standard that are created in order to account for ship geometry. These parameters have to be assumed by use of sound judgement. The numerous assumptions made on selection of load and ship geometry parameters may have led to some inaccuracies and errors in relation to the dimensioning in this thesis. One such error is the error in calculating the *Polar Code* design load. In the concluding phase of the master thesis the author discovered an error related to the design load calculated, and thus the dimensioning. One of the parameters in the design load pressure of the *Polar Code* is the ship displacement [kt]. Previously it was believed that this was the ship velocity in knots, and therefore the minimum value of 5 [kt] was used in the calculations. However, when realizing that this parameter is really the weight of the structure in kilotons it is clear that the dimensions obtained are non-conservative. When using the platform displacement of approximately 51 kilotons in the calculations the required thickness for the plate and dimensions stiffeners increase significantly. This makes the modelled ice belt under-dimensioned according to the requirements of PC4.

10.2 The Model

The structure was modelled as two column sections with a stringer in between the sections. This means that when the plates, bulkheads and stiffeners are loaded with the design loads, the loads act close to the boundaries of the model. This is unfavorable and has most likely influenced the results from the analyses.

By introducing an extra section, so that there would have been three sections, the loads could have been applied in the middle section. In this way the loads could get some distance to the boundaries. This would probably have given more realistic results.

The model created was fairly large due to the author's wish of being able to analyze the whole ice belt. This influenced the computational time and thus also chosen the mesh size for the analyses. Since the analyses that have been performed on the model were local, the load effects did not spread over the whole model. Therefore the model could have been divided into smaller parts. By dividing the model into several, smaller parts the computational time would have been reduced, and thus smaller mesh sizes could have been used.

The structural configuration of the ice belt is not designed for ice interaction. This have a large influence on how the loads are distributed. For example the stiffeners bend sideways when loaded due to their shape (L-bars). This is not optimal since the loads are not symmetrically distributed between components surrounding the stiffeners. The lack of stringer stiffness in the load direction in Area 3 and 4 is also a problem. If the structural configuration had been designed for the large ice loads, the load effects probably would have been reduced significantly.

10.3 Boundary Conditions

Regarding boundary conditions of the FE model there are many configurations to choose between. In this part of the discussion focus is put on fixed boundaries, boundaries fixed against rotations only and rigid body boundaries.

Analyzing the ice belt as a part of a larger structure by assuming fixed boundaries will give a conservative result with stresses in the boundaries that are higher than they would have been in reality. However, the stress out in the field would become lower than in reality. By modelling the ice belt with boundaries fixed against translations only, one allows for the boundaries to

rotate. This causes high stresses out in the field, and lower stresses in the boundaries. Boundaries fixed against translation are not a correct assumption since the column sections above and below the ice belt, in reality, will also be able to deform and by that carry load.

In this thesis boundaries fixed against horizontal translation are applied to the top and bottom edges of the structure. In addition, the edges along the bottom are fixed against vertical translation, in order for the structure to carry axial load, i.e. platform weight. This basically hinders the bottom boundary to rotate, making the selected boundaries asymmetric. Due to the boundary conditions the deformation of the structure is also asymmetric. This influences the results, since the top half of the structure becomes less stiff than the bottom half.

By using rigid body definition in Abaqus the problem with the bottom edge could have been dealt with. The way it works is that the motions of the top and bottom edges of the structure are governed by the motions of one reference node each. Boundary conditions can then be applied to the nodes. This allows for rotating boundaries and therefore it should have been applied. Setting up the boundary condition in this way was not done in the thesis due to that the author discovered the function too late.

10.4 Loads

The design load patch areas for the stiffeners are optimized for maximum load effects through experiments. However, this is not the case for the plates, bulkheads and stringer. These areas are chosen based on intuition and may not be the most critical, with respect to load effects, due to the size effect in ice loading.

In reality, the probability of large ice loads acting on the hull may not be the same for all sides of the ice belt. In the thesis such probabilities are neglected. However, if it is more probable that large ice loads act on the outer longitudinal side than on the inner side, the applied loads may be conservative for the inner side of the structure.

The local load calculation method from *ISO 19906* (equation (5.13)) which is applied for calculating the loads applied to the model, does not account for ice class. In other words, it is not given that a certain ice class will withstand the loads from it. The ice belt classed with Polar Class 4 appears, based on the results from the analyses, not to be able to withstand this load.

Also, the local load applied is based on measurements from the bottom-founded drilling barge Molikpaq and indentation tests. Since Molikpaq is a fixed structure, and ice loads on fixed structures generally are larger than on floating structures, the chosen load may be conservative for a semi-submersible. By using local loads that are more "custom-made" for semi-submersibles the results could would have been different.

10.5 Mesh Size and Element Type

The convergence check showed that by using the S8R5 or S8R elements mesh size would not have to be improved in order to obtain converged stresses. Therefore changing element type seems like an alternative to decreasing mesh. The S8R5 and S8R elements are based on thin-shell and thick shell theory, respectively. The required computational time for the S8R5 element is therefore significantly shorter than that of its counterpart. However, neither of these elements could be used without the analyses crashing. The reason for the crashes was not found, and therefore the S4R elements was used.

The choice of what mesh size that was to be used was largely based on the required computational time of the analyses. Since many analyses was performed the computational time had to be limited. This was not optimal for the results. Based on the convergence check and the mesh refinement study it was seen that stresses had not converged for the mesh size used, namely 100 mm. If the author had succeeded in isolating the areas of interest and giving them a finer mesh, while increasing the mesh size in the areas which were not of interest, the results would have been improved at the same time as computational time had been kept short. Another way of being able to increase mesh size is to divide the model into several smaller parts, as mentioned in sub-chapter 10.2.

11 Conclusion

The main objective of this thesis has been to perform structural analyses of a semi-submersible exposed to local ice loads and study the obtained results. This has been achieved by creating a realistic model of a component of a semi-submersible's hull that is likely to interact with ice, and analyzing it when exposed to ice loads, by help of the FE software Abaqus. In addition, a literature review on ice properties, ice mechanics, ice load formulation and methods for computation of load effects and structural resistance has been made.

The analyses that have been performed on the model, which is dimensioned according to Polar Class 4 from *Requirements concerning POLAR CLASS,* are nonlinear static analyses. Cases with design loads for plates, stiffeners, bulkheads and stringer has been studied separately. The structural response of the model when exposed to loads calculated from *ISO 19906*'s local load formulation for *thick, massive ice features* has been examined. Additionally, the capacity of the structure with respect to yielding and ultimate material stress has been checked.

The results from the analyses that consider the ISO load show that yielding occurs in the structure for most of the different cases. The yielding occurs to a large extent especially when the part of structure that has the weakest stringer structure is loaded.

The results from the analyses that consider the capacity in terms of yield stress and ultimate material stress shows that the largest stresses occurs in the stringer for all the cases, even though the applied loads act over the design load patches for plates, stiffeners or bulkheads. This shows that the stringer is the weak spot of the model in the analyses performed.

The stringer, which consists of plates, stiffeners and brackets, is neither configured nor dimensioned for ice loads. This is reflected by the results in terms of its high response. The results also show that the plates, stiffeners and bulkheads have lower response, and do not yield, when exposed to the ISO load in the areas where the stringer structure is stiff. By that it can be seen that the outer hull structure does not have to be strengthened further, in order to withstand the local ISO load, as long as the stringer is sufficiently stiff.

12 Further work

As can be seen from the discussion and conclusion, there are several uncertainties regarding dimensions, geometry, boundary conditions, loads, elements and mesh. Further work basically consists of improving all these uncertainties.

The model should be created with larger dimensions than those used in this thesis in order to comply with the rules of Polar Class 4. This will reduce the response of the structure when exposed to *ISO 19906's Local pressure for thick, massive ice features*, in addition to increasing its capacity.

An extra section could be introduced to the model, keeping the boundaries further away from the loads and limiting their own effect on the results. Also, introducing the rigid body definition, as mentioned in sub-chapter 10.3, would give better results in the analyses. This would allow both boundaries to rotate and thus the boundary conditions would have been symmetric.

The size effect included in the applied load calculation method makes finding the most critical load case a challenge. Experiments was performed in order to find the most critical load patch for the stiffeners, but not for the other components. By conduction such experiments for the other components the true critical load patch sizes and the loads that comes with them can be found. If the load used in this thesis are proved to be too conservative for column-based semi-submersibles or for the areas where such platforms are to operate, there may be possible to find a more suitable load.

The applied mesh size and element type in the analyses conducted are not optimal. By using a finer mesh size or a more suitable element, more accurate results would have been obtained. Further work with respect to meshing could be to creating a finer mesh in the areas that are to be considered, while having relatively coarse mesh for the rest of the structure.

13 References

ABAQUS. (2014). ABAQUS 6.14 Documentation. Retrieved 04.02, 2015, from http://abaqus.ethz.ch:2080/v6.14/index.html

Bell, K. (2013). *An engineering approach to finite element analysis of linear structural mechanics problems*. Trondheim: Akademika Publ.

DNV, D. N. V. A. (2013). Determination of Structural Capacity by Non-linear FE analysis Methods. DNV-RP-C208. www.dnv.no.

IACS, I. A. o. C. S. (2011). Requirements Concerning POLAR CLASS.

ISO:19906, I. S. O. (2010). *Petroleum and natural gas industries: Arctic offshore structures (ISO:19906)*. Geneva: ISO.

Løset, S., & Gudmestad, O. T. (2006). *Actions from ice on Arctic offshore and coastal structures*. St. Petersburg: Lan.

Mathisen, K. M. (2013). Lecture Notes in TMR4190 Finite Element Methods in Structural Analysis.

McClelland, B., & Reifel, M. D. (1986). *Planning and design of fixed offshore platforms*. New York: Van Nostrand Reinhold.

Michel, B. (1978). *Ice mechanics*. Québec: Les presses de l'Université Laval.

Moan, T. (2003). *Finite Element Modelling an Analysis of Marine Structures*. Marinteknisk Senter, Trondheim.

Motovated Design & Analysis. Retrieved 24.04, 2015, from http://www.motovated.co.nz/Tips-and-Tricks/inplane_large_displ.html

Offshore Energy Today. (2013). Retrieved 29.04, 2015, from http://www.offshoreenergytoday.com/deepsea-stavanger-rig-stays-with-bp-in-angola-until-november-2014/

Palmer, A., & Croasdale, K. (2013). *Arctic offshore engineering*. Singapore: World Scientific Pub.

Reddy, D. V., & Swamidas, A. S. J. (2014). *Essentials of offshore structures: framed and gravity platforms*. Boca Raton: CRC Press, Taylor & Francis Group.

Sakhalin Energy. (2014).   Retrieved 21.04, 2015, from http://www.sakhalinenergy.ru/ru/company/overview.wbp

Sanderson, T. J. O. (1988). *Ice mechanics: risks to offshore structures*. London: Graham & Trotman.

Timco, G. W., & Sudom, D. (2013). Revisiting the Sanderson pressure–area curve: Defining parameters that

influence ice pressure. *Cold Regions Science and Technology, 95*, 53-66.

Timco, G. W., & Weeks, W. F. (2010). A review of the engineering properties of sea ice. *Cold Regions Science and Technology, 60*, 107-129.

Wikipedia. (2015).   Retrieved 10.05, 2015, from http://en.wikipedia.org/wiki/Water#/media/File:Liquid-water-and-ice.png

World Meteorological Organization. (1970-2014). WMO Sea-Ice Nomenclature *Terminology - Volume 1*.

Zareh, H. (2011). Abaqus/CAE Material Nonlinearity Tutorial.   Retrieved 10.04, 2015, from http://www.ewp.rpi.edu/hartford/~sayrer/Master%27s%20Project/other/Research/plasticity_tutorial.pdf

Appendices

A. Stringer Drawing from Odfjell Drilling
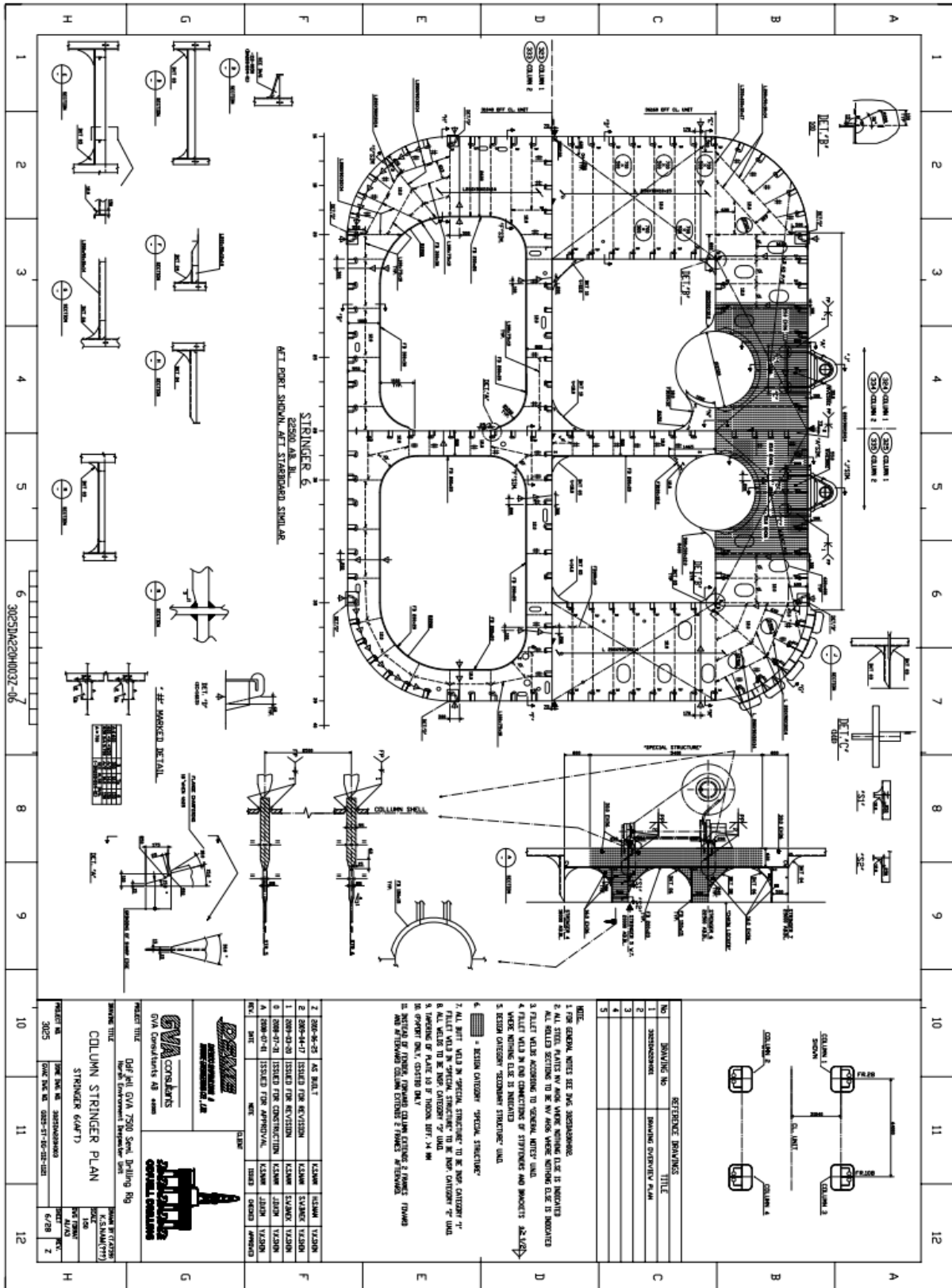
Figure A.1 – Stringer drawing provided by Odfjell.

B. Design Load from IACS

Input parameter

Ship displacement - v [kt]	5

Design Ice Loads

Polar class	Crushing Failure Class Factor - CFc	Flexural Failure Class Factor - CFf	Displacememt Class Factor - CFdis	Load Patch Dimension Class Factor - CFd	Longitudinal Strength Class Factor - CFl
PC1	17.69	68.6	250	2.01	7.46
PC2	9.89	46.8	210	1.75	5.46
PC3	6.06	21.17	180	1.53	4.17
PC4	4.5	13.48	130	1.42	3.15
PC5	3.1	9	70	1.31	2.5
PC6	2.4	5.49	40	1.17	2.37
PC7	1.8	4.06	22	1.11	1.81

Polar class	Bow shape coefficient fa3	Force F [MN]	Load patch aspect ratio - AR	Line load Q [MN/m]
PC1	0.6	29.73170986	1.3	14.52044796
PC2	0.6	16.62219392	1.3	8.867021585
PC3	0.6	10.18508546	1.3	5.750024705
PC4	0.6	7.563182271	1.3	4.450593783
PC5	0.6	5.210192231	1.3	3.270934956
PC6	0.6	4.033697211	1.3	2.499106122
PC7	0.6	3.025272908	1.3	1.989340783

Polar class	Pressure P [Mpa]	Design Load Patch (w=width, b=height)		Average Pressure Pavg [Mpa]
		w = F/Q [m]	b=Q/P [m]	
PC1	9.218993218	2.04757525	1.575057885	9.218993218
PC2	6.149085602	1.874608488	1.442006529	6.149085602
PC3	4.220054856	1.7713116	1.362547384	4.220054856
PC4	3.404667454	1.699364768	1.307203668	3.404667454
PC5	2.66952149	1.592875524	1.225288865	2.66952149
PC6	2.012840926	1.614055992	1.241581533	2.012840926
PC7	1.700580387	1.520741411	1.169801085	1.700580387

C. Local Ice Load Calculation

<table>
<tr><th colspan="4">Local Loads</th></tr>
<tr>
<th>Contact Area [m^2]</th>
<th>ISO 19906 - Local Pressure for a Thick Massive Ice Feature [Mpa]</th>
<th>CSA - Local Pressure for a Thick Massive Ice Feature [Mpa]</th>
<th>Palmer and Croasdale - Level ice up to 2m and FY-Ridges [Mpa]</th>
</tr>
<tr><td>0.2</td><td>22.83</td><td>19.01</td><td>10.73</td></tr>
<tr><td>0.35</td><td>15.43</td><td>14.37</td><td>8.11</td></tr>
<tr><td>0.5</td><td>12.02</td><td>12.02</td><td>6.79</td></tr>
<tr><td>1</td><td>7.40</td><td>8.50</td><td>4.80</td></tr>
<tr><td>1.5</td><td>5.57</td><td>6.94</td><td>3.92</td></tr>
<tr><td>2</td><td>4.56</td><td>6.01</td><td>3.39</td></tr>
<tr><td>2.5</td><td>3.90</td><td>5.38</td><td>3.04</td></tr>
<tr><td>3</td><td>3.43</td><td>4.91</td><td>2.77</td></tr>
<tr><td>3.5</td><td>3.08</td><td>4.54</td><td>2.57</td></tr>
<tr><td>4</td><td>2.80</td><td>4.25</td><td>2.40</td></tr>
<tr><td>4.5</td><td>2.58</td><td>4.01</td><td>2.26</td></tr>
<tr><td>5</td><td>2.40</td><td>3.80</td><td>2.15</td></tr>
<tr><td>5.5</td><td>2.24</td><td>3.62</td><td>2.05</td></tr>
<tr><td>6</td><td>2.11</td><td>3.47</td><td>1.96</td></tr>
<tr><td>6.5</td><td>2.00</td><td>3.33</td><td>1.88</td></tr>
<tr><td>7</td><td>1.90</td><td>3.21</td><td>1.81</td></tr>
<tr><td>7.5</td><td>1.81</td><td>3.10</td><td>1.75</td></tr>
<tr><td>8</td><td>1.73</td><td>3.01</td><td>1.70</td></tr>
<tr><td>8.5</td><td>1.65</td><td>2.92</td><td>1.65</td></tr>
<tr><td>9</td><td>1.59</td><td>2.83</td><td>1.60</td></tr>
<tr><td>9.5</td><td>1.53</td><td>2.76</td><td>1.56</td></tr>
<tr><td>10</td><td>1.48</td><td>2.69</td><td>1.52</td></tr>
<tr><td>10.5</td><td>1.48</td><td>2.62</td><td>1.48</td></tr>
<tr><td>11</td><td>1.48</td><td>2.56</td><td>1.45</td></tr>
<tr><td>11.5</td><td>1.48</td><td>2.51</td><td>1.42</td></tr>
<tr><td>12</td><td>1.48</td><td>2.45</td><td>1.39</td></tr>
<tr><td>12.5</td><td>1.48</td><td>2.40</td><td>1.36</td></tr>
<tr><td>13</td><td>1.48</td><td>2.36</td><td>1.33</td></tr>
<tr><td>13.5</td><td>1.48</td><td>2.31</td><td>1.31</td></tr>
<tr><td>14</td><td>1.48</td><td>2.27</td><td>1.28</td></tr>
<tr><td>14.5</td><td>1.48</td><td>2.23</td><td>1.26</td></tr>
<tr><td>15</td><td>1.48</td><td>2.19</td><td>1.24</td></tr>
</table>

D. Dimensioning According to IACS

Input parameters

alfa	90
beta'	0
Ship velocity - v [kt]	5
Stiffener spacing - s	0.8
Frame spacing - a [m]	2.5
Peak pressure factor - PPFp	1.2
Plating - Transversly Framed	1
Hull area factors for bow - AF	1
Yield stress [Mpa]	355
beff=500*s [mm]	400

Local Strength Requirements

Shell plate requirements

Polar class	Minimum required shell plate thickness - t=tnet+ts [mm]		t
	Plate thickness required to resist ice loads- tnet	Corrosion/Abrasion allowance - ts	
PC1	56.31121218	3.5	60
PC2	45.1458432	3.5	49
PC3	36.93229526	3.5	41
PC4	32.85728767	2.5	36
PC5	28.64580791	2.5	32
PC6	24.95479183	2	27
PC7	22.59968656	2	25

Frame geometry

Description	Symbol	Dimensions of PC4
Stiffener spacing [m]	s	0.8
Plate thickness [mm]	tp	40
Angle between plate and stiffener [deg]	phi	90
As built web thickness [mm]	tw	32
Flange thickness [mm]	tf	35
Width of flange [mm]	bf	150
Offset of web compared to stiffener [mm]	bw	75
Height of web [mm]	hw	375
Height of web + tf/2 [mm]	hfc	392.5
Stiffener height [mm]	h	410

Corrosion deduction - tc [mm]

Polar class	tc	Net web thickness twn=tw-tc [mm]	Net plate thickness tpn=tp-tc[mm]	Net flange thickness tfn=tf-tc [mm]
PC4	2.5	29.5	37.5	32.5

C200 Framing - general

Polar class	Actual net effective shear area of a framing member - Aw [cm^2]	Net x-sectional area of attached plate flange [cm^2]
PC4	108.1288965	300

Polar class	Net x-sectional area of the local frame [cm^2]	Actual net effective plastic section modulus - Zp [cm^3]
PC4	159.375	4027.606424

C300 Framing - Transversely framed side structures and bottom structures

Polar class	Lesser of a and b [m] LL	Y	Required effective shear area of a framing member - At [cm^2]	a1
PC1	1.575057885	0.684988423	340.2648483	
PC2	1.442006529	0.711598694	207.7853082	
PC3	1.362547384	0.727490523	134.7431766	
PC4	1.307203668	0.738559266	104.2929683	0.964524486
PC5	1.225288865	0.754942227	76.64943875	
PC6	1.241581533	0.751683693	58.56279143	
PC7	1.169801085	0.766039783	46.61720779	

Polar class	kw=1/(1+2*Afn/Aw) kw	zp [cm^3]	kz=zp/Zp kz	A1a	A1b
PC4	0.525844851	180.234375	0.044749749	0.619972519	0.679599321

Polar class	A1 = max(A1a,A1b) A1	Required net effective plastic section modulus - Zpt [cm^3]	Requirements	
			Aw>At	Zp>Zpt
PC4	0.679599321	3775.540577	OK	OK

C600 Framing - Structural Stability

To prevent local buckling of web			
Polar class	hw/twn	805/root(yield stress)	Requirement hw/twn < 805/root(fy)
PC4	12.71186441	42.72496384	OK

Polar class	twn	0.35*tpn*root(fy/ 235)	Requirement twn>0.35*tpn*root(fy / 235)
PC4	29.5	16.13167848	OK

To prevent local flange buckling of welded profiles			
Polar class	bf	5*twn	Requirement: bf > 5*twn
PC4	150	147.5	OK

E. Structural Response due to ISO Design Load

This part of the appendix presents plots of stress and displacement for the different cases which are not in the main report. Grey areas in the von Mises stress plots means stress higher than yield stress.

E.1 Plates

E.1.1 Corner plates

E.1.1.1 Area 3
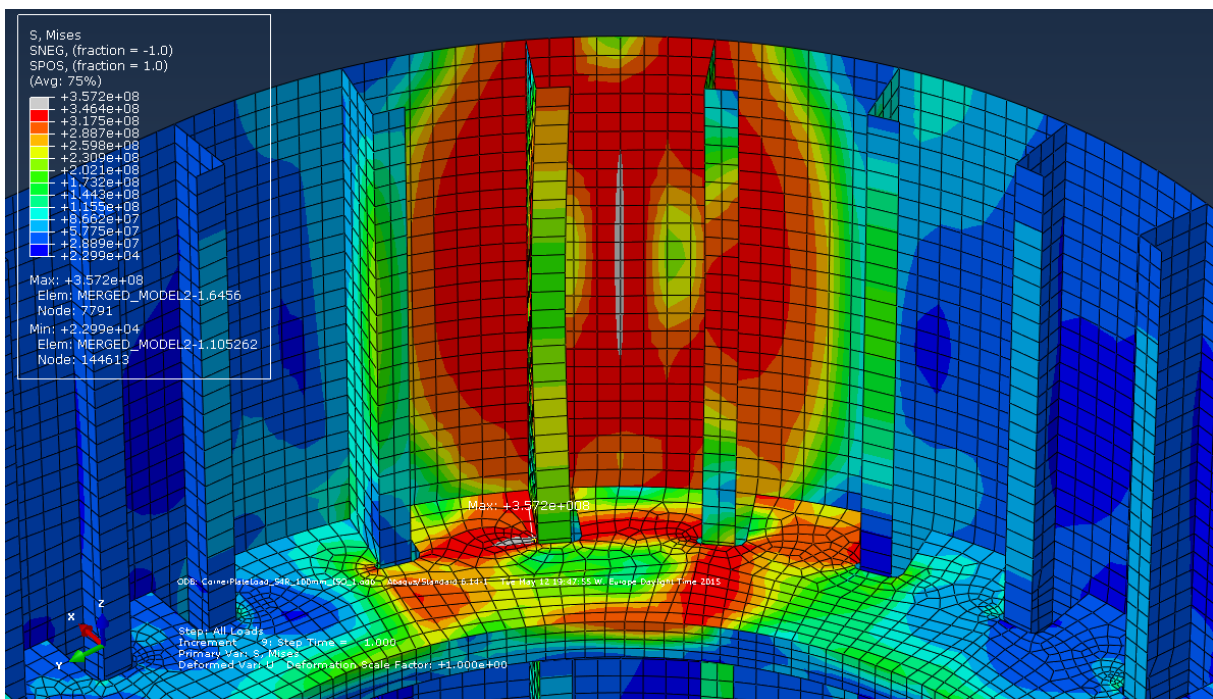
Figure E.1 – Response in von Mises stress due to design plate load at corner in area 3.
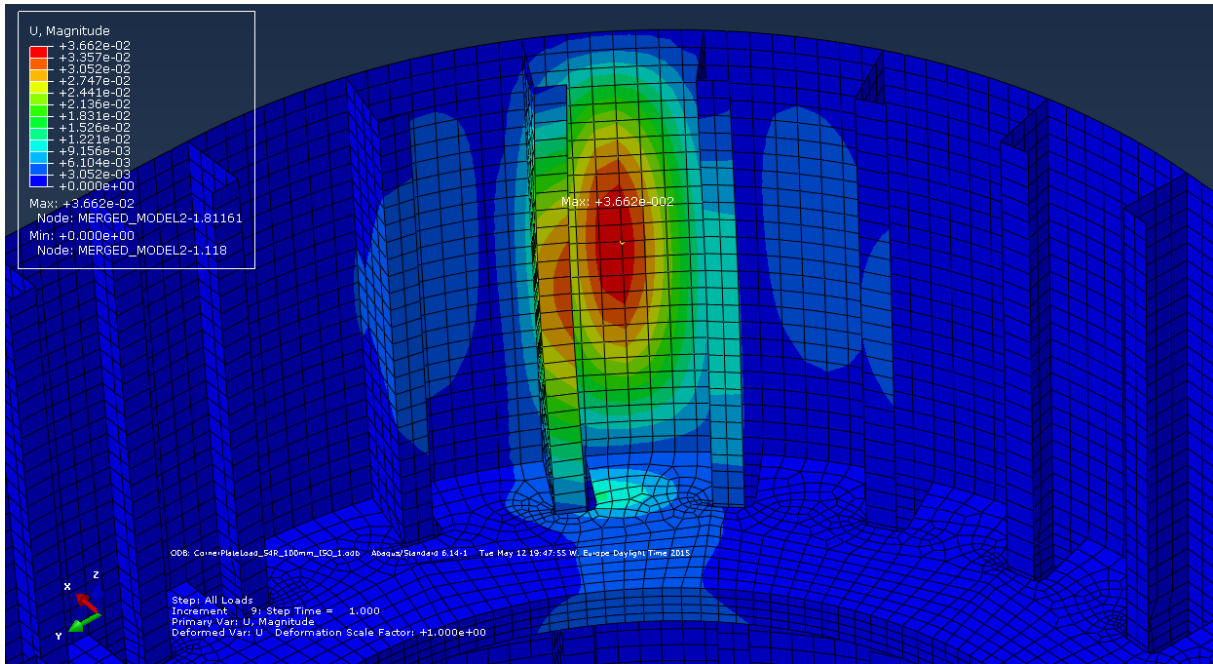
Figure E.2 – Response in displacement due to design plate load at corner in area 3.

E.1.1.2 Area 1
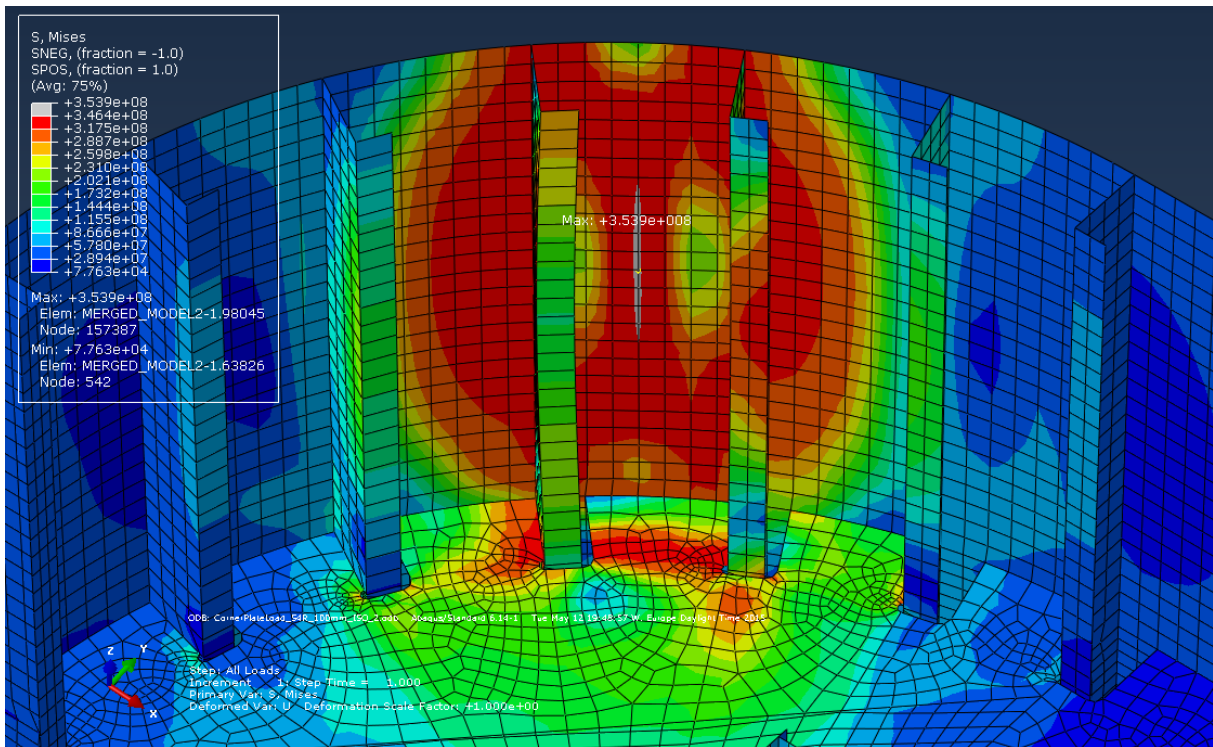
Figure E.3 – Response in von Mises stress due to design plate load at corner in area 1.
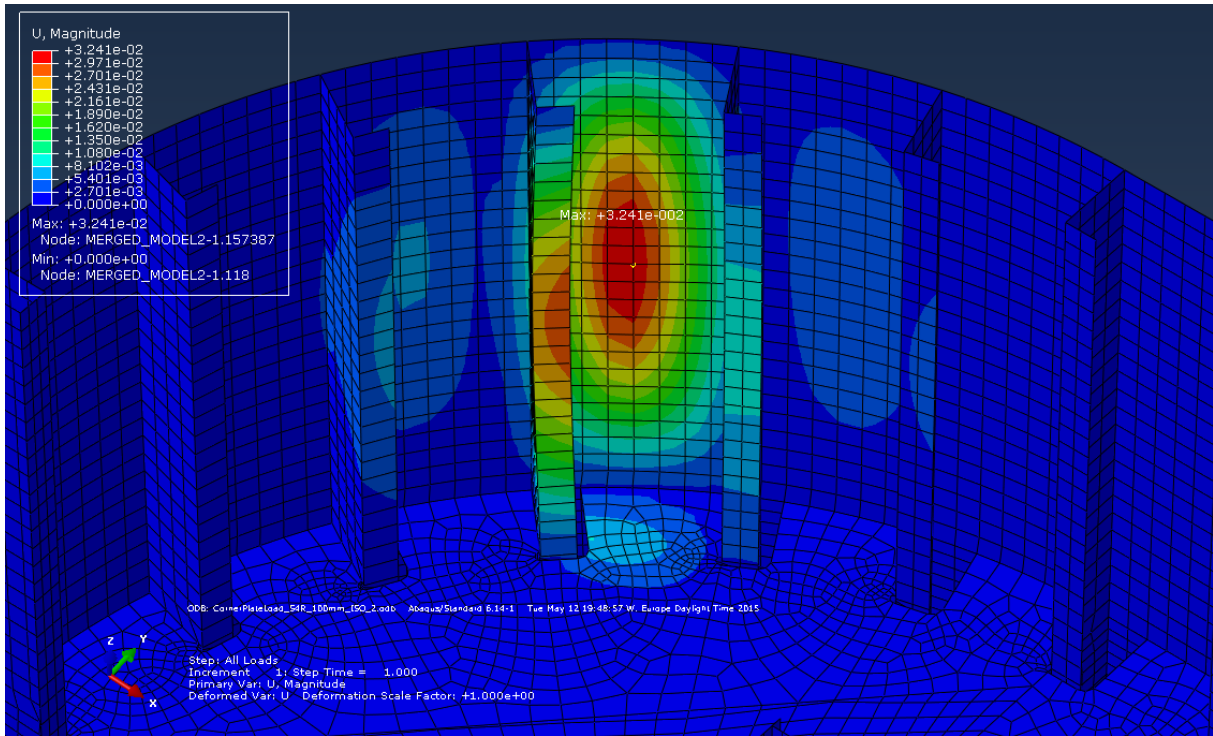
Figure E.4 – Response in displacement due to design plate load at corner in area 1.

E.1.2 Small plate on transverse side
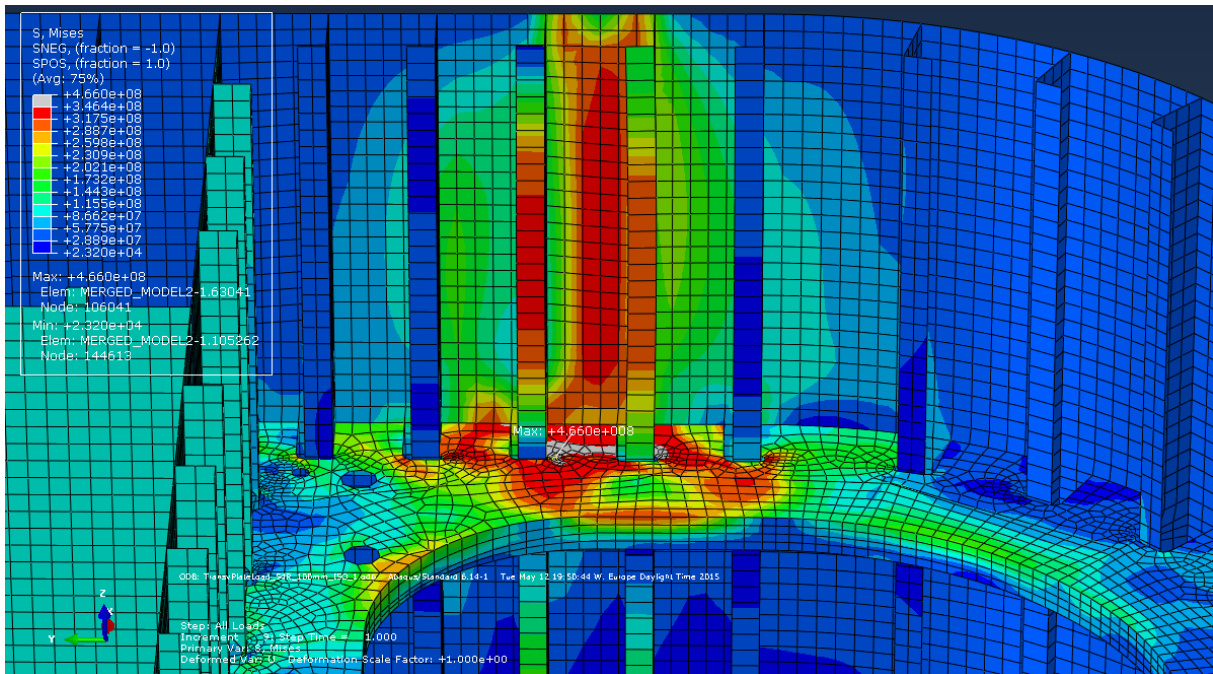
Figure E.5 – Response in von Mises stress due to design plate load at small plate on transverse side in area 3.
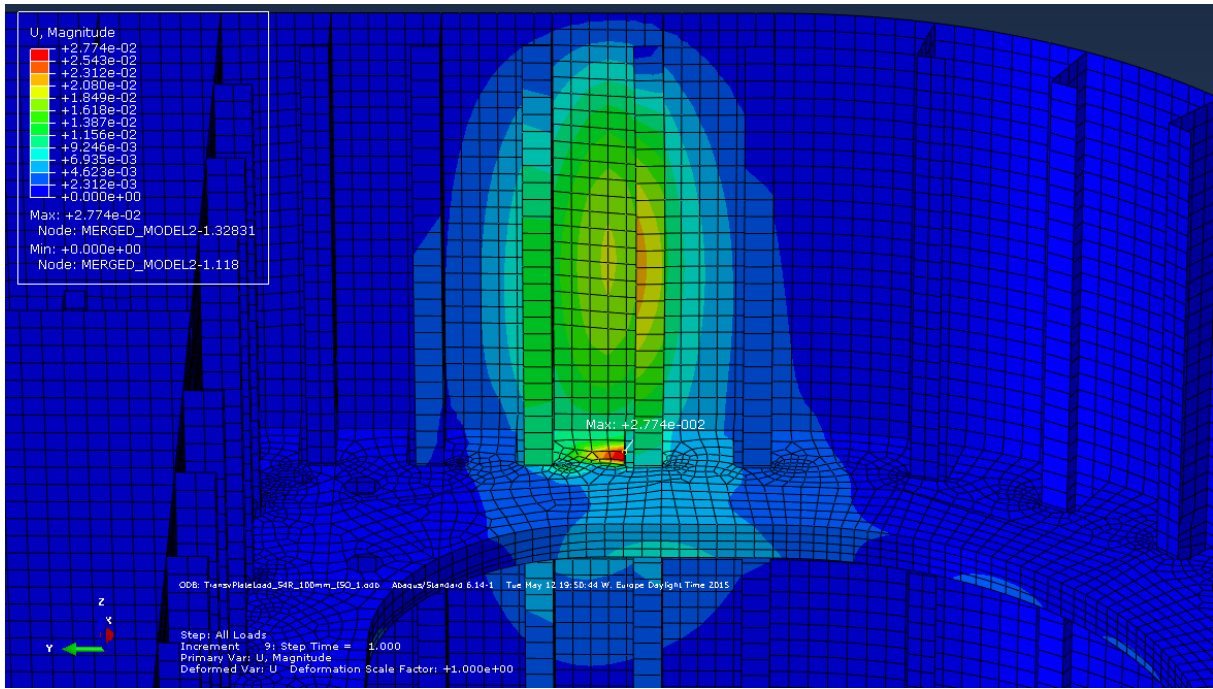
Figure E.6 – Response in displacement due to design plate load at small plate on transverse side in area 3.

E.1.3 Large plate on transverse side
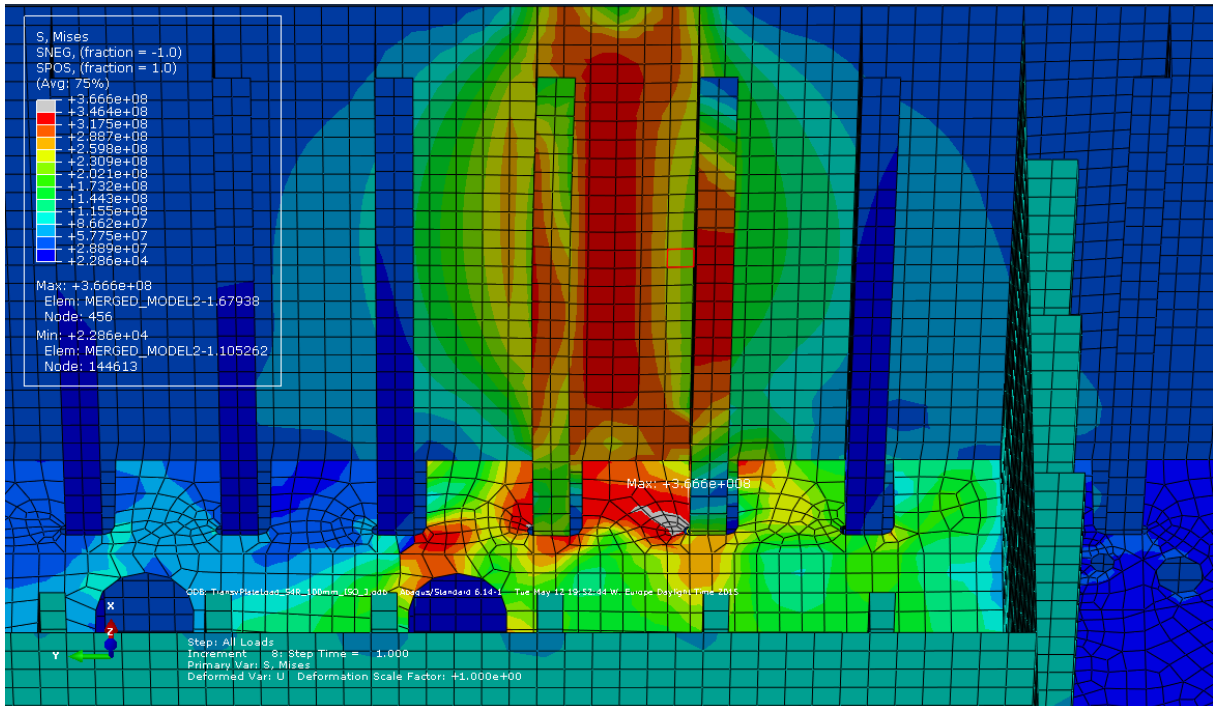
Figure E.7 – Response in von Mises stress due to design plate load at large plate on transverse side in area 2.

X
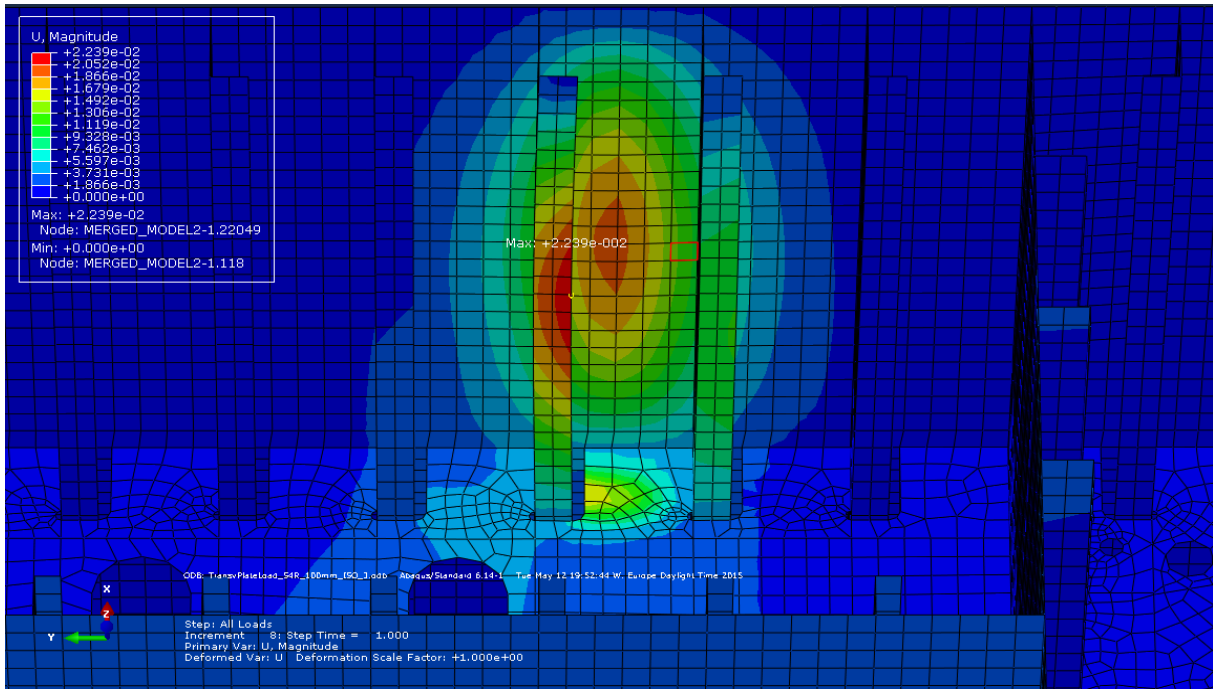
Figure E.8 – Response in displacements due to design plate load at large plate on transverse side in area 2.

E.2 Stiffeners

E.2.1 Transverse side of Area 3
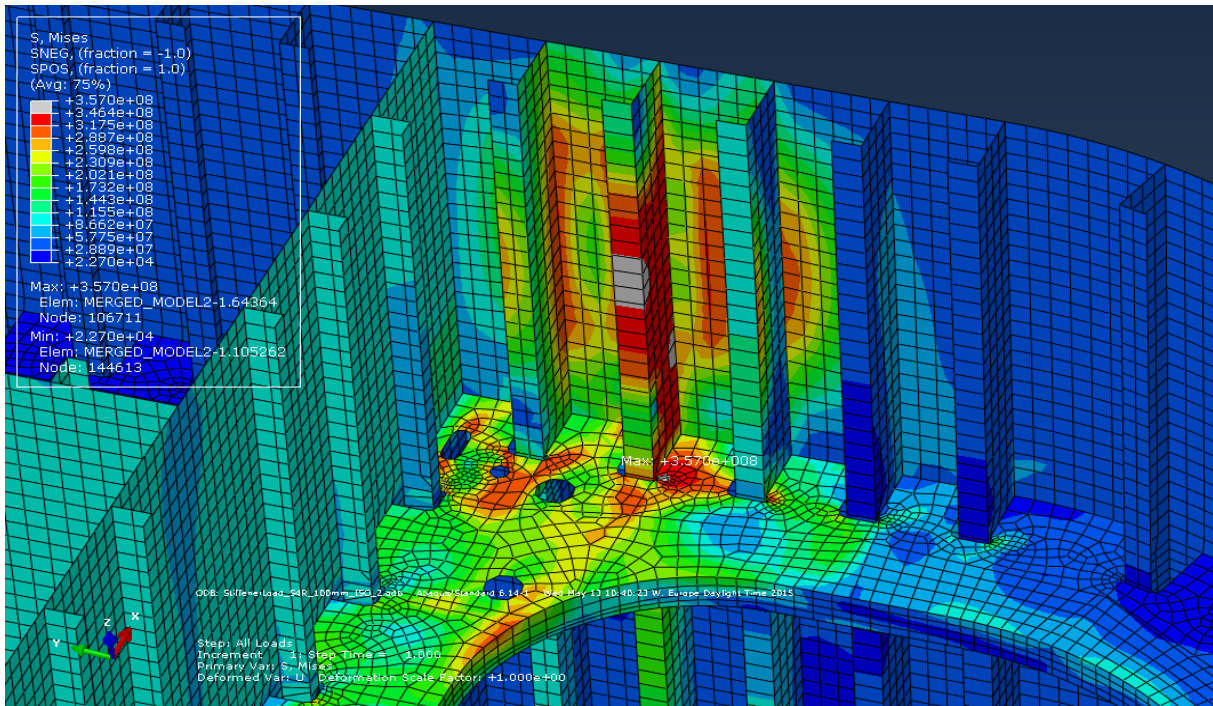
Figure E.9 – Response in von Mises stress due to design stiffener load at transverse side in area 3.
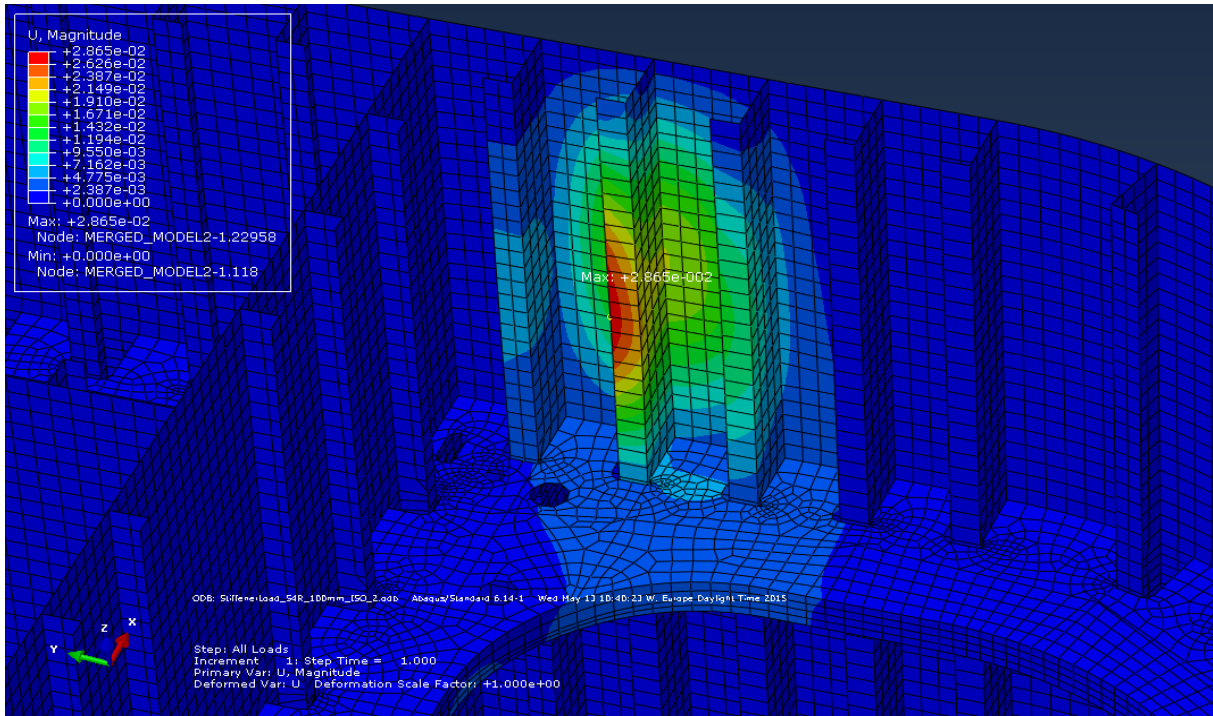
Figure E.10 – Response in displacements due to design stiffener load at transverse side in area 3.

E.3 Bulkheads

E.3.1 Transverse bulkhead

E.3.1.1 Area 1-2
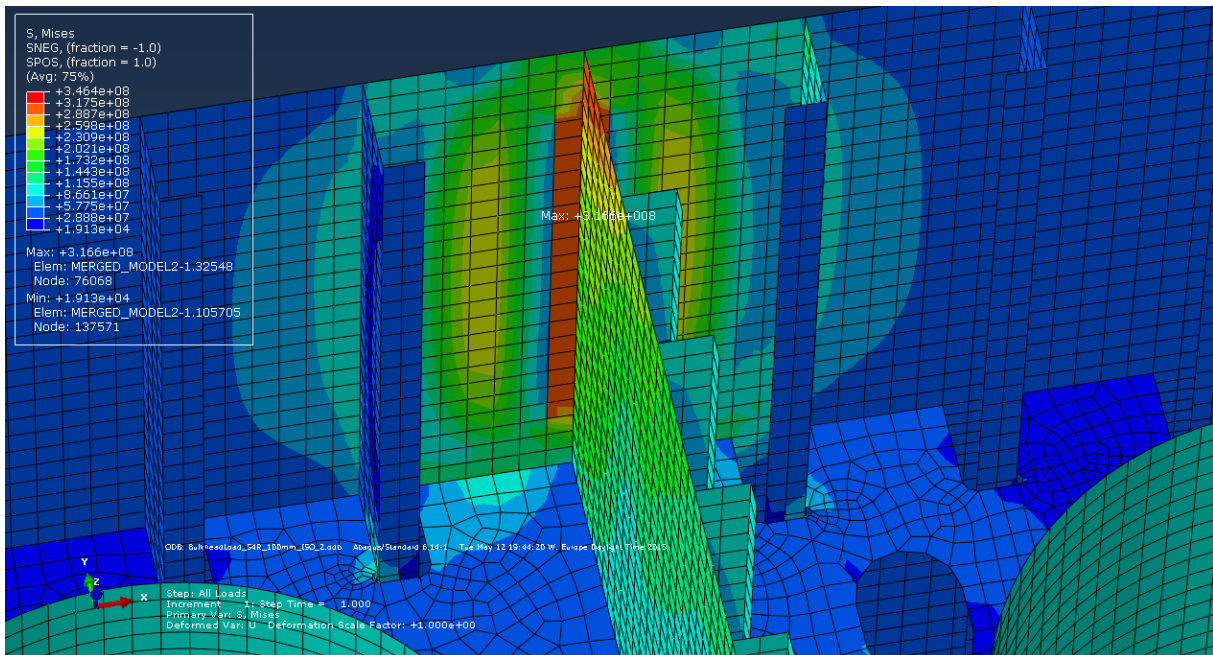
Figure E.11 – Response in von Mises stress for the transverse bulkhead in Area 1-2.
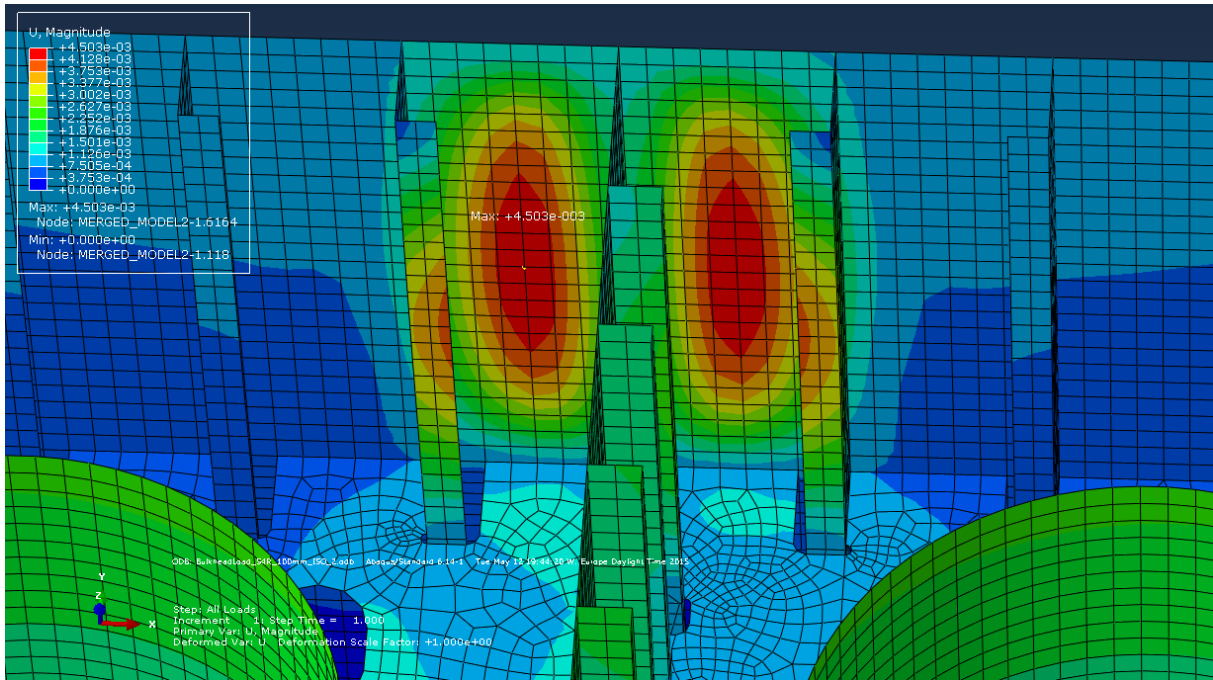
Figure E.12 - Response in displacements for the transverse bulkhead in Area 1-2.

E.3.1.2 Area 3-4
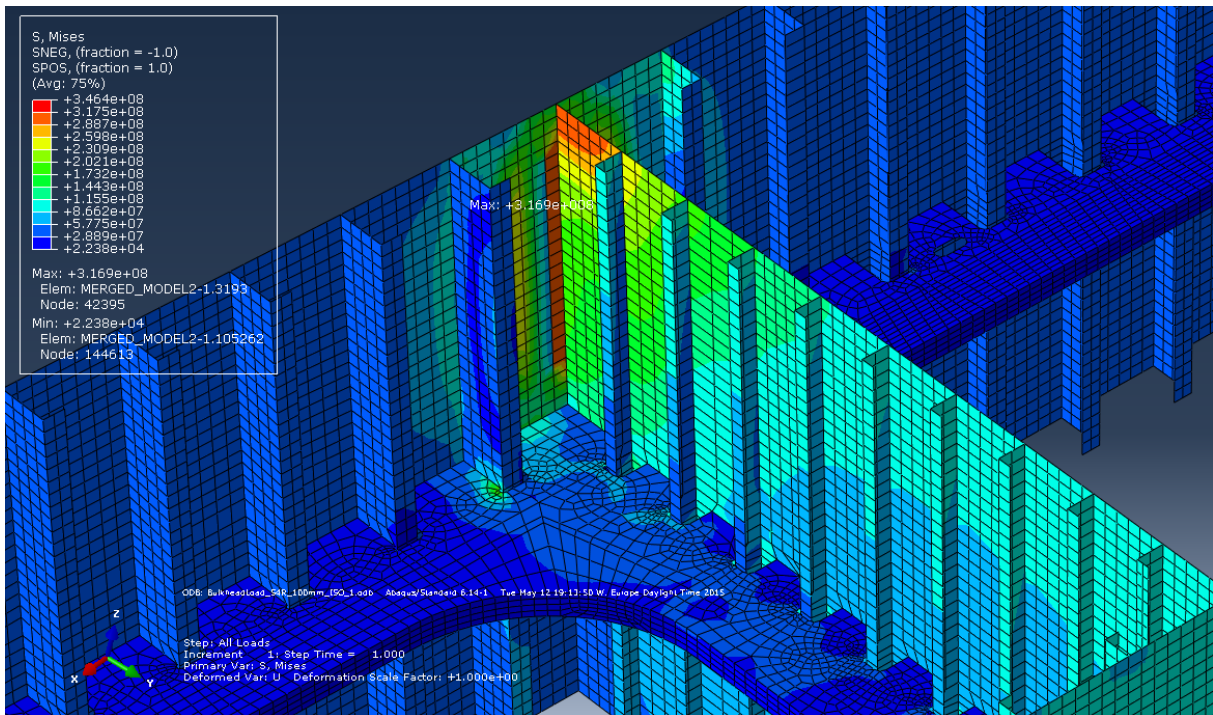
Figure E.13 – Response in von Mises stress for the transverse bulkhead in Area 3-4.
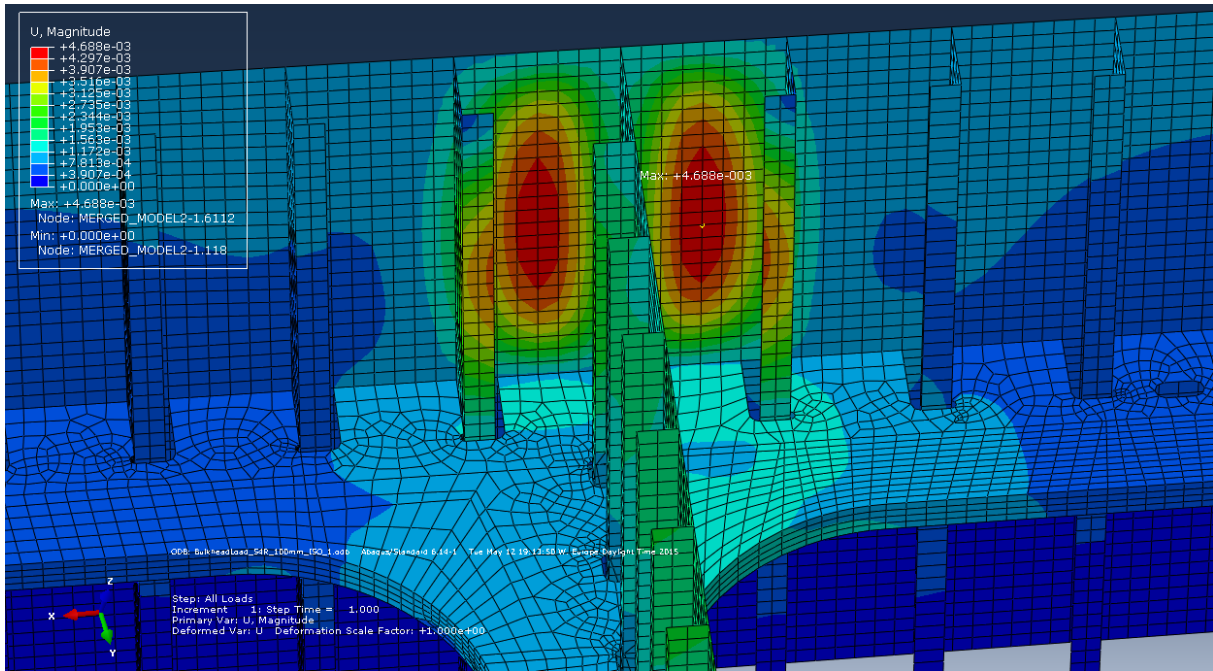
Figure E.14 – Response in displacements for the transverse bulkhead in Area 3-4.

E.3.2 Longitudinal bulkhead

E.3.2.1 Area 2-3
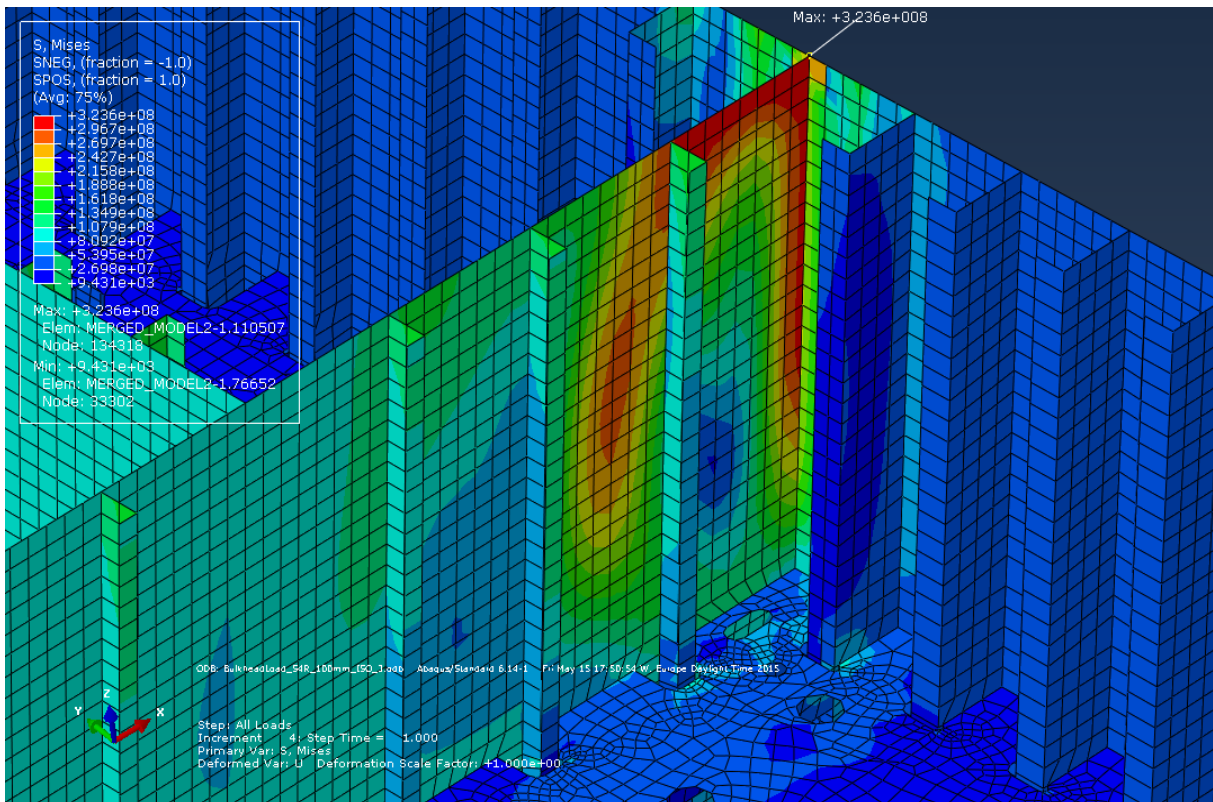
Figure E.15 – Response in von Mises stress for the longitudinal bulkhead in Area 2-3.
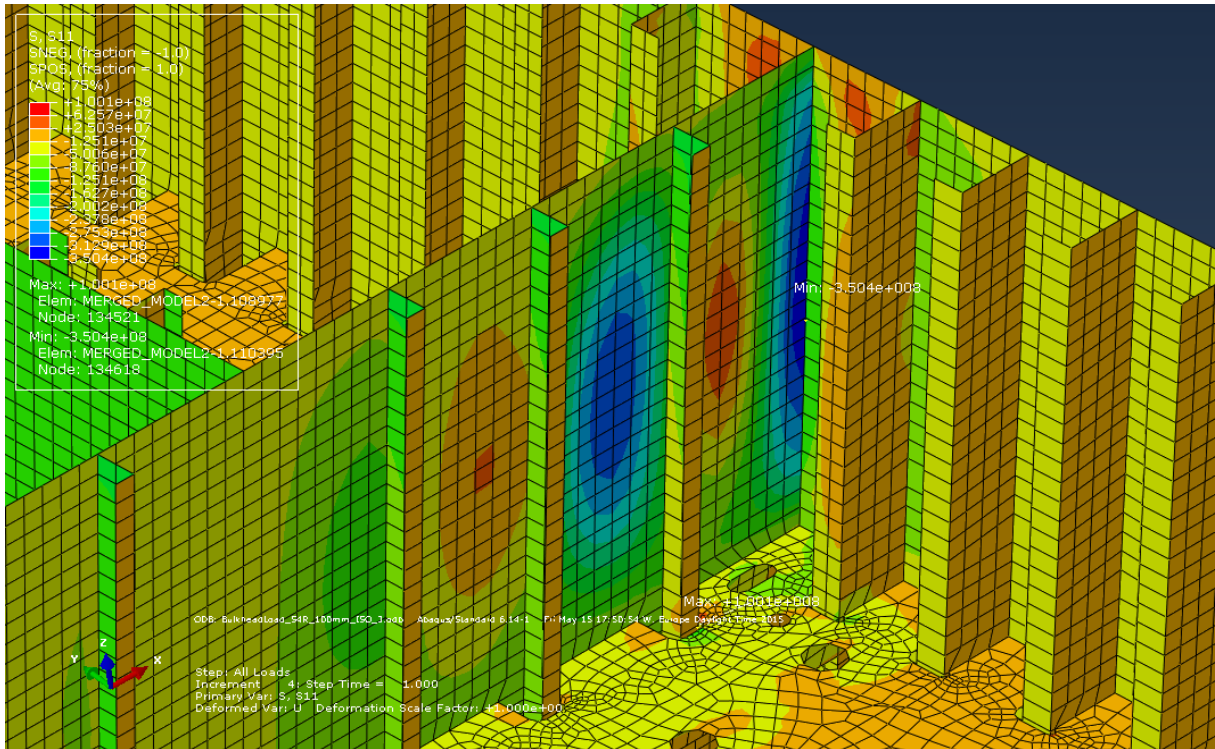
Figure E.16 – Response in stress in bulkhead direction for the longitudinal bulkhead in Area 2-3.

E.3.2.2 Area 1-4
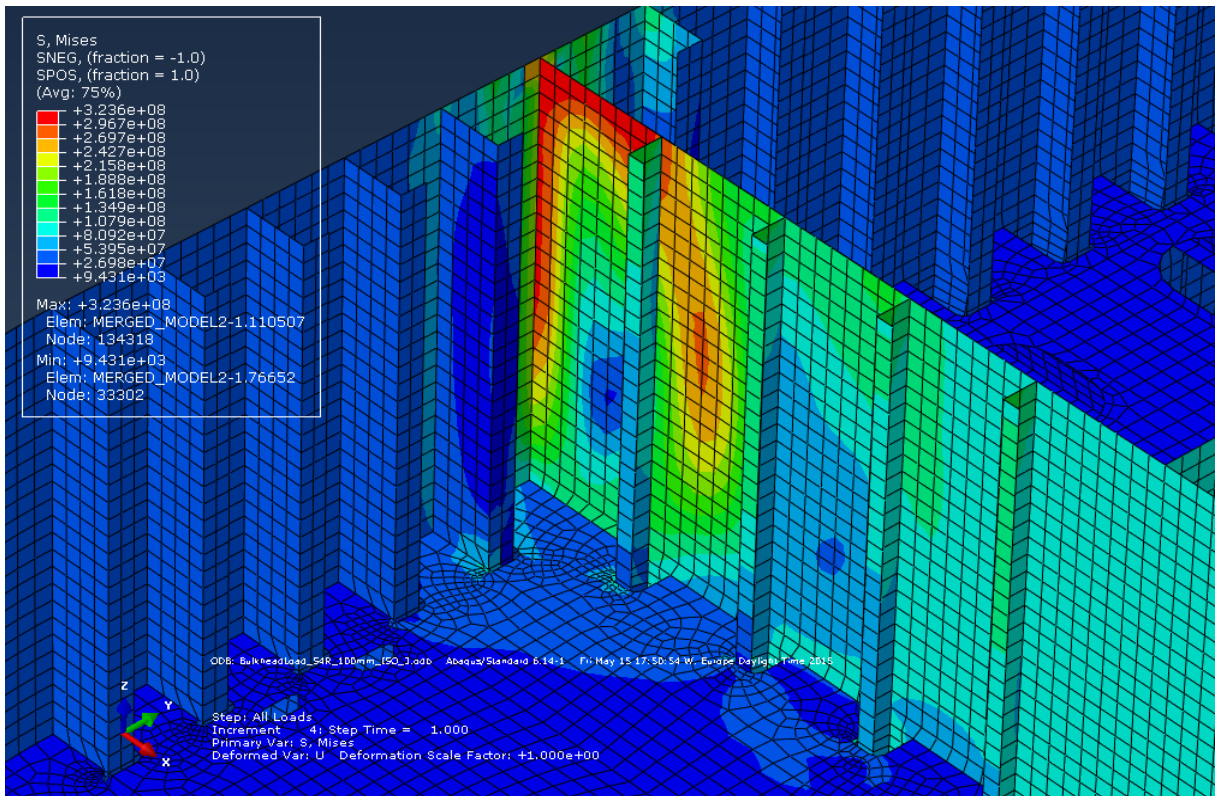
Figure E.17 – Response in von Mises stress for the longitudinal bulkhead in Area 1-4.
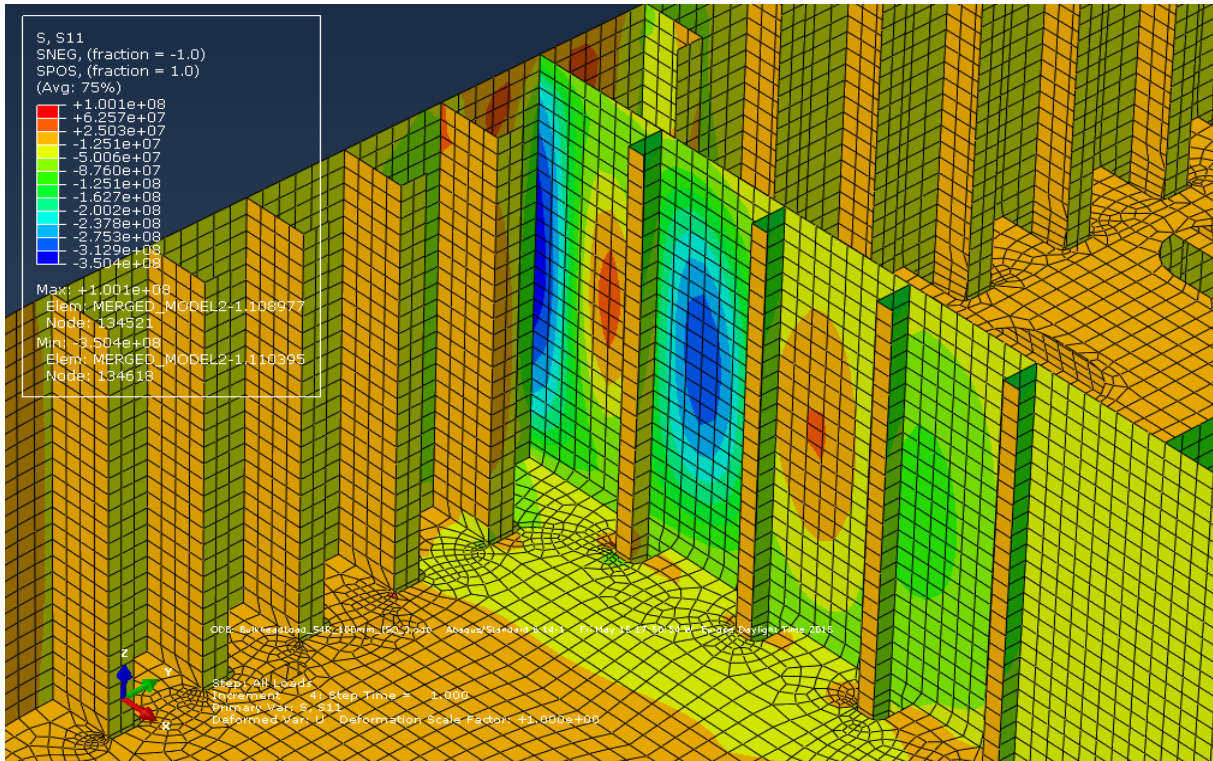
Figure E.18 – Response in stress in bulkhead direction for the longitudinal bulkhead in Area 1-4.
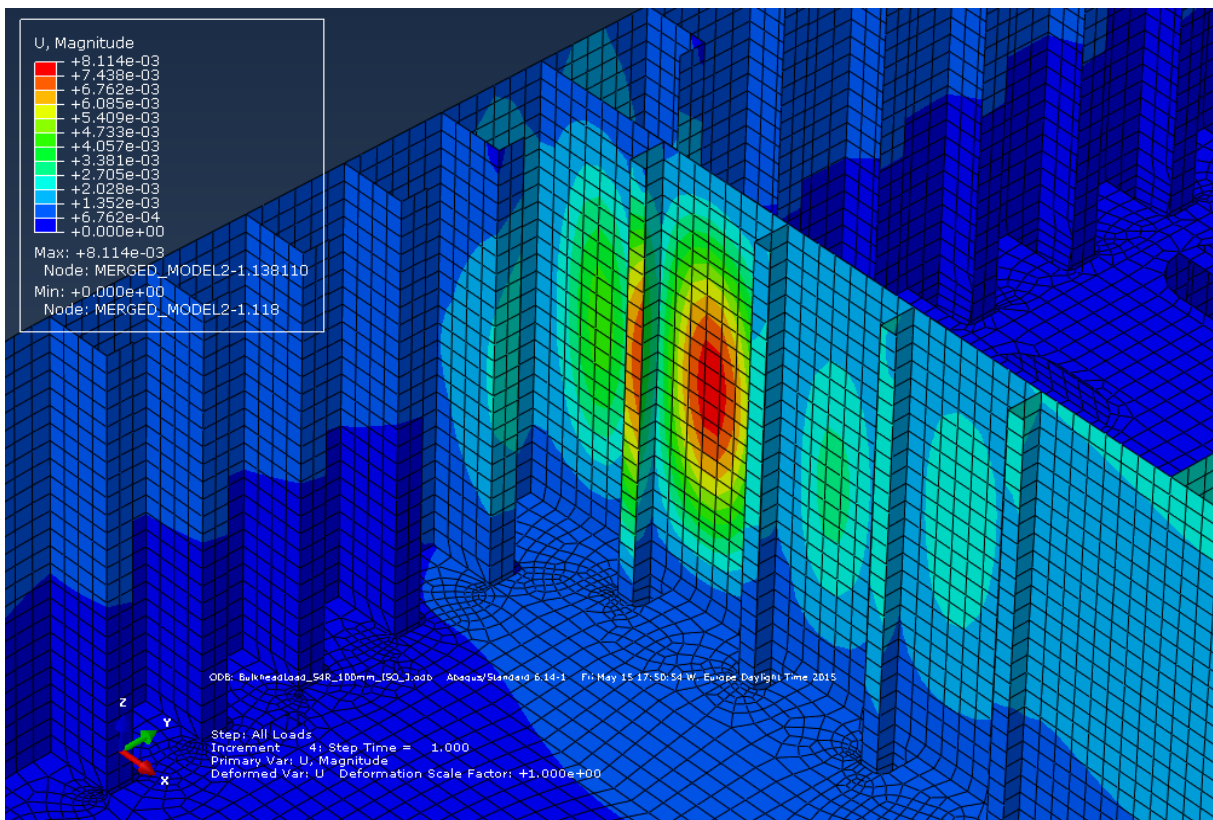
Figure E.19 – Response in displacements for the longitudinal bulkhead in Area 1-4.

XVI

E.4 Stringer

E.4.1 Transverse side of Area 1
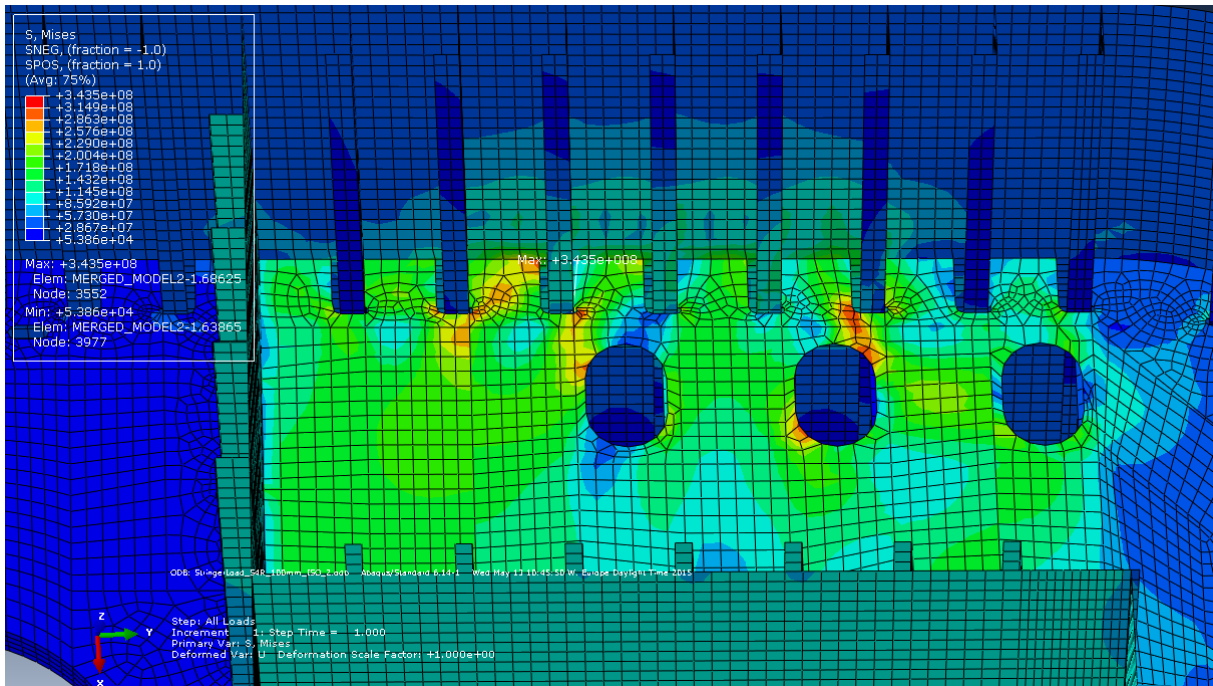
Figure E.20 – Response in von Mises stress for the stringer due to design stringer load on the transverse side in Area 1.
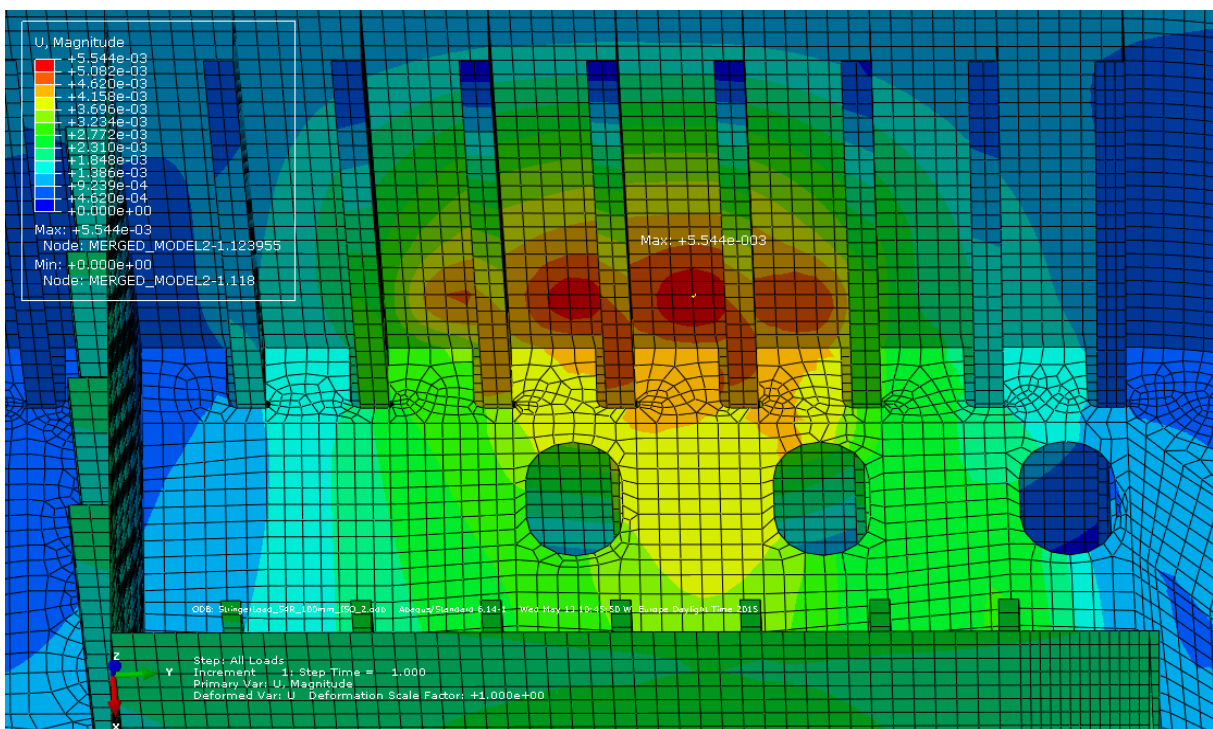
Figure E.21 – Response in displacements for the stringer due to design stringer load on the transverse side in Area 1.

E.4.2 Longitudinal side of Area 1
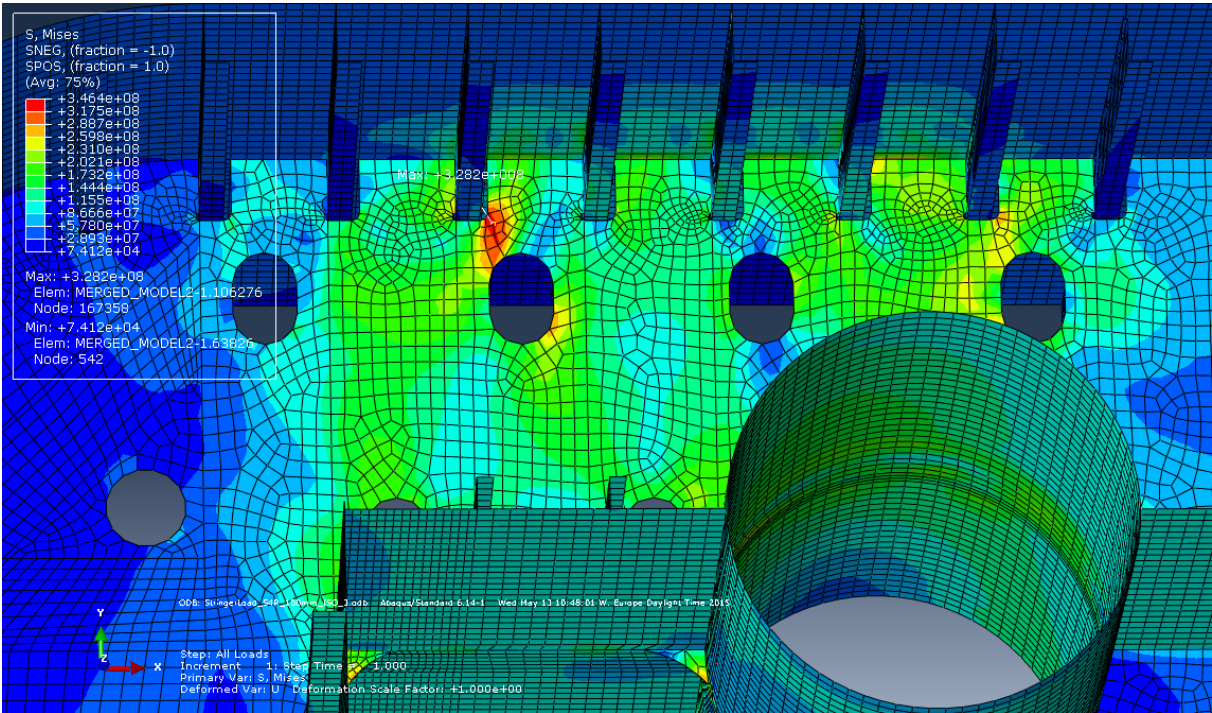
Figure E.22 – Response in von Mises stress for the stringer due to design stringer load on the longitudinal side in Area 1.
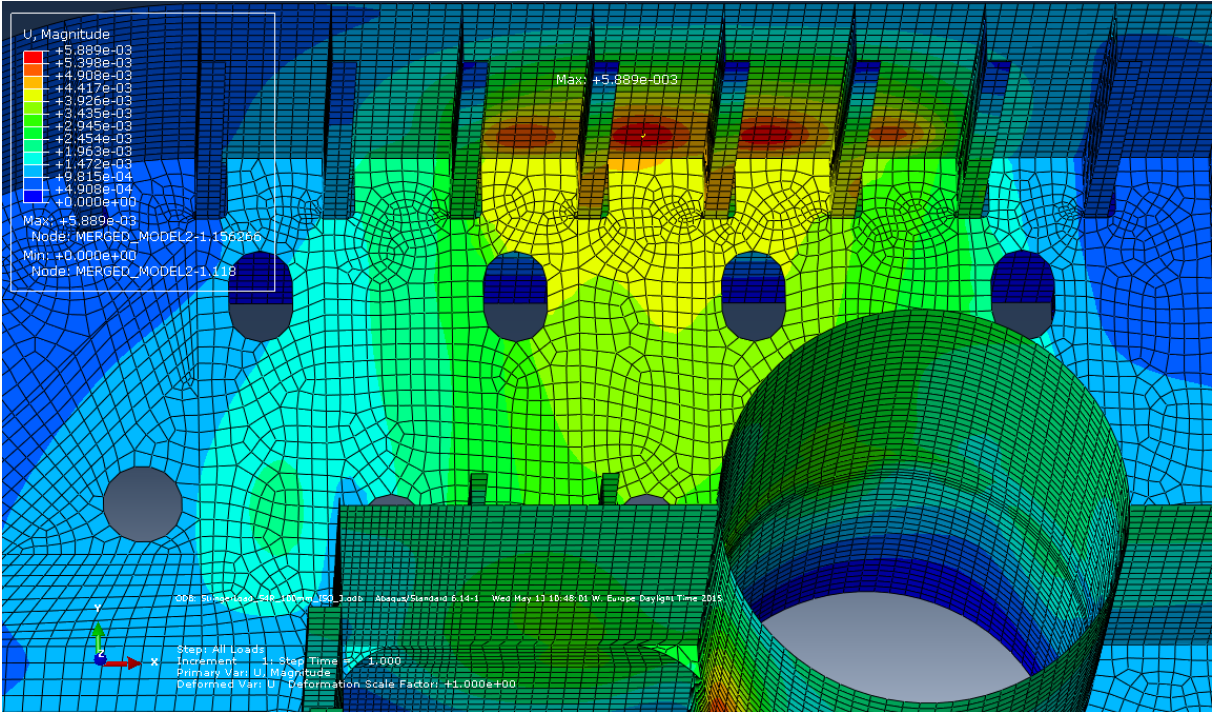
Figure E.23 – Response in displacements for the stringer due to design stringer load on the longitudinal side in Area 1.

XVIII

E.4.3 Longitudinal side of Area 3
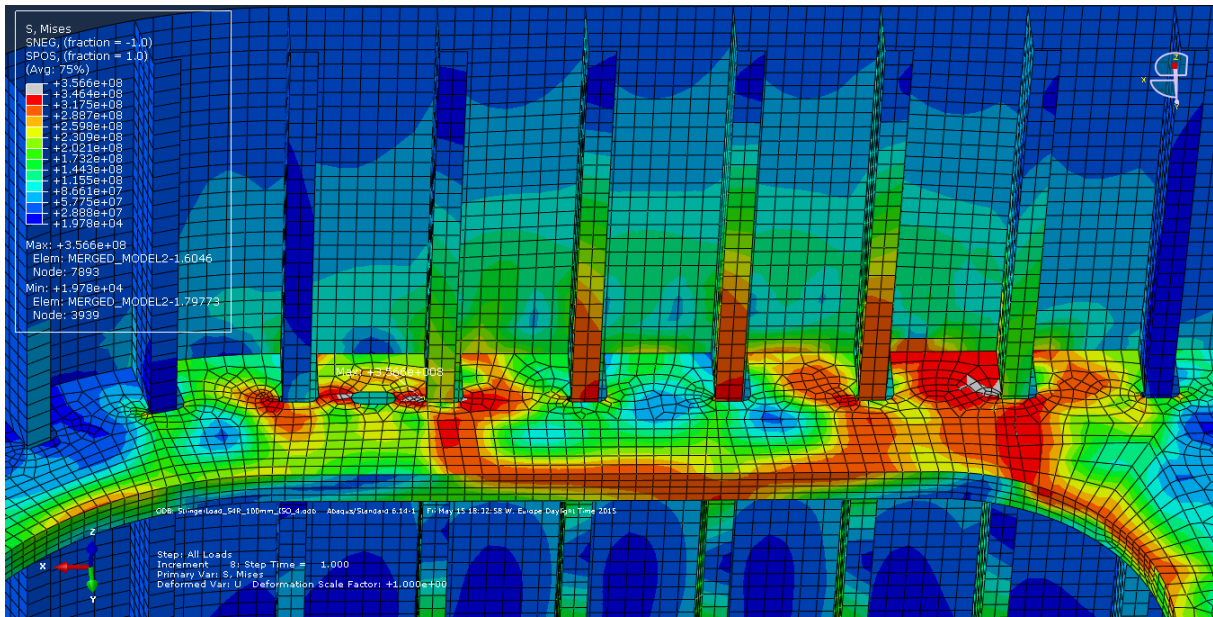
Figure E.24 – Response in von Mises stress for the stringer due to design stringer load on the longitudinal side in Area 3.
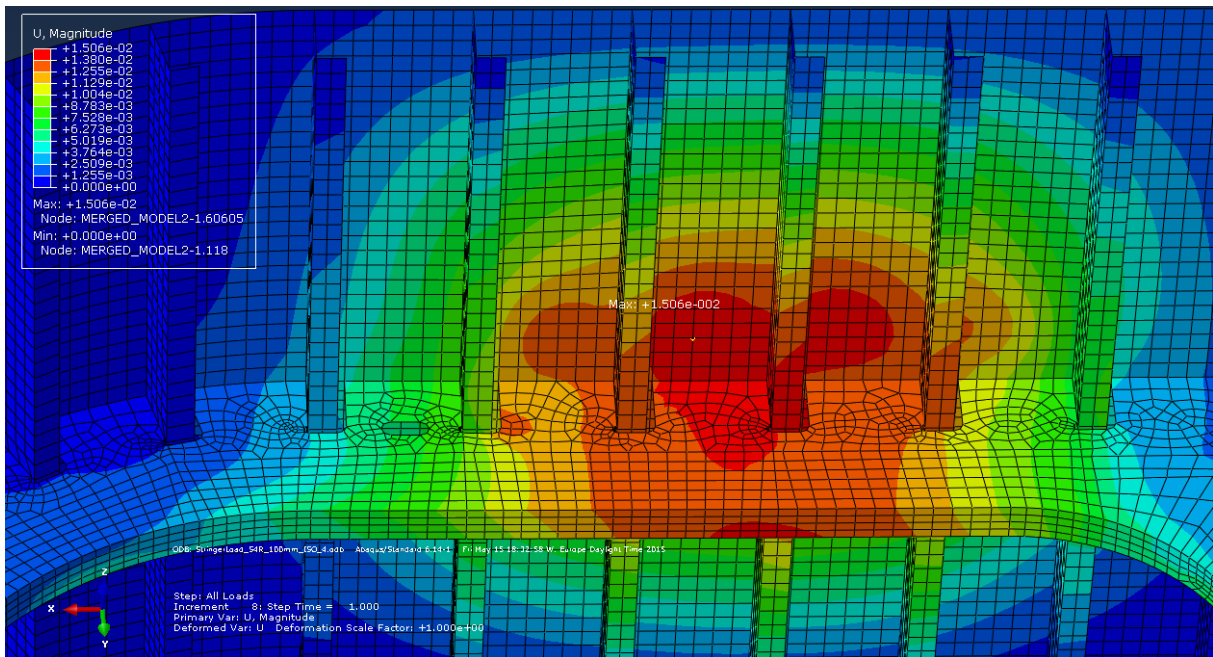
Figure E.25 – Response in displacements for the stringer due to design stringer load on the longitudinal side in Area 3.

E.4.4 Longitudinal side of Area 4
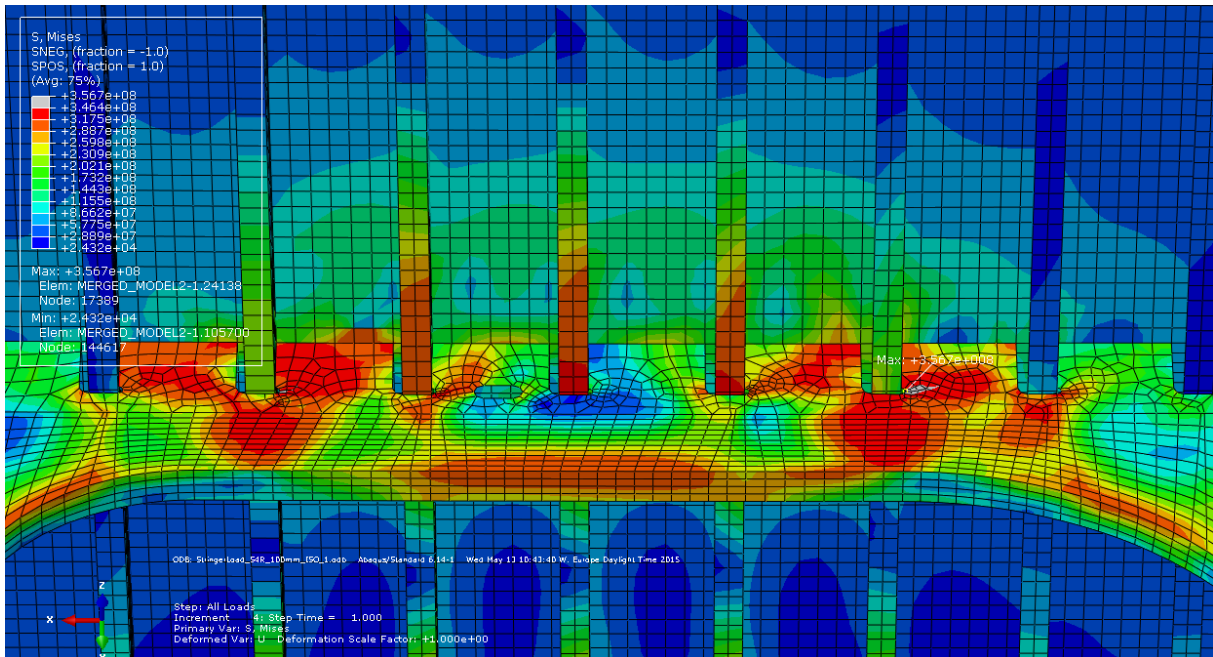
Figure E.26 – Response in von Mises stress for the stringer due to design stringer load on the longitudinal side in Area 4.
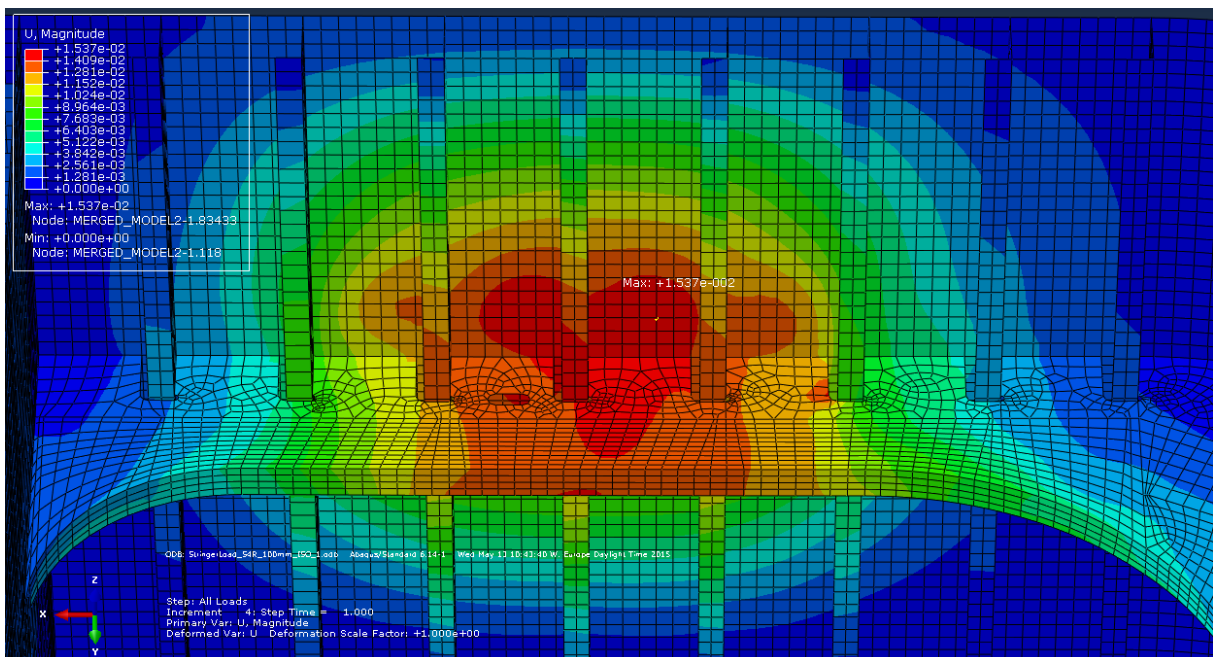
Figure E.27 – Response in displacements for the stringer due to design stringer load on the longitudinal side in Area 4.
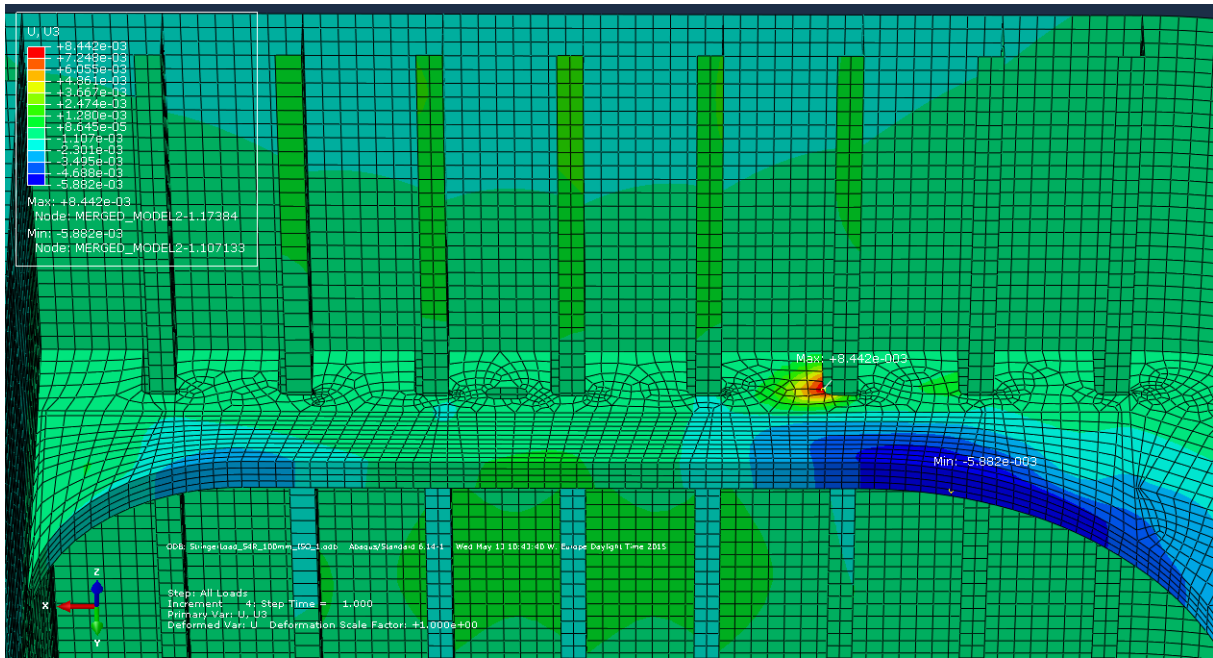
Figure E.28 – Response in vertical displacements for the stringer due to design stringer load on the longitudinal side in Area 4.

F. Local Capacity Study

F.1 Plate
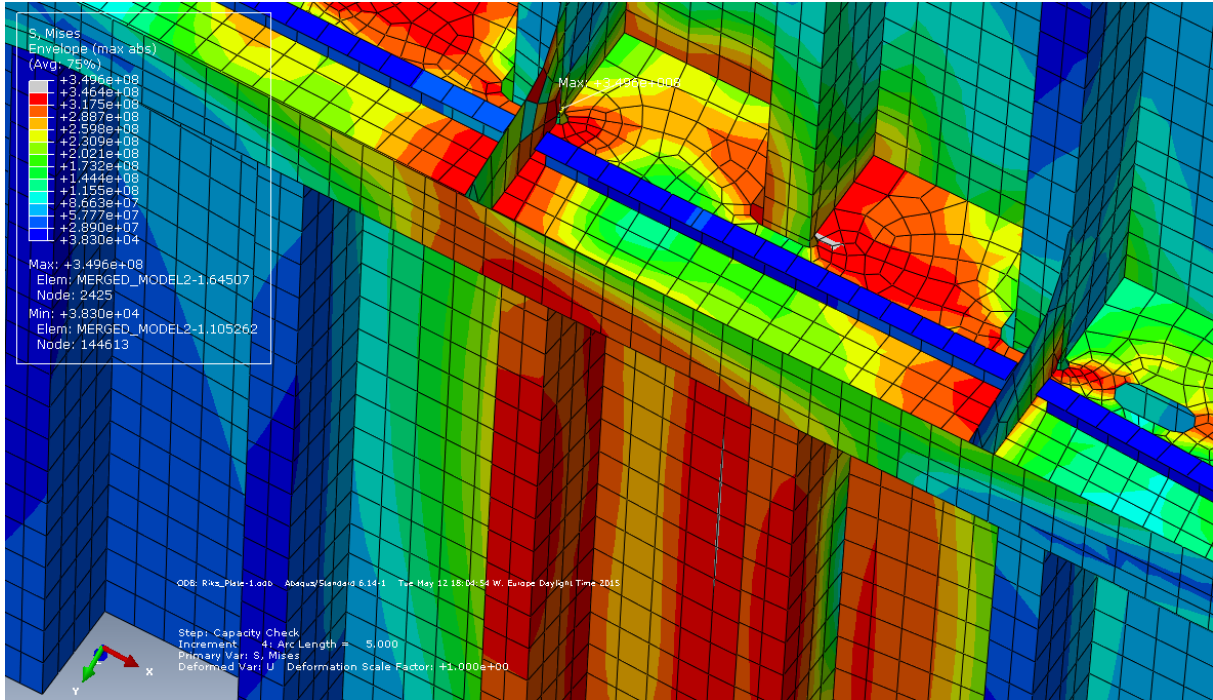
Figure F.1 – Response in von Mises at the step after first yield due to plate load.
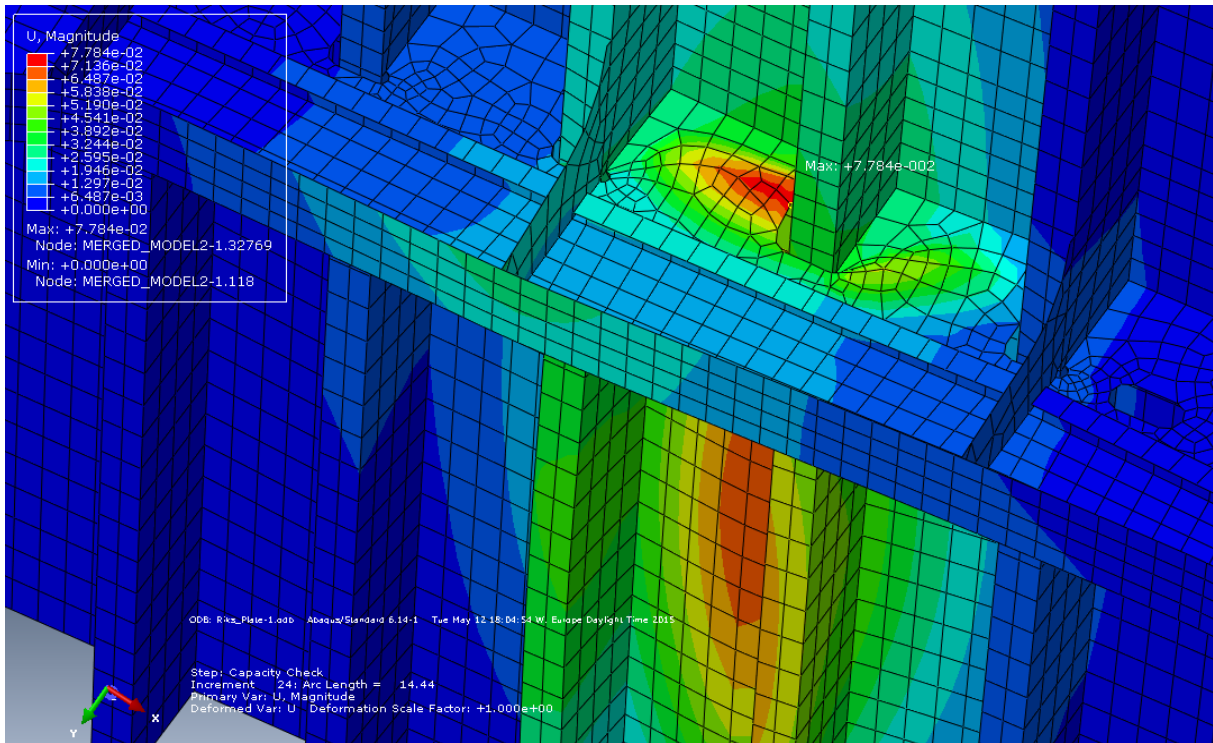
Figure F.2 – Response in displacements at ultimate stress due to plate load.

F.2 Stiffener
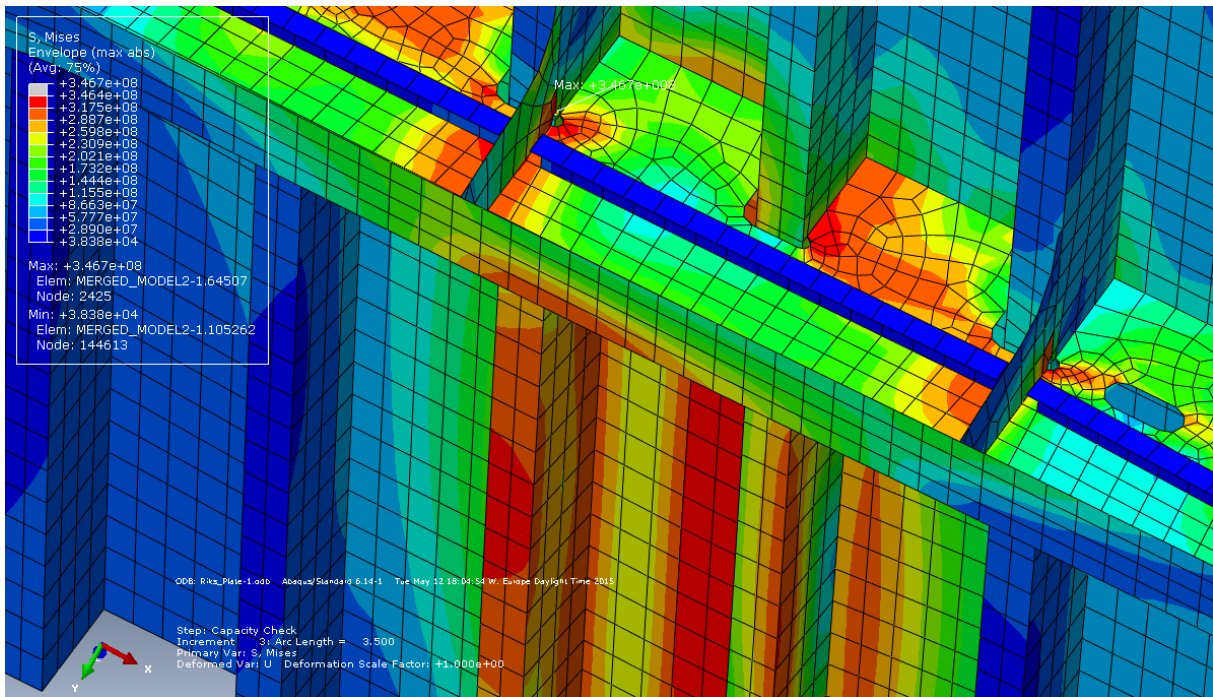
Figure F.3 – Response in von Mises at first yield due to stiffener load.
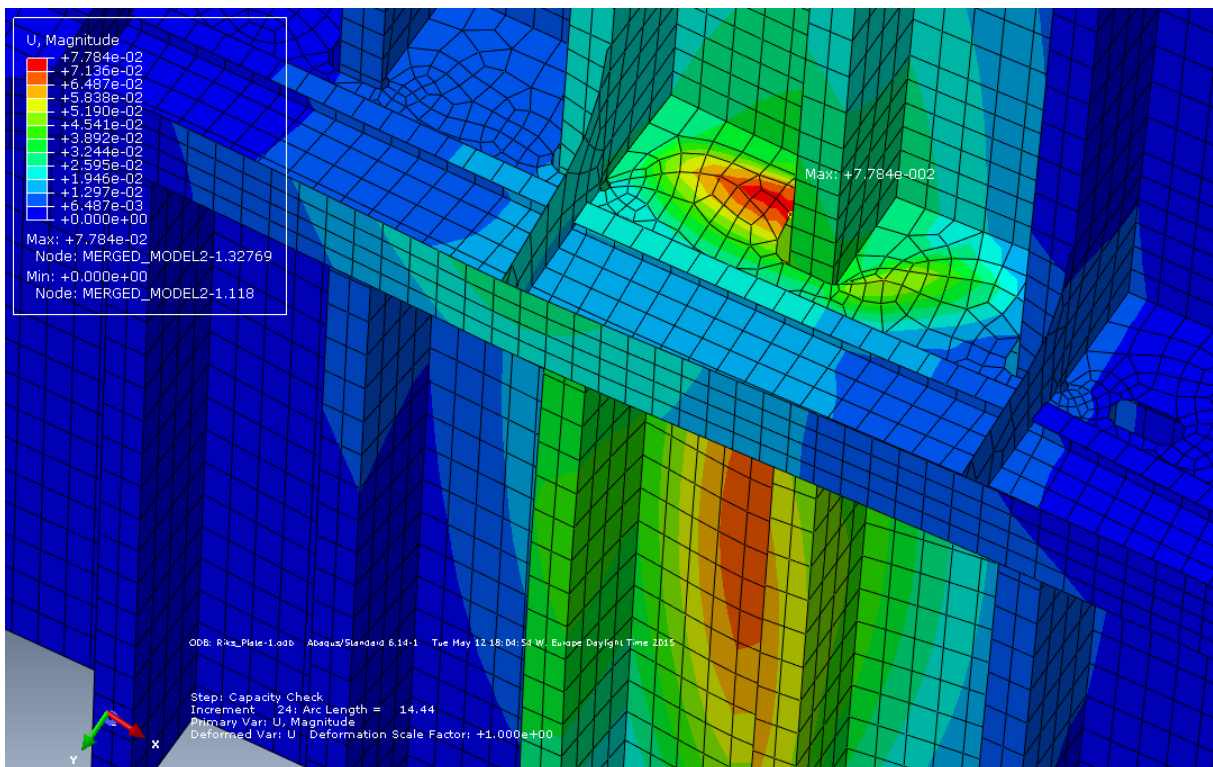
Figure F.4 – Response in displacements at ultimate stress due to stiffener load.

F.3 Bulkhead
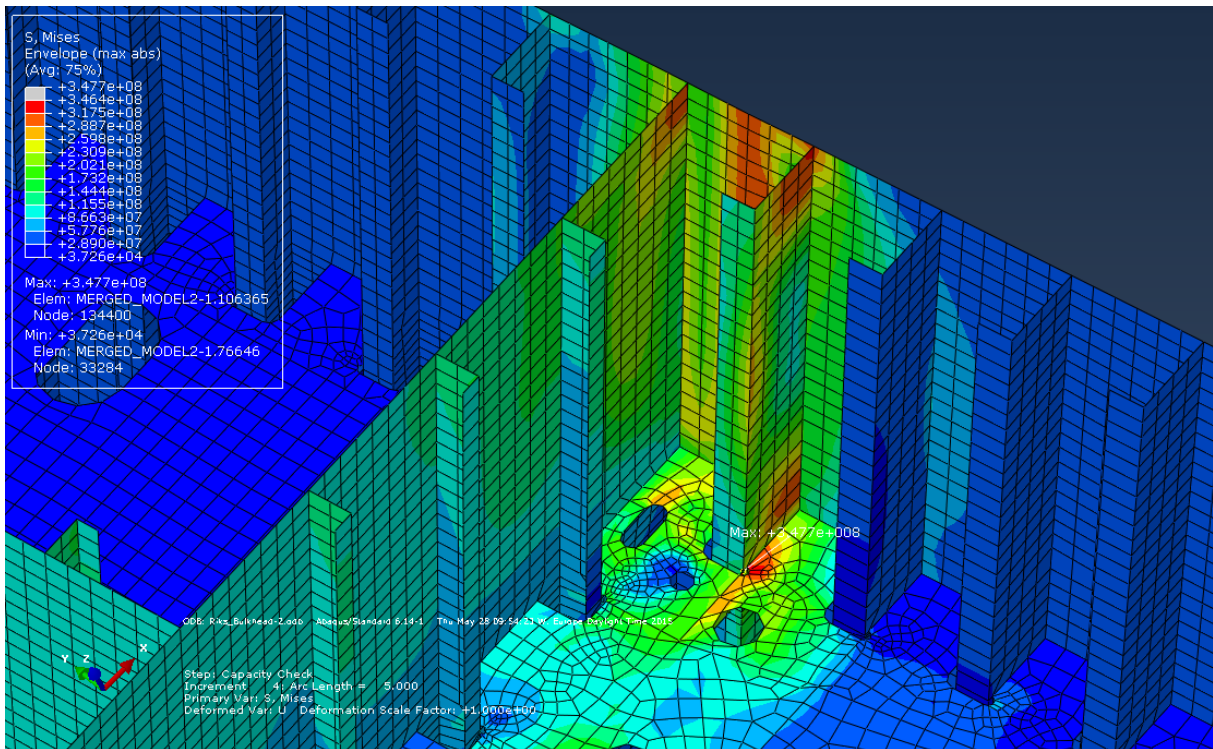
Figure F.5 – Response in von Mises at first yield due to bulkhead load.
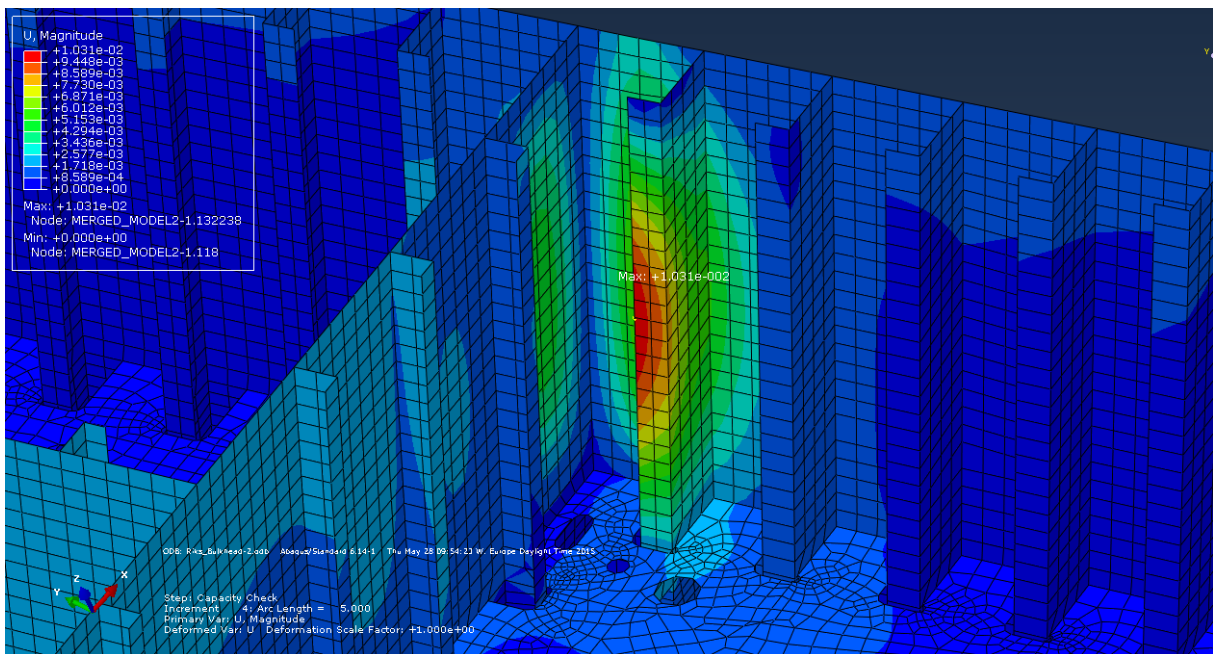
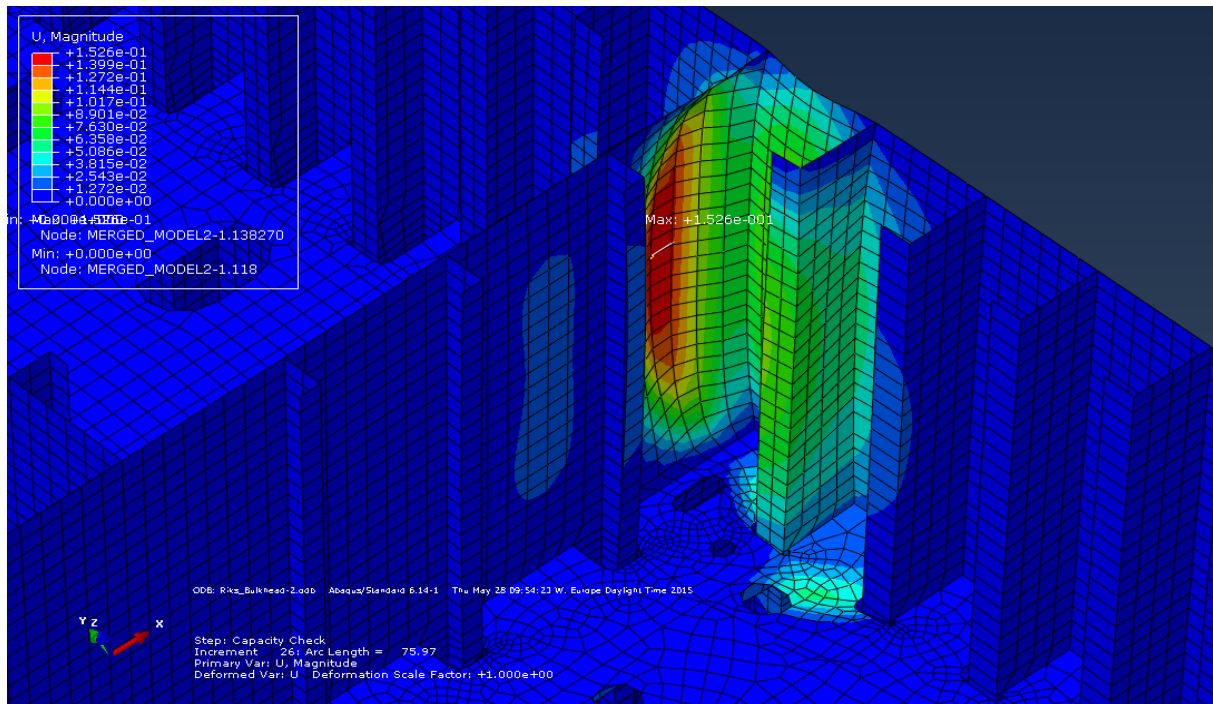**Figure F.6 – Response in displacements at first yield due to bulkhead load.**

Figure F.7 – Response in displacements at ultimate stress due to bulkhead load.
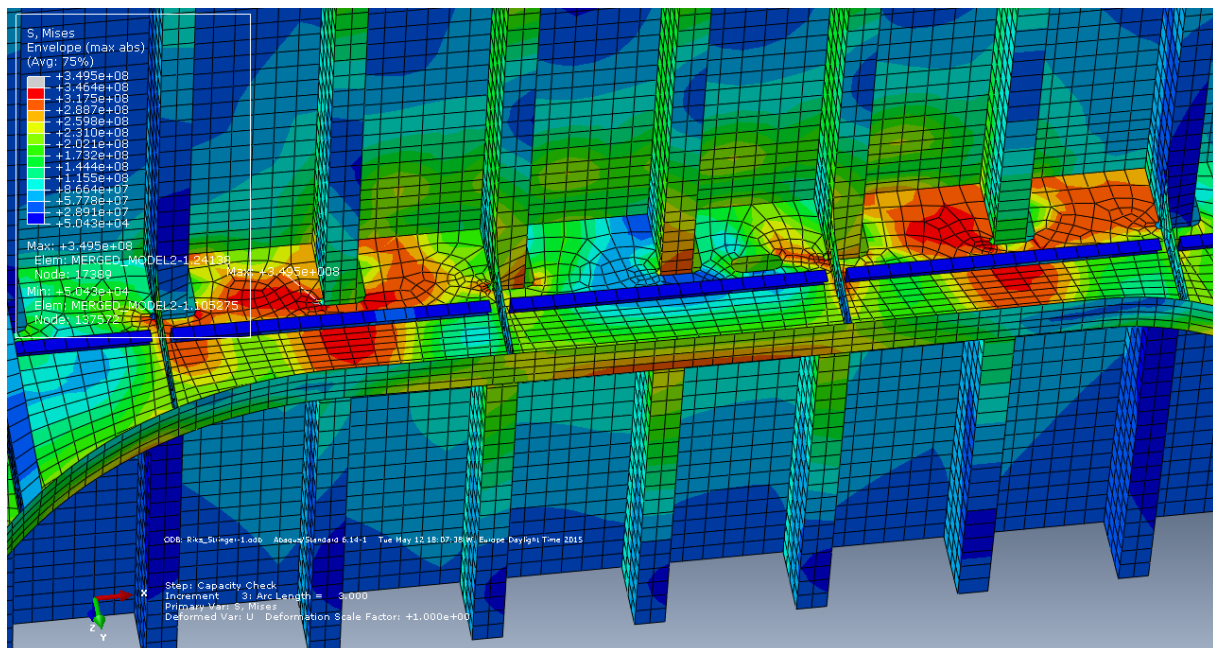
F.4 Stringer

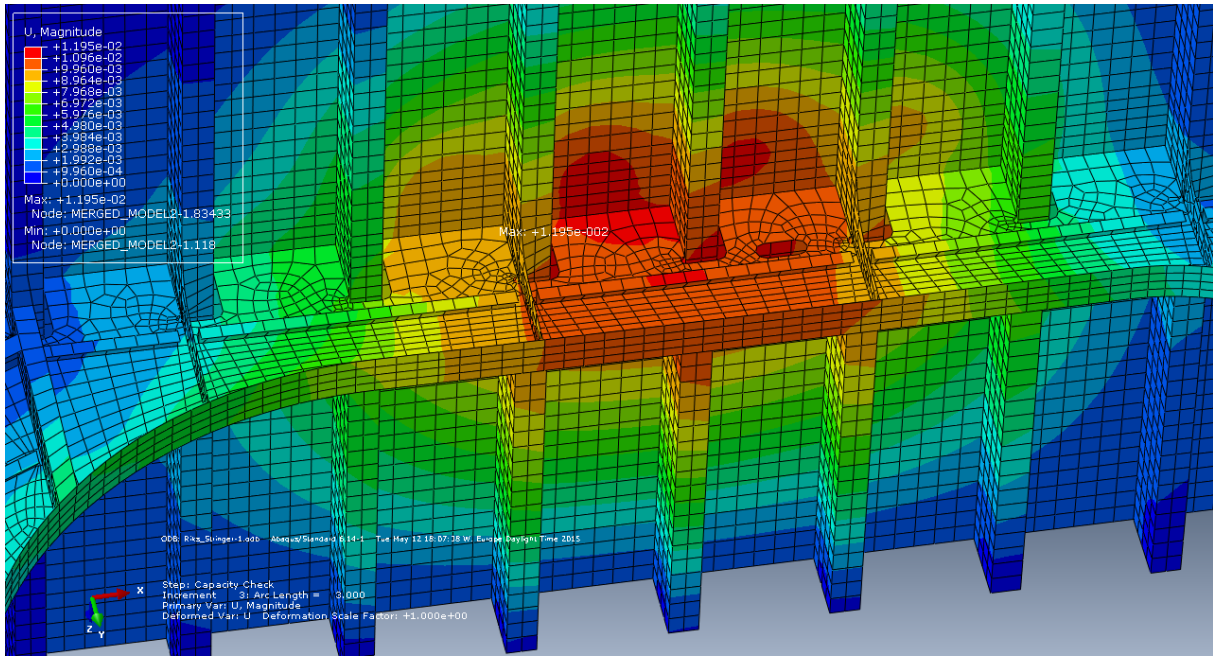**Figure F.8 – Response in von Mises stress at first yield due to stringer load.**

Figure F.9 – Response in displacements at first yield due to stringer load.
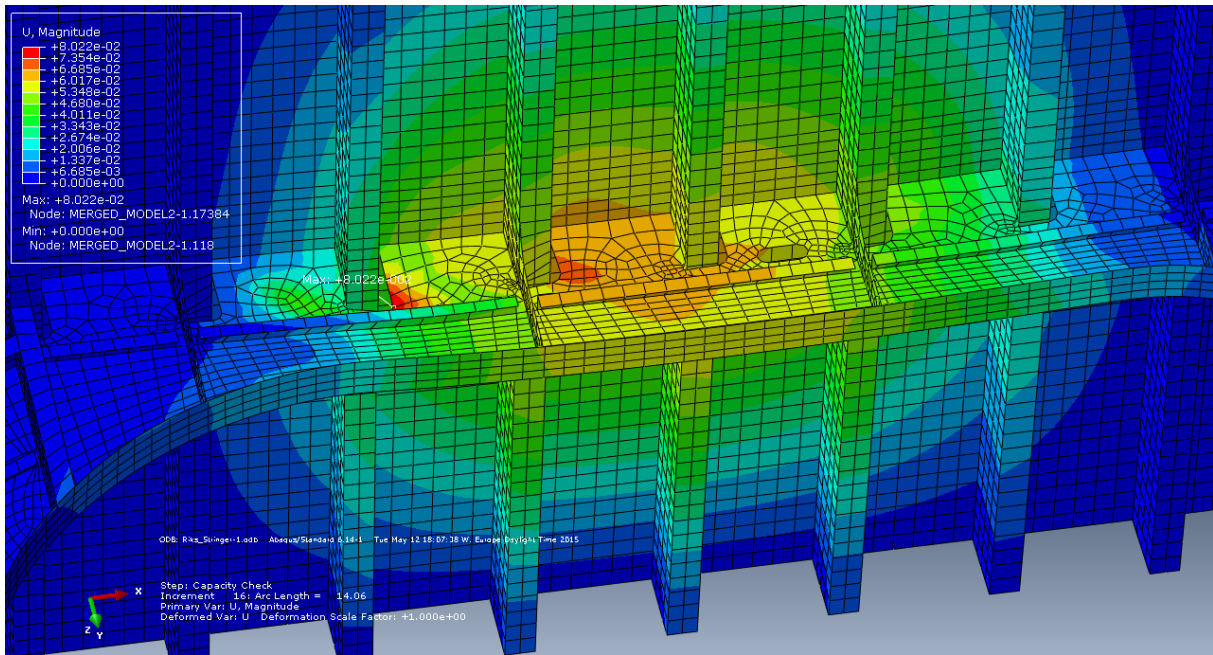

Figure F.10 – Response in displacements at ultimate stress due to stringer load.